NTNU

Norwegian University of
Science and Technology

A Multi-Horizon Stochastic Programming Approach to Optimal Component Sizing for The Strategic Microgrid Design Problem

Kristin Elise Skøyen Arnesen

Snorre Thorsønn Borgen

Industrial Economics and Technology Management
Submission date: June 2017
Supervisor: Asgeir Tomasgard, IØT
Co-supervisor: Gøril Forbord, Trønder Energi

Norwegian University of Science and Technology
Department of Industrial Economics and Technology Management

Problem Description

The objective of the strategic microgrid design problem is to identify the optimal size of the components in a stand-alone electricity grid configuration, considering the operational performance and costs over the lifetime of the system. The problem is subject to uncertainty in operational parameters, resulting in a stochastic model design. The desired output of the model are the suggested investments in components represented by the first stage decision variables. The problem considered in this thesis evaluates investments in battery units, solar photovoltaic panels, fuel based generators and wind turbines. Other considerations are battery lifetime calculations and degradation of battery performance.

In order to consider the operational performance and costs of today's investments over the lifetime of the system, the size of the stochastic program quickly becomes intractable for commercial solvers when considering realistically sized instances. The aim of this Master Thesis is therefore to develop a novel approach to modelling and solving the strategic microgrid design problem. The development of this novel approach includes:

Applying a multi-horizon information structure.

Testing various scenario generation routines in order to determine how to best represent the underlying data without compromising the quality of the solution.

A discussion on the level of detail necessary in the modelling of the components, and an analysis of the impact of various model formulations on computation time and the practical performance of the solution.

Implementation and testing of strategies for speeding up the solution process.

Preface

The content of this thesis is a continuation of Arnesen and Borgen (2016), and comprises the work performed during our last semester at the Norwegian University of Science and Technology. The thesis represents the completion of our Master of Science degree in Industrial Economics and Technology Management, with a specialization in TIØ4905 - Managerial Economics an Operations Research. The thesis was initially motivated by one of the co-authors, Snorre T. Borgen, and resulted in a collaboration with Trønder Energi. Through this collaboration, the initial ideas and motivation behind this thesis have developed to what is enclosed in the following pages.

We wish to express our gratitude towards those who have contributed to the content of this thesis, or been instrumental in the completion of it. First and foremost, we would like to thank our supervisor, Asgeir Tomasgard, for great academic insights. He has granted us a high degree of autonomy, while providing support and guidance in our learning process. We would also like to give a special thank to Christian Skar at the Department of Industrial Economics and Technology Management, for unwavering assistance, advice and motivation.

Throughout the process of producing this thesis, Trønder Energi have been accommodating in facilitating our research, and we wish to especially thank Gøril Forbord, Gunnar Aronsen and John Kristian Evjen for providing essential information and insights. Several of Trønder Energi's partnering institutions also deserve acknowledgement for providing technical insight and content, in particular Simen Karlsen from Powel and Lars Ole Valøen from Grenland Energy.

The support of our families, friends and classmates have kept us motivated in the process of producing this thesis, marking the end of our five year long adventure in Trondheim.

Trondheim, June 2017

Kristin Elise Skøyen Arnesen

Snorre Thorsønn Borgen

Abstract

This thesis studies the strategic microgrid design problem, and suggests a multi-horizon stochastic programming approach aiming to provide decision makers with valuable insights into the optimal component sizing in a stand-alone microgrid including renewable energy sources and energy storage systems. The components considered are photovoltaic panels, wind turbines, batteries and diesel generators.

The strategic microgrid design problem is subject to uncertainty in load demand, and in weather conditions, and due to modelling of the physical properties of components, it is a mixed integer problem. We present a novel approach to the strategic microgrid design problem, including the consideration of uncertainty in input parameters, component specific modelling, and the evaluation of long strategic horizons. Other important contributions are the inclusion of battery lifetime considerations and the possibility of reinvestments in battery units. The objective of the model is to provide a suggested investment decision, given as a number of specific types of components.

We propose to model the uncertainty with a multi-horizon information structure, separating the operational and strategic horizon of the problem. Exploiting the multi-horizon information structure, we design a scenario tree with representative profiles for predefined seasons in an effort to limit the size of the problem. The stability of the model is verified, and the decreased size of the problem facilitates for solving more realistic instances.

The computational performance is further improved by applying an alternative diesel generator formulation, leading to an average improvement in computation time for the smaller instances of more than 90% compared to the original formulation. The improvement is achieved without compromising the quality of the results. To further overcome the computational challenges faced by the problem, we propose a variety of speed-up strategies. The most promising approaches are a matheuristic, and applying a *Newton-Barrier* algorithm for the LP-relaxation, combined with an aggressive cut strategy.

The thesis gives a thorough introduction to the considerations necessary in a strategic planning phase of a microgrid. The main contribution is a novel mathematical model for the strategic microgrid design problem with a multi-horizon information structure, proven to perform as intended. In addition to this, we present a scenario generation algorithm that is shown to be stable with a given set of parameters, as well as numerous ways of improving the computational performance of the problem.

Sammendrag

Denne masteroppgaven studerer det strategiske mikrogrid-designproblemet, og formulerer en stokastisk optimeringsmodell med multi-horisont informasjonsstruktur. Modellen er utformet for å gi beslutningstakere verdifull innsikt i optimal dimensjonering av komponenter i et frittstående mikrogrid, bestående av fornybare energikilder og energilagringssystemer. Komponenter som vurderes er solcellepaneler, vindmøller, batterier og dieselgeneratorer.

Det strategiske mikrogrid-designproblemet er underlagt usikkerhet i last, og i værforhold, og er formulert som et blandet heltallsproblem for å kunne modellere de fysiske egenskapene til komponentene. Vi presenterer en ny tilnærming til problemet, som tar høyde for usikkerheten i last- og værdata, inkluderer komponentspesifikk modellering og evaluerer lange strategiske horisonter. Ytterligere bidrag er levetidsbetraktninger for batterienheten, samt muligheten for å reinvestere på et senere tidspunkt. Modellen har som mål å presentere en foreslått investeringsbeslutning, oppgitt som en kombinasjon av et antall forhåndsspesifiserte komponenter.

Vi foreslår å modellere usikkerheten med en multi-horisont informasjonsstruktur, som skiller mellom den operasjonelle og den strategiske horisonten i problemet. Videre utformer vi et senariotre med representative profiler for et sett forhåndsdefinerte sesonger, i et forsøk på å begrense problemets størrelse. Stabiliteten til scenariotreet verifiseres, og den reduserte størrelsen på problemet fører til lavere beregningstid.

Beregningsytelsen forbedres ytterligere ved å innføre en alternativ dieselgeneratorformulering, som fører til en gjennomsnittlig forbedring i beregningstiden for kortere strategiske horisonter på mer enn 90% sammenlignet med den opprinnelige formuleringen. Forbedringen i beregningstid oppnås uten å påvirke kvaliteten på resultatene. For å ytterligere eliminere de beregningsmessige utfordringene til problemet, foreslår vi en rekke strategier for å øke beregninshastigheten. Tilnærmingene som viste seg å være mest lovende er en matheuristikk, og å anvende en *Newton-Barrier*-algoritme for LP-relaksering kombinert med en aggressiv kuttstrategi.

Oppgaven gir en grundig innføring i nødvendige betraktninger i en strategisk planleggingsfase for et mikrogrid. Hovedbidraget er en ny matematisk modell for det strategiske mikrogrid-designproblemet med en multi-horisont informasjonsstruktur, som har vist ønskelig oppførsel. I tillegg presenterer vi en scenariogenereringsalgoritme som vi videre har vist at er stabil for problemet, samt utvalgte metoder som kan forbedre beregningsytelsen til problemet.

Contents

1 Introduction **1**

2 Background **3**

2.1 Microgrids and renewable energy sources 3

2.2 Trønder Energi and the Island Project 5

2.2.1 The Island Project 6

2.2.2 Scope and limitations for Trønder Energi 7

3 Literature review **9**

3.1 Stochastic programming 9

3.1.1 Formulation of the stochastic program 10

3.1.2 Solution methods for stochastic programs 12

3.1.3 Multi-horizon stochastic programming 12

3.2 The microgrid design problem 13

3.2.1 Optimal sizing of components in microgrids 13

3.2.2 Component modelling 16

3.2.3 A comparison to the capacitated lot sizing problem 21

4 Problem description **23**

4.1 Problem statement 23

5 Mathematical model **25**

5.1 Assumptions and simplifications 26

5.2 Information structure 28

5.3 Modelling Choices 31
5.3.1 Generator formulation 31
5.3.2 Battery formulation 32
5.3.3 PV 33
5.3.4 Considerations of a strategic model 33
5.4 Mathematical formulation - Base model 34
5.4.1 Sets, indices, parameters and variables 34
5.4.2 Multi-horizon stochastic model formulation 37
5.5 Continuous diesel generator formulation 46
5.6 Extensions to the model 48
5.6.1 Maximum PV-panel surface area 48
5.6.2 Degradation of battery capacity 48
5.6.3 Wind turbines 50
5.7 Strengthening the Big-M formulations 53
5.8 Challenges with solution procedure 55

6 Data analysis **57**

6.1 About the operational data 57
6.1.1 Analyzing the weather data 57
6.1.2 Analyzing the load data 59
6.2 Scenario generation 60
6.2.1 Choice of scenario generation method 60
6.2.2 The scenario generation algorithm 63
6.3 Evaluation of input parameters 66
6.3.1 Scaling Factor 66
6.3.2 Battery Parameters 66
6.3.3 Diesel generator parameters 67
6.3.4 Wind Parameters 69
6.3.5 PV parameters 69

6.3.6 Value of lost load 69

7 Computational study **71**

7.1 Hardware and software 72

7.2 Test Instances 72

7.3 Diesel generator formulations 73

7.4 Stability testing 75

7.4.1 In-sample stability 76

7.4.2 Out-of-sample stability 77

7.4.3 Testing the stability of the MISSMDP 78

7.5 Improved implementation 84

7.5.1 Heuristics 84

7.5.2 Pre-processing for a lower bound 86

7.5.3 Solver Settings 87

7.6 Value of information and the stochastic solution 90

7.6.1 The expected value of perfect information and the value of the stochastic solution 90

7.6.2 The expected value of planning with battery lifetime and degradation 91

7.6.3 The vaule of the MISSMDP 92

7.7 Practical analysis 94

7.7.1 Battery 94

7.7.2 Changing future prices 95

7.7.3 Changing load demand 96

7.7.4 Comparing cost per kW/kWh - approach to the MISSMDP 97

8 Future research and concluding remarks **99**

8.1 Future research 99

8.2 Concluding remarks 101

Bibliography **105**

A Mathematical Model - base **113**

B Mathematical Model - full **115**

C Notation - Full **118**

D Component data and input parameters **121**

E Statistical property match calculations **123**

F Calculations VSS and EVPBD **125**

G Results from Chapter 7.5.1 **126**

Abbreviations

DG	-	Distributed generators
DM	-	Decision Maker
GA	-	Genetic Algorithms
LCC	-	Life Cycle Cost
LCOE	-	Levelized Cost of Energy
LOLP	-	Loss of Load Probability
LP	-	Linear Programming
LPSP	-	Loss of Power Supply Probability
MCS	-	Monte Carlo Simulations
MIP	-	Mixed Integer Programming
MINLP	-	Mixed Integer Nonlinear Programming
O&M	-	Operation and Maintenance
PoE	-	Power Electronics
PS	-	Pattern Search
PSO	-	Particle Swarm Optimization
PV	-	Photovoltaic
RES	-	Renewable Energy Sources
R&D	-	Research & Development
SOC	-	State of Charge

List of Figures

2.1 The microgrid concept 4

2.2 Map of existing subsea cables at Froan (Sørburøy, Nordøya and Sauøya) and Gjessingen 7

4.1 Schematic energy flow for the strategic microgrid design problem 24

5.1 Complete information structure for the multi-stage optimization problem 29

5.2 Multi-horizon information structure for the MISSMPD. 30

5.3 Linear fuel consumption relationship for diesel generator 40

5.4 Example of approximated fuel consumption curve for the diesel generator . . . 46

6.1 Historic daily means of wind speed throughout the year 58

6.2 Historic hourly mean irradiance throughout the day for every month 59

6.3 Probability distribution of historical irradiation data and a generated scenario tree 64

6.4 Probability distribution of historical wind data and a generated scenario tree . . 65

6.5 Probability distribution of historical load data and a generated scenario tree . . 65

6.6 Fuel consumption curves for generators of different sizes; production in kW on x-axis; consumption in l/h on y-axis 68

6.7 Aggregated fuel consumption scatter plot for diesel generator with linear regression and approximated fit 68

7.1 Objective values for $GEN1$ and $GEN2$ on all four tests on instance 1. Bottom parts are investment costs, top parts are operational costs. 75

7.2 Average Coefficient of Variation [%] from in-sample stability tests on instance 1 and 2 80

7.3 Average computation time for in-sample Stability tests on instance 1 and 2 . . . 81

7.4 Objective values of solving the MISSMDP on ten different scenario trees with 72 operational horizons and 30 scenarios, run on instance 1-4 (5, 10, 20 and 30 strategic periods) 87

List of Tables

2.1 Partnering institutions - The Island Project 6

3.1 Article overview: Selected articles adressing the microgrid design problem . . . 16

5.1 Main assumptions of the problem 27

5.2 Main assumptions of the problem (extended) 31

5.3 Sets 35

5.4 Indices 35

5.5 Parameters 36

5.6 Variables 36

5.7 New notation for continuous diesel generator formulation 47

5.8 New notation for limiting PV-panel surface area 48

5.9 New notation for battery degradation 49

5.10 New notation for wind turbines 51

6.1 Variance in load data 60

7.1 Details of computer and solver used in computational study 72

7.2 Instances 73

7.3 Results from testing the different generator formulations, $\Delta\%_{RC}$ is the relative change in computation time, $\Delta \mathbf{z}^*$ is the absolute difference in objective values, and $\Delta \mathbf{z}^*_{RC}$ is the relative change from $GEN1$. 73

7.4 Further results from testing $GEN1$ and $GEN2$ on instance 1. 74

7.5 Combinations tested for deciding parameters in in-sample stability testing . . . 79

7.6 Results from in-sample stability testing. CV is calculated over ten runs, $^{\Delta CV}/_{\Delta|T^S|}$ is the change in CV relative to increase in strategic periods. 82

7.7 Relative difference in out-of-sample stability testing 83

7.8 Average computation time and objective value with 0.7% and 5% tolerance gap, and the relative change. 85

7.9 Average objective value and computation time from including a lower bound, found by solving the MISSMDP for a lower number number of strategic periods, together with the relative change in computation time. 87

7.10 Average computation time by default, with the *Newton-Barrier* (N-B) LP-relaxation algorithm and with the N-B and an aggressive cut strategy (cut-str), as well as the respective relative change (Rel chng) 89

7.11 Average VSS and EVPBD for all combinations with instance 3 and 4 for the MISSMDP, % refers to the average relative change in objective value compared to the *EEV* and the FRP. 93

7.12 Objective values of the MISSMDP when solving with constant fuel cost, or an increasing/decreasing fuel cost, with either 5% or 10% yearly increase, or 5% yearly decrease. 96

7.13 Objective values of the MISSMDP when solving with stable future load demand, a 2.5% yearly increase, and a 2.5% yearly decrease. 97

7.14 Objective value of MISSMDP considering all components and considering only the "cheapest" components 98

C.1 Sets 118

C.2 Indices 118

C.3 Parameters 119

C.4 Variables 120

D.1 Input parameters for PV-panels 121

D.2 Input parameters for battery units 121

D.3 Input parameters for wind turbines 121

D.4 Input parameters for diesel generators 122

D.5 General list of input parameters for the model 122

F.1 VSS and EVPBD for all combinations with instance 3 and 4 for the MISSMDP 125

G.1 Testing the matheuristic of increasing tolerance gap from 0.7 % to 5% on instance 3. Table shows average computation time and objective value with 0.7% and 5% tolerance gap, and the relative change on 4 different scenario trees. . . 126

G.2 Testing the matheuristic of increasing tolerance gap from 0.7 % to 5% on instance 4. Table shows average computation time and objective value with 0.7% and 5% tolerance gap, and the relative change on 4 different scenario trees. . . 126

Chapter 1

Introduction

Secure supply of energy has become an expectation in developed parts of the world. Modern society, with complicated infrastructure and information channels, is highly dependent on a stable supply of energy in order to maintain the "status quo". The International Energy Agency estimates global investments in the energy sector from 2003 - 2030 to be $16 trillion if the aging infrastructure is to cope with the introduction of more renewable energy without compromising security, reliability and quality of power supply (Schwaegerl and Tao, 2014).

Microgrids are becoming increasingly relevant as an energy system configuration, as distributed generators relying on renewable energy sources are getting cheaper and more efficient. These solutions are, according to Soshinskaya et al. (2014), expected to play a significant role in future electricity supply. Traditionally, microgrids have been promoted in remote areas with poor infrastructure. The recent increase in reliability of renewable technology and batteries, has introduced the idea of microgrids as a solution in countries where infrastructure is more developed and there are high requirements to the performance of the electricity system.

Norway is a country with an abundance of potential locations for microgrids due to steep mountains, deep fjords, thousands of islands and long distances between populated areas. There is a great opportunity for value creation by developing a solid investment scheme for microgrids in the Norwegian power grid, as delivering electricity to remote areas through an aging regional grid can be expensive. Installation of optimally sized microgrids could reduce the need for grid expansion in the traditional sense (Hatziargyriou et al., 2007) and be an economically efficient option in these locations.

The majority of the published research on microgrids is focused on optimal operation and component sizing. Less attention has been awarded to strategic decision making related to the optimal sizing of microgrid components considering the lifetime of the system, and stochastic

operating conditions. As microgrids are becoming more relevant as a viable alternative for energy supply in remote areas, it is important to bear in mind the total lifetime costs of such a solution and to consider the uncertainty in future conditions.

It is the goal of this thesis to present a generic mathematical model for the strategic microgrid design problem, considering the lifetime of the microgrid and uncertainty in future operating conditions. The model should provide important insights for decision makers in the strategic planning phase of a microgrid project, regarding the sizing of the necessary components. In collaboration with Trønder Energi, we study a specific case where a microgrid is considered to be a viable option for energy supply. By applying stochastic programming, we formulate the mixed integer stochastic strategic microgrid design problem (MISSMDP), designed to provide optimal investment decisions in components for a microgrid. The MISSMDP is evaluated on a variety of measures, and several extensions and improvement strategies from literature is applied in an effort to increase the value of the program.

The content of this thesis is structured in the following order: Providing context for the research problem, Chapter 2 presents some background covering microgrids, as well as the case study initiated by Trønder Energi. Chapter 3 presents a study of available literature concerning state of the art research on relevant topics, confirming the academic relevance of our work. In Chapter 4, we describe the problem studied in this thesis in more detail. Chapter 5 presents the modelling approach along with the major assumptions of the MISSMDP, and states the suggested mathematical formulation of the problem together with suggested reformulations and extensions. In Chapter 6, we explain and analyze the stochastic input data, present a scenario generation algorithm, and evaluate the remaining input parameters. Chapter 7 provides a comprehensive computational study, beginning with a discussion of the alternative formulations suggested in Chapter 5. The study moves on to testing the stability of the MISSMDP, followed by a detailed technical and practical analysis. Chapter 7 also includes an evaluation of the value of accounting for uncertainty and increasing the information level in the model. The chapter is concluded by suggesting potentially interesting areas of future research. Finally, Chapter 8 presents a conclusion to our work.

Chapter 2

Background

Before discussing the strategic microgrid design problem in more detail, this chapter is included to provide a context and motivation for the work presented in this thesis. The chapter begins with an introduction to microgrids as an energy system, and is concluded with details of the case study provided by Trønder Energi.

2.1 Microgrids and renewable energy sources

A microgrid is a smaller grid consisting of distributed generators (DGs), loads, energy storage, and power electronics, and is often described as a smaller part of a distribution grid with local power sources. Microgrids appear in a large variety of scales, and they are defined by their function rather than their design or size (Soshinskaya et al., 2014). CIGRÉ, the International Council on Large Electric Systems, provides the following definition of microgrids:

"Microgrids are electricity distribution systems containing loads and distributed energy resources, (such as distributed generators, storage devices, or controllable loads) that can be operated in a controlled, coordinated way either while connected to the main power network or while islanded. (CIGRÉ, 2010)"

Microgrids are rarely discussed without the mentioning of distributed energy resources, which includes DGs, distributed storage and active loads. DG relates to smaller generator units that can be distributed along the grid where needed, rather than centralized at large generation facilities (Soshinskaya et al., 2014). Some common types of DG are internal combustion engines of various kinds, gas turbines, biofuel technologies, microturbines, photovoltaic (PV) panels, fuel cells and wind turbines. DGs based on renewable energy sources (RESs) are usually the preferred

option in microgrids, as they are convenient in remote areas and emission free. Additionally, the IRENA (2015) report states that with the recent price development, RESs are proven to be the economically superior solution for islanded microgrids compared to a purely diesel generator based solution. However, as DG technologies based on RESs are subject to intermittent behaviour, they can cause disturbances if connected directly to the utility grid (Hatziargyriou et al., 2006). This has led to an increased interest in subsystems or microgrids as a means to include DGs (Lasseter, 2002).

In a microgrid, distributed storage devices are often included in order to contribute when production is not perfectly matched to load demands, and thus enhance the overall performance of the system. Possible storage options are batteries, flywheels, energy capacitors, compressed air and pumped hydroelectric storage and so on (Soshinskaya et al., 2014). Currently, batteries are the most common technology for energy storage in microgrids.

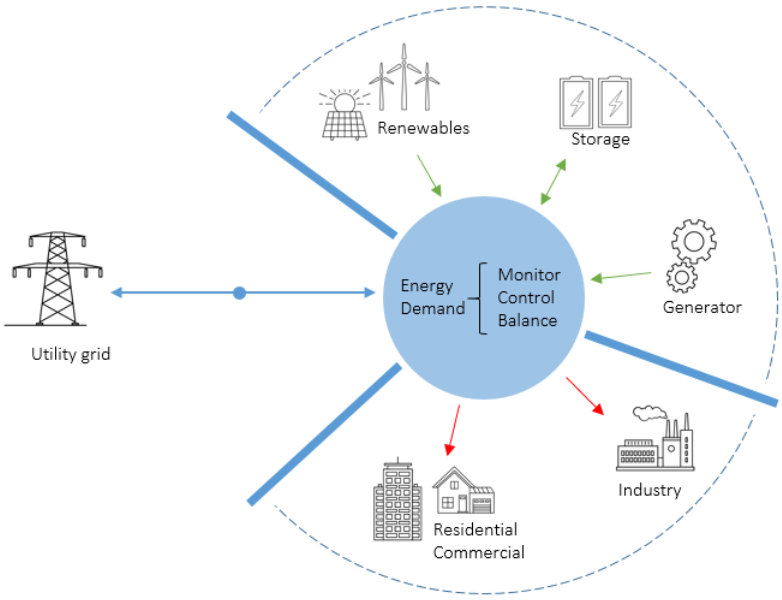

Figure 2.1: The microgrid concept

Figure 2.1 illustrates the microgrid concept, where production of energy and the covering of demand is monitored and controlled by a central management system. The figure highlights three essential features of a microgrid, being local load, local microsources and intelligent control (Schwaegerl and Tao, 2014). The microgrid in Figure 2.1 also has a connection to the utility grid. This is not always the case, and it is therefore important to distinguish between what is known as islanded or stand-alone microgrids, and grid-connected microgrids. Stand-alone microgrids are mainly interesting for remote electrically non-integrated areas, such as geographical islands (Hatziargyriou et al., 2007). Microgrids are also discussed in terms of combined heat and power (CHP), where waste heat from electricity production is used to cover parts of the heat load. Lasseter and Paigi (2004) points out that these configurations will increase the efficiency

of the systems drastically, while Schwaegerl and Tao (2014) suggests that the opportunity to locally utilize the waste heat is the key economic potential for installing thermal generation at customers premises, especially in colder climate countries.

The challenges in proper design and management when implementing DGs based on RES, are accelerating the interest in microgrid research (Sachs and Sawodny, 2016a). Control and design of grid-connected microgrids is considered a difficult task, as the system should disconnect from the main grid upon disturbances (Lasseter and Paigi, 2004). The issue of control and operation becomes even more challenging when considering several interconnected microgrids, also referred to as multi-microgrids. In this thesis, however, we study stand-alone microgrids with no possibility to connect to the main grid. Thus, the control aspect will not be further elaborated on. The possibility of heat transfer from the DGs is considered a potential perk of the installed system configuration, and not included in the modelling presented in this report. In the case of long-term islanded operation, a microgrid is subject to high requirements on storage capacity or demand side flexibility in order to provide continuous supply of all loads (Schwaegerl and Tao, 2014). This makes the access to an accurate decision making tool regarding the design of the microgrid even more important.

2.2 Trønder Energi and the Island Project

This thesis is written in collaboration with Trønder Energi, a regional Norwegian power company, more specifically the Trønder Energi New Renewables department. In order to test the model that this thesis proposes, Trønder Energi has provided case studies from their ongoing research and development (R&D) project - The Island Project - where they are studying the market potential for installation of microgrids. The motivation for the project is that microgrids could benefit society in two ways; decreased costs of energy, and a potentially higher security of supply. Currently, the project considers stand-alone microgrids on islands in the open sea outside of Trondheim. Gøril Forbord, Simen Karlsen (Powel), Gunnar Aronsen and John Kristian Evjen have provided the necessary information. Additionally, the R&D project at Trønder Energi has partnered with the institutions listed in Table 2.1.

Table 2.1: Partnering institutions - The Island Project

Institution	Area of competence
Grenland Energy	Battery technology
Powel	Optimal operation/design of microgrids
NTNU	Kjell Sand [Power Engineering]
	Asgeir Tomasgard (and us) [Industrial Economics]
CenSES	Sustainable energy research

2.2.1 The Island Project

The regional grid in Norway is well developed, and most citizens experience a reliable power supply and low loss of load probability (LOLP). The electricity grid is however aging, and there is an urgent need for a high number of reinvestments. Several islands and remote areas require disproportionally large investments to cover the load demand of very small settlements. Trønder Energi wishes to consider DG-based microgrids using RES as an alternative to reinvestments in the transmission grid.

Trønder Energi are studying three island locations in the sea outside the fjord of Trondheim; Froan, Gjessingen and Halten. Froan and Gjessingen have previous connections to the regional grid. Both are pictured in Figure 2.2, along with the subsea cables connecting the islands. Common for all cases is the need to invest in new connections in order to stay connected and ensure security of supply.

Froan

Froan is an archipelago, and the island of Sørburøy has the only permanent settlement. Sørburøy maintains approximately 30 permanent residents, and has an elementary school and a small grocery store. Sørburøy is almost split in two, and the northern part, where most permanent households are, is commonly called Nordøya. There is also activity on a third island, Sauøya, and all islands have several vacation homes. Trønder Energi are currently measuring load demand from all substations on Froan and Gjessingen. The islands are flat and rocky with good conditions for generating wind power, and an abundance of space for PV-panels. A challenge with installing wind turbines on Froan is its status as a bird sanctuary. Trønder Energi is currently studying alternative turbine technologies that are less harmful for birds than traditional turbines in order to overcome this problem.

Froan is the first archipelago to participate in a possible pilot microgrid project. According to Trønder Energi Nett, who owns the regional grid to which these islands are currently con-

nected, their connection is prone to faults as they experience a relatively higher LOLP than the national average. Reinvesting in the grid connection will amount to an investment in excess of 30 MNOK, and a microgrid could thus be a good alternative.

Figure 2.2: Map of existing subsea cables at Froan (Sørburøy, Nordøya and Sauøya) and Gjessingen

Gjessingen and Halten

Gjessingen is an island south of Froan, having only one permanent resident. It does however, as Froan, have several vacation homes and more or less the same geographical features. As seen in Figure 2.2, Gjessingen is linked to the same mainland subsea cable as Froan.

Halten has no permanent residents, but there are vacation homes, a lighthouse and a seasonal restaurant. The island has no current connections to the regional grid, and electricity is provided from a diesel aggregate.

2.2.2 Scope and limitations for Trønder Energi

The overall objective of Trønder Energi is to explore alternatives to grid investments, and ways of integrating distributed energy resources and RES. They aim to study the inclusion of a great variety of possible technologies, including bio-gas, hydrogen, wind, solar, batteries and other storage solutions. The optimal configuration could also include some limited capacity from the regional grid, as well as fuel-based generators. The main goal is a general decision making tool that can be changed and adapted to include a variety of functionality and different technologies.

If Trønder Energi invests in microgrid technology and pilot projects on Froan, Gjessingen or Halten, they are obliged to guarantee similar or better security of supply (or lower LOLP) than what they are currently experiencing. This is due to Norwegian regulations provided by the Norwegian Water Resources and Energy Directorate. According to Trønder Energi, Norwegian laws also state that in order to disconnect customers from the regional grid, the customers have to waive their right to grid connection.

Another challenge is to determine ownership of the microgrid, necessary responsibilities, pricing scheme and so on. These challenges arise as the customers of the stand-alone microgrid are not subject to the same market mechanisms and pricing mechanisms as other customers, since the owner of the microgrid will in effect become a monopolist. The customers do, however, have a right to see the same power price as the rest of the country.

As microgrids can be thought of as a kind of monopoly, regulation of microgrids is extremely important. A question arising, is whether it is possible to operate microgrids within existing frameworks, or will new regulations and regulatory institutions have to be established. These last two paragraphs are included to reveal the entire problem of implementing microgrids in an established energy system faced by Trønder Energi. In this thesis, however, we focus on the determination of optimal sizing of the system given restrictions on performance.

Chapter 3

Literature review

This chapter provides an introduction to the existing literature that is relevant to the problem studied in this thesis. The first part of the literature review gives a short introduction to the main ideas and definitions of stochastic programming, as well as a review of multi-horizon stochastic programming. This forms the basis for the model design and mathematical formulation proposed in Chapter 5. Subsequently, a comprehensive review of literature concerning the microgrid design problem is provided. The literature review is concluded with a comparison of the stochastic microgrid design problem to the capacitated lot sizing problem.

3.1 Stochastic programming

One of the first attempts of including uncertainty in linear programming (LP) problems is found in Dantzig (1955), where the recourse model with uncertain decision variables included in the objective function was introduced. In this model, it is distinguished between what decisions have to be made prior to gaining certainty, and what decisions can be delayed until more information is available. In deterministic LP-models, there is generally not a clear distinction between what is known, and what information is still uncertain when a decision is made. Applying deterministic models to problems where the future is uncertain, basing the estimates on best-guesses or expected values, might result in misleading and very inflexible solutions (Higle and Wallace, 2003).

Stochastic programming considers problems where some decisions have to be made prior to obtaining important information about future conditions (King and Wallace, 2012). A stochastic programming approach relates uncertainty and information structure to different stages in time, and allows the decision maker (DM) to distinguish between decisions that have to be made un-

der uncertainty and decisions that can be delayed until information is revealed (Higle, 2005). Wallace (2003) define uncertainty, or randomness, as lack of predictability of outcomes. When discussing decision making under uncertainty, or stochastic programming, we understand uncertainty as parameters which we do not know the realization of, but we do know the underlying probability distribution of the uncertain parameters (Wallace, 2003). The assumption of known (possibly joint) probability distribution is fundamental to stochastic programming (Higle, 2005).

3.1.1 Formulation of the stochastic program

By considering different realizations of the uncertain parameters, represented by scenarios, decisions can be made by collectively considering all possible outcomes (Higle, 2005). King and Wallace (2012) illustrates the idea by describing a two-stage recourse problem, where each stage represent a level of information. In the first stage, decisions have to be made under uncertainty, while the DM can adapt the decisions in the second stage. The ability to adapt is often referred to as "recourse", and the two-stage problem is therefore called the recourse problem (Birge and Louveaux, 2011). The distinction between stages was introduced by Dantzig (1955), who formulated the classical two-stage stochastic linear program with fixed recourse, as rendered by Birge and Louveaux (2011):

$$\min z = c^T x + E_\xi[\min q(\omega)^T y(\omega)] \tag{3.1}$$

$$s.t. \qquad Ax = b \tag{3.2}$$

$$T(\omega)x + Wy(\omega) = h(\omega) \tag{3.3}$$

$$x \geq 0, y(\omega) \geq 0 \tag{3.4}$$

where ω represents a random event, x is the first-stage decision, and $y(\omega)$ is the second stage decision. Fixed recourse refers to the parameters related to the second-stage decision variable, W, not being subject to uncertainty. Further more, stochastic programs are often described mathematically by the deterministic equivalent problem (DEP). For a two-stage program with fixed recourse, Birge and Louveaux (2011) describe the deterministic equivalent by the objective function. They explain that the deterministic equivalent has an objective containing a deterministic term based on the first-stage decision $c^T x$ and the expectation of the second-stage objective depending on all possible realizations of the random variables given the chosen first-

stage decision, $q(\omega)^T y(\omega)$. For a given realization of ω, the second-stage value function is given as

$$Q(x,\xi(\omega)) = \min_y \left\{ q(\omega)^T y | Wy = h(\omega) - T(\omega)x, y \geq 0 \right\} \tag{3.5}$$

where $\xi(\omega)$ refers to the realization of all random variables ξ given the random event ω. Birge and Louveaux (2011) then define the expected second-stage value function to be

$$\mathscr{D}(x) = E_\xi Q(x,\xi(\omega)) \tag{3.6}$$

resulting in the DEP, given as

$$\min z = c^T x + \mathscr{D}(x) \tag{3.7}$$

$$s.t. \qquad Ax = b \tag{3.8}$$

$$x \geq 0 \tag{3.9}$$

In most cases, however, it is impossible to account for all possible realizations of the random variables. Therefore, the DEP is usually solved for a set of discrete scenarios, joined in a scenario tree designed to replicate the underlying stochastic processes (King and Wallace, 2012). Higle (2005) describes a scenario tree as *"a structured distributional representation of the stochastic elements and the manner in which they may evolve over the period of time represented in the problem (Higle, 2005)"*. In a simple two-stage model, a scenario-tree consists of a first stage node, connected to the possible second stages with branches, representing the transition from the first to the second stage.

The two-stage recourse problem can be extended to the multistage case. It is however two-stage problems that are studied in this thesis, and we will therefore not discuss the possible extensions in this chapter.

3.1.2 Solution methods for stochastic programs

Assigning a value to the flexibility of delaying decisions is what distinguishes a stochastic model from a deterministic one (Higle and Wallace, 2003). However, with many stages and multiple scenarios, the stochastic problem often becomes large and difficult to solve with deterministic solution methods. Accordingly, solution methods that are designed to exploit the structure of the stochastic models could be applied (Birge and Louveaux, 2011). Several approaches and methods are discussed in the literature, with much emphasis on decomposition methods. Birge and Louveaux (2011) provides a thorough presentation of the L-shaped method, also known as an adaption of Bender's decomposition, and mention several alternative decomposition approaches based on inner linearization.

3.1.3 Multi-horizon stochastic programming

As stochastic problems often become very large and unmanageable, extensive research has been devoted to manipulating the structure of the problems in order to make them more manageable in size. Kaut et al. (2013) studies a special class of stochastic problems, often referred to as infrastructure-planning models, and introduce a restructuring of the scenario tree that shrinks the size of the problem. The approach is called multi-horizon stochastic programming, and the idea is to distinguish between two types of uncertainty; strategic and operational uncertainty. In an infrastructure-planning problem, the DM often has to make strategic investment decisions that depend on the performance of the investments under operational uncertainty. Such problems often become very large in size, as one has to branch on uncertainty on both a strategic and operational level. The multi-horizon optimization model suggest that when strategic uncertainty does not depend on operational uncertainty, and strategic decisions do not directly depend on operational decisions undertaken in the preceding operational periods, it is possible to model the operational stages directly into the strategic decision node. Kaut et al. (2013) also stresses that for the approach to be exact, there can be no actual connection between the decisions made in the operational scenarios of two separate strategic decision nodes.

The multi-horizon optimization approach is illustrated by Kaut et al. (2013) on a simple example of installing PV-panels on a house. A more complex case is studied in Hellemo et al. (2013), where a natural gas infrastructure design is modelled with operational nodes embedded in the strategic nodes. Relevant to the problem discussed in this report, Kaut et al. (2013) suggest that other areas that could benefit from multi-horizon stochastic programming is, among others, the energy planning sector and design of robust power networks that includes RES.

3.2 The microgrid design problem

The majority of the existing research and literature on sizing of components in microgrids takes a purely deterministic view. This research is therefore able to incorporate relatively accurate mathematical representations of the components and their interactions, without making the problem computationally intractable. In recent years, increased focus has been directed towards the consideration of the uncertainty in such problems, and methods for handling the complex mathematical formulations describing the components. In this chapter, we study the optimal sizing of components in microgrids by providing a brief introduction to the different formulations and focus that researchers have adopted in their work on the topic. This is followed by a more detailed description of the modelling of specific components relevant to this thesis, and a comparison between the strategic microgrid design problem and the classical capacitated lot sizing problem.

3.2.1 Optimal sizing of components in microgrids

The first relevant literature addressing the component sizing problem is found in Lee and Chen (1995), who developed a battery energy storage sizing algorithm utilizing advanced multi-pass dynamic programming. According to Gao (2015), the most common algorithms used in solving the deterministic component sizing problem today, are particle swarm optimization (PSO), Genetic Algorithm (GA), common LP, and Dynamic Programming (DP). A comprehensive and informative review of research on the microgrid design problem, often referred to as hybrid energy system design, can be found in Chauhan and Saini (2014). Furthermore, a review on simulation optimization for stand-alone hybrid renewable energy systems can be found in Bernal-Agustín and Dufo-López (2009).

As the optimal component sizing problem in its essence is a multi-objective optimization problem (MOP), the literature studies several different combinations of objectives, and proposes a variety of approaches to account for difficulties in determining optimal solutions. Common objectives considered are cost, reliability, emissions or a combination of the aforementioned. Arabali et al. (2014) even considers social acceptance as an objective of the optimization. In most cases, though, the optimal microgrid design problem considers a trade off between cost, defined in various ways (LCOE, Life Cycle Cost (LCC), Total System Cost (TSC), Total Investment Cost (TIC), Annualized system cost (ASC), Capex, Net Present Cost (NPC)), and reliability, defined in various ways (Loss of Power Supply Probability (LPSP)/LOLP, Energy Index of Reliability (EIR)). Sachs and Sawodny (2016a), Katsigiannis et al. (2010), Wang and

Singh (2009) and Arabali et al. (2014) are all examples of problem formulations with multiple objectives, where an a posteriori approach is chosen. They use either the weighting method or the ε-constraint method, resulting in a Pareto-front of non-dominated solutions with different trade offs between the objectives.

Much of the relevant literature mentioned in Chauhan and Saini (2014) considers either rule based approaches for the energy management part of the optimization, or they include linear approximations of the nonlinear component models. Others, such as Sachs and Sawodny (2016a), stress the fact that in order to achieve realistic results, the system should be modelled explicitly, as simplifications could lead to high power losses when operating the system according to plan. Sachs and Sawodny (2016a) propose a deterministic multi-objective mixed integer nonlinear optimization problem (MINLP), that places great emphasis on exact modelling of components, batteries and power electronic (PoE) layout in particular. The problem is solved in different layers using a variety of heuristics combined with simulation. There is no actual optimization related to the choice of components, but the performance of a given configuration is evaluated and then reconsidered in an iterative procedure.

The presence of multiple objectives, non-linearity in component modeling and mixed integer programming formulations result in problems that are difficult to solve with exact optimization techniques, even when not considering the stochastic behaviour of different parameters such as weather data and load demand. In several articles, including Askarzadeh and dos Santos Coelho (2015), Upadhyay and Sharma (2015), Hassan et al. (2015) and Sharafi and ElMekkawy (2014), PSO meta-heuristics are utilized to solve the nonlinear and complex optimization problems. The combination of PSO and simulation allows for accurate modelling and evaluation of different solutions to the optimization problem. Upadhyay and Sharma (2015) evaluate the performance of several solution methods, including PSO, GA and the simple deterministic microgrid design software HOMER. GA's are also found in Fossati et al. (2015) and Sachs and Sawodny (2016a). Other solution methods and heuristics applied to solve the deterministic MINLP version of the microgrid design problem, or parts of it, include artificial bee colony algorithm (Singh and Kaushik, 2016), simulated annealing (Ekren and Ekren, 2010), simulated annealing in combination with tabu search (Katsigiannis et al., 2012), improved bat algorithm (Bahmani-Firouzi and Azizipanah-Abarghooee, 2014) and adaptive neuron fuzzy algorithm (Jeyaprabha and Selvakumar, 2015).

Of the limited literature that incorporates some degree of uncertainty in their approach to optimal component sizing, Kuznia et al. (2013) is the most noteworthy. In contrast to the purely deterministic models, a high emphasis is here placed on formulating linear models and convex solution spaces. However, there are various ways to model and account for uncertainty in the problem, and stochastic programming, presented earlier in this chapter, is merely one of them.

Tina et al. (2006) studies a solar-wind system as both stand-alone and grid-connected, and present a probabilistic approach based on the convolution technique to incorporate the fluctuating nature of the input data relating to resources and load. Nogueira et al. (2014) provides a methodology for component sizing and simulation of a stand-alone PV-wind-battery microgrid, and use a statistical model based on a Beta and Weibull probability density function to account for the uncertainty in power produced by solar and wind in a simulation based LP. Kishore and Fernandez (2011) argue that for reliability studies relating to PV-wind power systems, analytical methods do not properly represent its random nature and component failures. Therefore, they provide a reliability analysis approach called 'well-being analysis', that is based on a combination of probabilistic and deterministic methods using Monte Carlo Simulations (MCS). Paliwal et al. (2014) argue that MCS are too computationally burdensome, and therefore develop a novel probabilistic battery state model to be used in an analytical technique for microgrids with intermittent RES. In Arabali et al. (2014), the authors present a sophisticated reliability model, based on a method developed by Wang and Singh (2009). The work in Arabali et al. (2014) is some of the first published research that includes a possibility to perform load shifting.

Some stochastic programming models have been applied to model the microgrid design problem, although most have focused only on optimal storage capacity. This is most likely due to the limitation of commercial solvers to efficiently deal with the complexity of stochastic mixed integer program (MIP) models for the microgrid design problem (Kuznia et al., 2013). Abbey and Joos (2009) employ a stochastic optimization approach to the rating of energy storage systems, while Brown et al. (2008) models the uncertainty of renewables in optimization of pumped storage capacity. Niknam et al. (2012) proposes a stochastic programming model for optimal energy management in a grid connected microgrid studying a 24h horizon. They consider uncertainties related to forecasted values of load demand, output power of wind and PV units, as well as market price.

The first, and to the authors knowledge only, publication on stochastic programming optimization for the microgrid design problem with RES is found in Kuznia et al. (2013). They present a stochastic MIP model including RES, represented by wind power, as well as energy storage units, thermal units and a transmission network. They develop a customized solution algorithm based on a Benders' decomposition with two additional types of cutting planes; Pareto-optimal cuts generated using a modified Magnanti-Wong method (Magnanti and Wong, 1981), and cuts generated from a maximum feasible subsystem. The algorithm outperformed a commercial solver consistently for all problem sizes tested. Kuznia et al. (2013) use a simple model for generators, in order to potentially limit the complexity of the problem. The modelling of the energy storage unit resembles traditional warehouse modelling, where the only differences from classical inventory problems are efficiency losses. They include no slack in energy balance, saying that all demand should be met, and therefore gives no measure of reliability. Further-

more, they consider a planning horizon of only one year. Suggested further research includes expanding the model to consider multiple renewable resources simultaneously and allowing construction at different times in the planning horizon (i.e. reinvestment).

A selection of the aforementioned literature representing the wide focus in research on component sizing in microgrids is included in Table 3.1.

Table 3.1: Article overview: Selected articles adressing the microgrid design problem

Authors	**Det/Stoc**	**Components**	**Objective**	**Solution Method**
Arabali et al. (2014)	Stoc	PV/Wind/Bat	Min Cost (CapEx+O&M)	PS + GA
Sachs and Sawodny (2016a)	Det	PV/Bat/Diesel	Min LCOE, Capex, Emissions	MINLP, NSGA-II
Kuznia et al. (2013)	Stoc	Wind/Bat/Grid/ Thermal	Min CapEx+O&M	SMIP, Benders++
Paliwal et al. (2014)	Stoc	PV/Wind/Bat/Diesel	Min Lifetime cost	PSO
Katsigiannis et al. (2010)	Det	PV/Wind/Biodiesel/ Hydrogen	Min LCOE & Emissions	GA
Askarzadeh and dos Santos Coelho (2015)	Det	PV/Wind/Bat	Min LCC	PSO
Sharafi and ElMekkawy (2014)	Det	PV/Wind/Bat/ Diesel/Hydrogen	Min total cost, emissions, LOLP	PSO
Niknam et al. (2012)	Stoc	PV/Wind/Bat	Min total cost, emissions	TLBO Simulation

To the best of our knowledge, there exists no literature considering the combination of taking into account a high degree of uncertainty in operational input parameters and long strategic horizons, including lifetime considerations for batteries, and the opportunity to reinvest at a later point in the planning horizon.

3.2.2 Component modelling

Models for optimal sizing of energy storage and power generation units in microgrids should ideally be able to evaluate the transient performance of the components considered. This requires complex mathematical representations of the components. Furthermore, the performance of technical components is highly dependent on non-linear relationships with operational parameters such as weather and load (Sachs and Sawodny, 2016a). Such complex modelling of components leads to non-linear and non-convex models that are challenging to solve. Thus, for a mathematical model to provide insights reflecting an acceptable level of the actual physical properties and behavior of each component, the chosen level of detail in the mathematical modelling requires careful consideration. This section provides a literature review of the mathematical modelling of the components relevant for this thesis.

Photovoltaic panels

Yang et al. (2008) applies a comprehensive model of the PV-system and the battery unit in an optimal component sizing algorithm. The PV-system is modeled in three parts, being PV-array power model, solar radiation on PV-module surface, and PV-module temperature model. The optimal slope angle of the PV-modules is also considered in the optimization procedure. The PV-module temperature model considers the thermal energy exchange of the module with its environment through the main heat transfer paths; convection and radiation heat transfer from the front and the back. The complexity in the PV-system modelling results in a relatively accurate representation of the component, but also a non-linear model. A similar level of detail in a strategic optimization model would quickly become intractable with today's computation technology.

Sachs and Sawodny (2016a) presents a less detailed, but still relatively accurate, modelling of PV-panels resulting in non-linear constraints for the optimization model. The PV-model considers mounting and orientation of the panels, as well as irradiance data when determining DC output of the PV-units.

The above mentioned articles have a strong focus on PV-panel modelling and exact modelling of components in general. Other articles, however, with a broader focus on the energy balance in a system, employ far simpler models of power production from PV-panels. One such formulation is found in Dragičević et al. (2014), determining power production based on parameters such as surface area, irradiation, and efficiency measures. This simple modelling allows for more complex solution spaces, and it can be argued that such a model is sufficient for operational evaluation in a strategic design problem.

When considering long-term planning horizons, it is interesting to discuss the lifetime and degradation of components. A thorough analytical review on PV-panel degradation rates is presented by Jordan and Kurtz (2013). It presents results showing that the median value for performance degradation in PV-panels is about 0.5% per year. This is assumed to be sufficiently low to be neglected in a strategic microgrid design process.

Batteries

The mathematical modelling of battery performance ranges from simple inventory formulations to highly complex theoretical and empirical models (Xu et al., 2016). The more complex models try to overcome the most challenging obstacle when modelling the battery; the non-linear degradation over time.

Diminishing storage capacity in battery units occurs mainly due to the effect cyclic charging and discharging has on the electrochemical material in the battery. Each cycle can be said to be responsible for a marginal loss in battery life. Since batteries are rarely operated on a regular full-cycle basis, a highly accurate model would need to quantify the amount of equivalent full state of charge (SOC) cycles that the battery experiences under arbitrary charging behavior. A rainflow cycle-counting algorithm (Downing and Socie, 1982) has been successfully and widely applied for this purpose.

Dragičević et al. (2014) presents a deterministic robust MIP formulation for the microgrid design problem, focusing on the modelling of the battery degradation in lead-acid and Li-ion batteries. A rainflow cycle-counting algorithm is applied to count cycles. The proposed model is solved using CPLEX software with promising results in terms of computational burden.

Bordin et al. (2017) also focuses on inclusion of the battery degradation processes, but in linear programming models for optimal management of off-grid systems. They suggest a method for addressing how different operational patterns of an off-grid power system impacts the battery degradation costs. This is done by developing a methodology to include the battery degradation processes in the optimization model, through the definition of battery degradation costs which incur as the battery is being used. In order to do this, they consider total energy throughput as a measure for the lifetime of the battery, and use the maximum amount of full cycles to calculate the maximum allowed energy throughput. A detailed and complex Kinetic Battery Model, as described in Manwell and McGowan (1993), is used to describe the performance of the battery. The battery technology that forms the basis of the analysis in Bordin et al. (2017) is lead acid batteries. For lead acid batteries, partial cycles is regarded as negative, and limiting the number of partial cycles becomes an objective. However, when looking at Li-ion batteries other effects may be more prominent. de Vries et al. (2015) identify two effects that extends cycle life in Li-ion batteries. They find that cycle life of Li-ion cells can be increased inversely proportional to depth of discharge and that cycle life can be increased by charging from a lower state of charge.

Another method developed specifically for application in microgrids, or hybrid energy systems, can be found in Scioletti et al. (2016). A thorough explanation of why neglecting the rate-capacity effect, which is often the case in similar problem formulations, can lead to overestimation of battery capacity is presented. Next, they provide a detailed physics-based integer-linear model in order to account for as much of the non-linear, non-convex effects that the battery introduces as possible. A drawback is that the linear formulation still includes a bilinear term, that is suggested handled by the approach given in McCormick (1976).

Sachs and Sawodny (2016a) uses a model of the battery units that considers nominal voltage and SOC, and the battery discharge is modelled using the basic Shepherd equation explained in Shepherd (1965). In describing the behaviour of the battery and determining SOC in each time period, Sachs and Sawodny (2016a) employ a variety of nonlinear and differential equations in addition to the basic Shepherd equation resulting in a complex, but rather exact modelling of the batteries. These non-linearities are, as mentioned previously, handled by solving the problem using a GA.

Several microgrid design problems place little emphasis on the exact modelling of batteries, and simply give a set maximum lifetime, independent of operation. However, some articles, like Yang et al. (2007), use a method that incorporates two variables called battery float life and battery cycle life. Battery float life is a maximum calendar lifetime, and battery cycle life is related to the actual operation of the battery. Whichever reaches its defined maximum first defines the maximum lifetime of the battery. Zhao et al. (2013) employs another quite simple approach, well suited for linear problems, presenting a simple warehouse modelling of the battery units. They add a lifetime cost in the objective function to account for lifetime considerations based on Ampere-hour (Ah) throughput, adjusted for varying effect on lifetime degradation dependent on current SOC when throughput occurs.

Diesel Generators

One of the major challenges in mathematical modelling of diesel generators is related to the non-linear relationship between power output and fuel consumption. This non-linear relationship is caused by startup effects and the efficiency of the generator. Another challenge is related to minimum load requirements.

A common way of dealing with fixed operating costs in diesel generators is by defining a binary variable representing the operation state (on/off) and a continuous variable representing output power per generator. This approach is utilized in e.g. Sachs and Sawodny (2016a), Sharafi and ElMekkawy (2014) and Kuznia et al. (2013). The use of binary variables allows the mathematical program to account for start-up effects, and minimum production constraints, while retaining linear properties. Sachs and Sawodny (2016a) also define a minimum off time where the diesel generator is not available for use.

Another approach to modelling non-linear relationships is to use special ordered sets, as discussed in Williams (1993), creating piece-wise linear curves and defining an ordered variable that represents weights for each of the corner points. This approach is not dependent on explicit binary variables, but relies on rules related to what variables are allowed to take on a value in

order to reach all points on the curve. Although the formulation is continuous, the ordered sets hold some integer properties complicating the solution process.

Abbey and Joos (2009) and Vrettos and Papathanassiou (2011) focus on a more thorough modelling of diesel generators. They define three distinct operating strategies that lead to three different formulations for the optimization problem. Other articles, however, simply define a fixed efficiency and marginal cost, and allow the size of the diesel generator to be a function of maximum load demand in the system (Jeyaprabha and Selvakumar, 2015; Kolhe et al., 2002). Another approach is to simply assume a linear function relating fuel consumption to power production (Katsigiannis et al., 2010).

Most of the above mentioned approaches rely on the use of binary or integer variables, or ordered sets, often leading to rapidly increasing computation time. In Doorman (2016), an alternative non-integer generator formulation used in the Norwegian EFI's Multi-area Power-market simulator (EMPS) model is presented. In this formulation, continuous variables between 0 and 1 are used to relate start-up costs and operational costs to the energy produced by thermal generation units. The method relies on linear representations of the generator, and is mostly relevant for larger generation plants and strategic planning horizons.

Wind Turbines

Wind turbines convert the kinetic energy from wind into electrical energy. There are no direct marginal cost related to the conversion of energy, such as the cost of fuel for a diesel generator, but there are other marginal costs related to the production of wind power. These marginal costs are commonly grouped under the term Operation and Maintenance (O&M) costs. Blanco (2009) found that marginal O&M costs for a European wind turbine are estimated to be between 1 to 2 Eurocents per kWh produced wind power. This coincides with recent official numbers reported by the International Renewable Energy Agency (IRENA) (IRENA, 2016).

A typical wind turbine power output characteristic can be approximated by a linear function of wind speed between cut-in wind speed and rated wind speed, and stays constant at the rated power output when wind speed is above rated wind speed and below cut-off wind speed. This approach is widely adopted in literature, among others it is used in Tina et al. (2006), Arabali et al. (2014), Yang et al. (2007), and Zhao et al. (2013)

Others approximate the wind turbine power output between cut-in and rated wind speed as a quadratic or cubic function of wind speed. An example of literature using a quadratic equation to model this relationship can be found in Nogueira et al. (2014). There are also many examples

of literature using a cubic equation, some of these are Alsayed et al. (2014), Askarzadeh and dos Santos Coelho (2015), Sharafi and ElMekkawy (2014), and Chauhan and Saini (2014).

Stability in Microgrids

When introducing a high share of intermittent renewables such as wind and photovoltaics to a microgrid, or any energy system at all, requirements for spinning reserves are often imposed by relevant authorities. Spinning reserves, often referred to as regulation reserves, normally consist of conventional power sources, such as coal fired plants, fuel based generators, and reservoir based hydro power. They should be able to respond within seconds or minutes, which is why they have the name "spinning" (Papavasiliou et al., 2011). A spinning reserve requirement allows the system operator to compensate for unpredictable imbalances between load and generation capacity due to the intermittent behaviour of the renewable energy sources (Ortega-Vazquez and Kirschen, 2009). Estimating the necessary size of the spinning reserve that a system operator should provide in order to respond to generation outages, frequency drops and forecast errors, becomes increasingly difficult with higher renewable energy penetration in the system (Ortega-Vazquez and Kirschen, 2009).

Microgrids are also subject to spinning reserve requirements, and operational modelling of microgrids for that reason often account for these requirements. Spinning reserve requirements are included in several models that have an operational focus, such as those found in Chen et al. (2011) and Sachs and Sawodny (2016b). Some strategic formulation also consider spinning reserves, and we find examples of that in Scioletti et al. (2016) and Niknam et al. (2012). These are however rather the exception than the rule, and most of the approaches to the strategic microgrid design problem discussed in this thesis do not explicitly consider spinning reserve requirements.

3.2.3 A comparison to the capacitated lot sizing problem

Kuznia et al. (2013) provides a simplified model description for stochastic optimization of a microgrid configuration. In this model description, they state that the operational part of the strategic microgrid design problem can in simple terms be described as a flow problem, where power production from different sources flow to a load - either directly or via a battery unit. Available power sources in the system is defined by the strategic design part of the problem, and there are corresponding capacity limits on both production, flows, and storage in the battery

unit. Based on this, Kuznia et al. (2013) suggests that their problem has a strong connection to the classical capacitated lot sizing problem.

The capacitated lot sizing problem is a classical optimization problem, known for being $\mathscr{NP}$-hard and therefore difficult to solve. There exists a variety of lot sizing problems, and the classical capacitated lot sizing problem (CLSP) is just one of many specific variants (Karimi et al., 2003). It is characterized as a single level production planning problem with finite planning horizon and known dynamic demand. Production in each period is constrained by capacity limits, and there are costs related to production, inventory and setup.

Kuznia et al. (2013) prove that their strategic microgrid design problem, based on the role of the storage device in the system and the system flow balance dynamics, in its general form has the structure of the CLSP. The problem they describe can thus be proven to be $\mathscr{NP}$-hard.

In the review of different formulations of the strategic microgrid design problem, several solution methods were briefly mentioned. Among them were a variety of simulation techniques, optimization simulation, different heuristics, teaching-learning-based optimization, and combinations of the aforementioned. Common for most of the research on optimal microgrid design, is that by introducing complexity to or increasing the dimensions of the problem in one form or another, obtaining exact solutions prove to become difficult.

Being able to compare and relate the strategic microgrid design problem to known optimization problems is valuable in determining how to evaluate, define and design solution algorithms for the problem. Karimi et al. (2003) suggests that solution methods for the CLSP can be categorized into exact methods consisting mostly cutting plane algorithms, specialized heuristics and mathematical programming based heuristics. Accordingly, Kuznia et al. (2013) exploit the structure of their problem and develop a Bender's decomposition method with additional types of cutting planes, in combination with heuristic strategies for improving the performance of the algorithm.

Chapter 4

Problem description

In this chapter we provide a description of the MISSMDP, presenting details regarding the considerations that should be modelled. The problem statement is based on our work in Arnesen and Borgen (2016), and many of the considerations will therefore bear resemblance to what is found in that report.

4.1 Problem statement

The objective of the MISSMDP is to find the optimal combination of the components in a simple grid configuration, while minimizing the costs over the lifetime of the system (Total lifetime Costs (TLC)). Costs are associated with initial investment cost of components (CapEx), re-investments and (O&M) costs . There is also a high cost associated with not covering load. The microgrid is designed to provide sufficient coverage of demand over the lifetime of the system, while the performance of the components over time are restricted by their physical constraints.

This thesis focuses on a system comprised of PV-solar panel(s), wind turbine(s), a backup generator and a battery energy storage unit. There is operational uncertainty related to irradiance, wind speed and load demand. The problem is therefore split into stages. The first stage decisions represent the specific PV-panels, wind turbines, generators, and energy storage units that are invested in. After the first stage, several recourse decisions are possible. These are related to reinvestment in battery unit and the actual operation of the microgrid. The decisions are evaluated based on the operational performance of the system, balancing production, storage and load. The desired output of the model are the first-stage decision variables, which will serve as decision support for DMs in the strategic planning phase of designing a microgrid.

Figure 4.1 illustrates the possible flows of energy in the system. There are capacity constraints on production, battery storage, as well as flows to and from the battery. A lifetime of several decades is expected for the system.

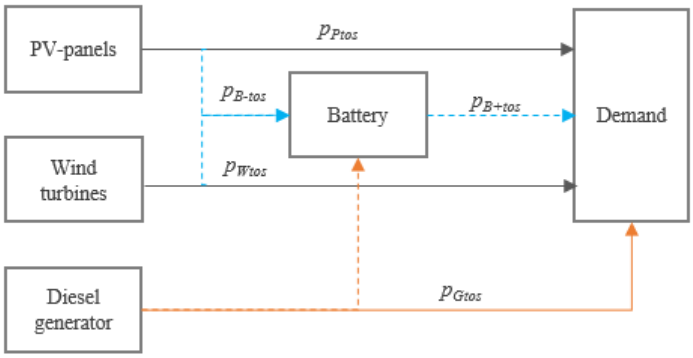

Figure 4.1: Schematic energy flow for the strategic microgrid design problem

The power produced by the PV-panels depends on the type and amount of panels invested in, in the first stage, as well as the uncertain weather data given as input. The same is true for wind. Wind power production is also limited by maximum and minimum wind speeds for the different turbines. A possibility to invest in fuel-based generators is included in order to increase the reliability of the system. When included, a fuel-based generator acts as a backup power supply and is defined by high operating costs and high flexibility. The generator also has a maximum and minimum capacity and is characterized by a fuel consumption that is dependent on power production.

Battery units introduce time dependency to the problem, because the battery SOC at any given time is dependent on the SOC in the previous time steps. The rated energy and power capacity defines boundaries on the operation of the chosen battery. The SOC is updated in every operating period, based on the SOC in the previous operating period and energy charged or discharged to/from the battery in the current period. The battery unit has a lifetime defined by a maximum number of cycles. A cycle is a full charging and discharging of the battery unit. The lifetime of the battery unit is therefore highly dependent on how it is operated, and when the battery lifetime is depleted, a reinvestment in a new battery is necessary.

Finally, our industry partner (Trønder Energi) would like to limit the use of non-renewable energy sources. The problem therefore includes the possibility to enforce a renewable energy fraction, ensuring that the proportion of energy provided by RES is equal to a predefined percentage of total load demand.

Chapter 5

Mathematical model

This chapter presents the mathematical model developed for the MISSMDP defined in Chapter 4. The first part of the chapter explains our assumptions in the proposed formulation together with their implications and significance. After this, a discussion on our choices and considerations for the information structure and model design is given. Next, a brief introduction to the notation of the mathematical model is provided, before we present and explain the base model formulation in detail. The next part of this chapter introduces an alternative diesel generator formulation and extensions to the model. Finally, the Big-M formulations are strengthened, and the chapter is concluded with a discussion of challenges regarding solution procedure.

Throughout this chapter, we often refer to a version of the mathematical program called *the base model*. This is the model described in Arnesen and Borgen (2016), which is a variety of the MISSMDP considering, PV-panels, batteries and diesel generators. The final and full mathematical model provided in Appendix B is the base model including all reformulations and extensions suggested in this chapter.

Additionally, we use the term "component specific" in our explanations and discussions. As explained in the problem statement in Chapter 4, the objective of the MISSMDP is to determine optimal combination of components, resulting in component specific considerations in the model design.

5.1 Assumptions and simplifications

There are eight main assumptions of the problem, all listed in Table 5.1. The first assumption is that partial load shedding is possible in the microgrid. This assumption makes it possible to model the energy balance as an equality constraint without making the problem prone to infeasibility. If the microgrid in any given operational period has insufficient power production or energy stored to supply the full load, the system will either experience a fault (such as frequency drops and eventually complete blackouts) or it will have to shed the excess load demand. Control systems are assumed to be in place allowing partial load shedding, while still providing power to the remaining load.

Assumption number two concerns the maximum charging and discharging power of the battery unit. It is assumed, in collaboration with Trønder Energi, that the maximum charge and discharge power of the battery unit is set equal to the maximum load demand recorded from historic measurements with a time resolution of one minute in the area of the potential microgrid. In the event of a coincidence between peak power demand and zero power production during the course of an operating period, this assumption ensures that given a sufficient level of energy stored in the battery, there is still power capacity available to prevent faults in the system. The inclusion of this assumption accounts for the stability of the system.

Assumption number three concerns the direct operational marginal costs of producing electricity from PV-panels. There are no direct costs associated with utilizing sun as a source of energy, and the costs related to the production of electricity from PV-panels are thus limited to maintenance costs. As PV-panels are virtually maintenance free, these costs are negligible.

Assumption number four is also related to costs, more specifically the costs of buying equipment and fuel. In the current formulation, these costs are assumed to be constant throughout the planning horizon. With a planning horizon of up to several decades, providing meaningful estimates of future costs is a complicated task, and fully including this uncertainty could drastically increase the complexity of the model. In the scope of this thesis, it was deemed necessary to make the assumption of constant equipment and fuel costs throughout the planning horizon for the simplification of the model.

In order to resemble a realistic decision, the optimization model only allows investment in one battery unit and one generator. This is the fifth main assumption. Battery units come in different sizes, price ranges, and with different specifications. According to our industry partner, Trønder Energi, a DM would choose a single battery unit capable of performing to his or hers preferences. Similarly, a DM would choose to invest in one generator with sufficient

capacity, rather than several smaller ones. Assumption number five is not relevant for PV-panels and wind turbines, as a DM may choose to buy several different types, as well as more than one unit of each type.

As mentioned in Chapter 4.1, the possibility to re-invest in the battery unit should be incorporated in the model. However, a simplification is introduced in the sixth assumption, stating that reinvestments are only available for the initially chosen battery unit. This assumption is added for ease of modelling.

Assumption number seven only applies to the base model formulated in Chapter 5.4, and is related to the performance of the battery. It is assumed that there is no gradual degradation of the battery capacity during its lifetime. Accordingly, battery capacity is constant, and power capacity of the battery is likely to be overestimated towards the end of its lifetime. Although neglected in this problem statement, the modelling of degradation of the battery capacity is a possible extension to the model.

The final major assumption of the problem is related to the fuel consumption of the diesel generator. Fuel consumption is dependent on the power production, and the relationship is not necessarily linear due to start up and shut down effects. In order to decrease the number of binary variables introduced in the mathematical formulation, as well as to ensure a linear and convex problem, the relationship between power production and fuel consumption is assumed linear for the diesel generators.

Table 5.1: Main assumptions of the problem

Assumption	**Description**
Assumption 1	Partial load shedding is possible
Assumption 2	Maximum (dis)charging power of the battery unit is equal to maximum load
Assumption 3	No direct costs of producing electricity from PV-panels
Assumption 4	Constant costs for equipment and fuel in the future
Assumption 5	Only one battery unit and one generator can be invested in
Assumption 6	Re-investments are only available for the initially chosen battery unit
Assumption 7	No degradation of the battery energy storage capacity
Assumption 8	Linear relationship between power produced and fuel consumed for the generator

5.2 Information structure

The model we present is a stochastic optimization model considering the lifetime of a stand-alone microgrid, in order to evaluate optimal component sizing in an initial investment decision. There are continuous, integer and binary decision variables incorporated in the model. The MISSMDP is modelled as a stochastic program, due to operational uncertainty in load demand, wind speeds and irradiance. When we use the term operating conditions, we refer to the combination of load demand, wind speed, and irradiance. The length of an operational period is defined as input to the model and can be adjusted to fit the purpose of the user. A one hour resolution is chosen for the explanation of the model design.

In designing a stochastic optimization model, the definition of the information structure is crucial. At the beginning of the planning horizon, decisions have to be made regarding investment in components for the microgrid. These are the first-stage decisions, and they will have an impact on all consecutive decisions during the lifetime of the system. At this point in time, the future operating conditions are uncertain. To avoid an excessive number of branches, and to simplify the stochastic program, we introduce an important assumption relating to the structure of the mathematical program: Assumption number 9 states that operating conditions for all operational periods (operational decision nodes) within an operational horizon are revealed at the beginning of each operational horizon.

Once the discrete operating conditions are revealed, decisions on how to utilize the available system design in order to cover demand are made for every operational period. The operational decisions are the recourse decisions of the problem, constrained by the first stage variables. The operational horizon is one year, and at the beginning of the next year a new branching on operating conditions takes place. In every strategic decision node, it is possible to reinvest and replace the battery unit. The described decision process is repeated for the defined lifetime of the system, with strategic investment decisions made at the beginning of each year, followed by operational decisions for a set of operational scenarios within the given strategic period (year). This results in a multi-stage scenario tree, containing both hourly and yearly decisions.

The information structure described in the above paragraph is illustrated in the scenario tree in Figure 5.1. The grey nodes represent strategic decisions. The strategic horizon of the problem is the entire lifetime of the system. The white nodes represent operational decisions. The figure illustrates an example with the first three strategic periods of the planning horizon shown explicitly. From each strategic decision node, there are two branches representing two operational scenarios. Within each operational scenario, the first three periods are included, while the remaining periods are represented by the dotted line reaching the next strategic decision

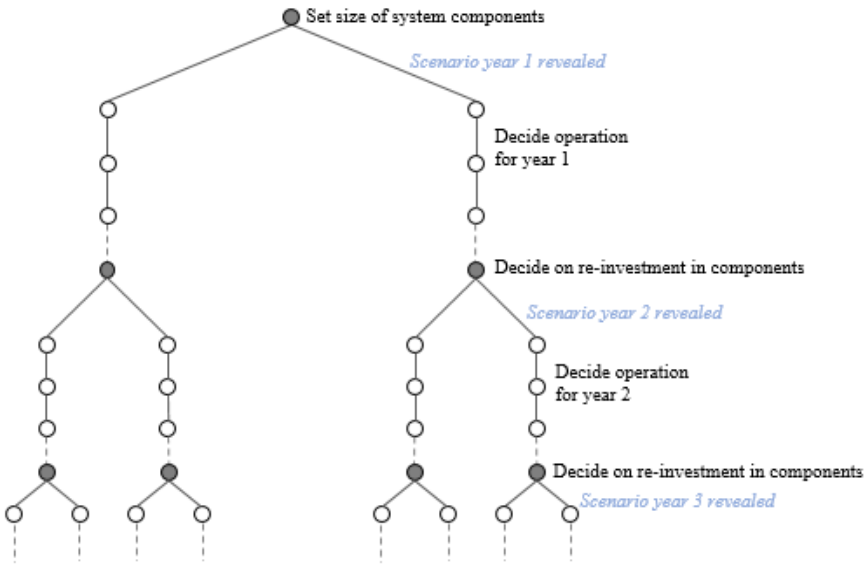

Figure 5.1: Complete information structure for the multi-stage optimization problem

node. The text on the right hand side of the figure describes when uncertainty is revealed and what decisions are made in each node. The different scenarios are illustrated by the solid line between strategic nodes and each branch of operational nodes.

Figure 5.1 shows only two branches, while in reality the number of branches would be much higher. Given b branches, and supposing the number of branches is equal for all n strategic periods in the defined lifetime of the system, the information structure will consist of b^n scenarios. Additionally, if each strategic period contains t operational nodes, every scenario will consist of $(t \times n)$ operational decisions to be made with respect to all components included in the system. Considering a situation with b = 10 and n = 30, the number of scenarios amounts to 10^{30}. Consequently, the information structure in Figure 5.1 leads to fast growing scenario trees when studying longer strategic horizons with several operational scenarios.

The MISSMDP bears resemblance to the infrastructure-planning models discussed in Kaut et al. (2013). For information structures consisting of decisions with different time horizons, they suggest a multi-horizon formulation as an alternative mathematical model design. In a multi-horizon information structure, the strategic time horizon is separated from the operational time horizon, as shown in Figure 5.2. The figure shows a scenario tree consisting of strategic nodes with an embedded operational profile. The strategic decisions depend on the overall operational performance, and it is considered sufficient to branch between the strategic stages in the strategic model. This approach allows the model to use operational decisions to evaluate the strategic decisions without excessive branching. There are however two conditions that have to be satisfied for the multi-horizon formulation to be exact.

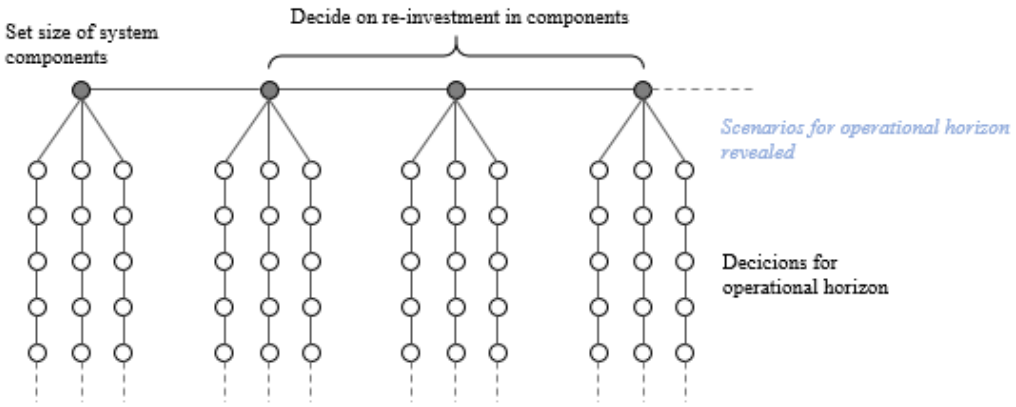

Figure 5.2: Multi-horizon information structure for the MISSMPD.

First of all, the strategic uncertainty must be independent of the operational uncertainty. Operational uncertainty can on the other hand be dependent on the strategic uncertainty. When only considering uncertainty in operating conditions, the uncertainty is isolated to the operational level alone and the first condition for exact multi-horizon model formulation is satisfied. The second condition states that there cannot be interdependency between the operational scenarios of different strategic nodes. This condition is not entirely met, as the decisions made in the operational scenarios will affect the lifetime and performance of storage devices in the following strategic nodes. However, the interdependency in our problem can be sufficiently taken into account by only considering the expected value of the interdependent variable from each operational horizon, making an indirect link instead of a direct link (Assumption 11). Another issue is that the storage devices may have a SOC higher than zero at the end of an operational horizon. If considering sufficiently long operational scenarios, it is a valid simplification to disregard this connectivity between operational horizons and start the SOC at zero for all operational scenarios (Assumption 10). This means that the first condition is fully met, while the second condition leads to some simplifications in the operational model. The multi-horizon formulation is therefore not an exact reformulation of the original scenario tree in Figure 5.1. The simplifications are however expected to be of little consequence to the final optimal first stage solution.

Using a multi-horizon information structure with uncertainty on the operational level, reduces the amount of scenarios from b^n to bn, which is a significant reduction. Figure 5.2 illustrates a multi-horizon information structure for the MISSMDP with $b = 3$ branches in the operational horizon, and no strategic uncertainty. Without the strategic uncertainty, the multi-horizon information structure has similar properties to that of a regular two-stage stochastic model.

As a result of the above discussion, we have chosen to use a multi-horizon information structure when modelling the MISSMDP. Three assumptions should be added to Table 5.1 from Chapter 5.1. These are assumption 9, 10 and 11, and all eleven assumptions are summarized in Table 5.2 below.

Table 5.2: Main assumptions of the problem (extended)

Assumption	Description
Assumption 1	Partial load shedding is possible
Assumption 2	Maximum (dis)charging power of the battery unit is equal to maximum load
Assumption 3	No direct costs of producing electricity from PV-panels
Assumption 4	Constant costs for equipment and fuel in the future
Assumption 5	Only one battery unit and one generator can be invested in
Assumption 6	Re-investments are only available for the initially chosen battery unit
Assumption 7	No degradation of battery energy storage capacity
Assumption 8	Linear relationship between power production and fuel consumption for generator
Assumption 9	Operating conditions are known prior to each operating period
Assumption 10	Battery SOC is zero at the beginning of each operating horizon
Assumption 11	Total number of used battery cycles can be calculated as an expected value

5.3 Modelling Choices

In this section, we discuss considerations and choices we have made when designing the mathematical representation of technical components in the microgrid. As explained in Chapter 4, the problem description is based on the work found in Arnesen and Borgen (2016), and we will therefore place emphasis on adjustments and changes made to the formulation proposed in that report.

5.3.1 Generator formulation

In Arnesen and Borgen (2016), a binary generator formulation based on the approach in Sharafi and ElMekkawy (2014) and Kuznia et al. (2013) was used in the mathematical model. The binary variable in the formulation takes the value 1 if a generator is running, otherwise 0, allowing for an appropriate linear approximation of the fuel consumption. The same binary variable can be used to apply minimum limits on ramping of the generator, and other specifications.

Upon inspection of the branch and bound tree obtained when solving the model in Arnesen and Borgen (2016), we found that a lot of computation time was spent branching on the generator binary variable. In an effort to decrease computation time, we have chosen to study and consider other ways to model the generator.

An alternative to the binary formulation, attempting to replicate the characteristics and properties of the binary start/stop variable, is the non-integer formulation suggested in Doorman (2016). When tested on our strategic model, however, we found weaknesses in the relationship between the continuous (0-1)-variables and the component specific decision variables deciding which generator to invest in. As there is a cost related to consumption of fuel, it is invested in an unnecessarily large diesel generator, allowing the continuous variables related to fuel cost to assume low values while still providing enough energy to the system. Additionally, the low values assumed by the continuous variables led to weak minimum limits on the generator.

As the binary variable in the original generator formulation is the complicating factor, we suggest that it is possible to replace it with a simple continuous diesel generator model with an approximated linear fuel consumption curve. Preliminary testing of this formulation has shown a drastic decrease in computation time. It is however possible that the quality of the practical solution suffers from the approximations, and the lost ability to model limits on minimum ramping of the generator.

The original binary formulation from Arnesen and Borgen (2016) is included in the base model (Chapter 5.3). The simple continuous diesel generator model is presented as an alternative formulation in Chapter 5.4. The performance of the two formulations is compared and discussed in the computational study (Chapter 7).

5.3.2 Battery formulation

As for the generator formulation, the component specific decision variables result in some challenges when modelling the behaviour of the chosen battery unit. Many of the articles mentioned in the literature review strives to be as exact as possible, while maintaining linear characteristics (Scioletti et al., 2016; Bordin et al., 2017). However, when considering the choice between different components and thus component specific parameters, it proved difficult to retain the linearity in these formulations.

In Arnesen and Borgen (2016), we present a linear battery formulation with component specific parameters, that incorporates ideas from Dragičević et al. (2014) and Kuznia et al. (2013) when modelling the behaviour of the battery. The battery model presented in this thesis is to a high degree based on this work.

The inclusion of battery lifetime calculations and reinvestment decisions is one of the major contributions of our model, but also one of the more challenging processes to model mathematically. As the problem is of a strategic nature and spans long time horizons, we propose a simplified lifetime calculation basing the reinvestment decisions on an average energy throughput of the battery. The idea of basing lifetime calculations on energy throughput is adopted by Bordin et al. (2017) and Zhao et al. (2013), and facilitates for a linear but relatively accurate modelling of battery lifetime. In this thesis we present a simplified battery model that includes battery lifetime calculations, while allowing the model to keep its multi-horizon structure.

5.3.3 PV

The detailed PV-panel modelling mentioned in the literature review will, if implemented in a strategic model, lead to great challenges in terms of solution procedures. Therefore, it is assumed sufficient to model the PV-panel according to the work found in Dragičević et al. (2014), calculating PV-power production as a function of the parameters surface area, irradiation and efficiency.

5.3.4 Considerations of a strategic model

In the mathematical formulation presented in Arnesen and Borgen (2016), constraints on spinning reserves related to the power produced by PV-panels are included. This is a relevant constraint in an operational problem, when deciding how to dispatch energy resources, but it does not provide any particular insight in a strategic problem. Inspection of the solutions obtained when solving different instances with and without the spinning reserve constraints revealed that they have little impact on the strategic solution, and limited impact on the computational time. As the constraints in most cases are redundant, we have chosen to not include them in the formulation that we present in this thesis.

5.4 Mathematical formulation - Base model

Based on the problem statement in Chapter 4 and the assumptions and modelling choices stated in the beginning of this chapter, the MISSMDP is formulated as a multi-horizon stochastic mixed integer optimization problem, minimizing total costs over the lifetime of the system. It considers both a strategic, and an operational horizon, allowing the DM to make investment decisions based on expectations of the future operating conditions and the performance of the chosen components.

In Arnesen and Borgen (2016), a mathematical model is formulated for the MISSMDP with batteries, PV-panels and diesel generators. In this chapter, we present a version of this model - a base model - before we provide further extensions including all the characteristics described in the problem statement.

Assumptions related to the technical modelling of specific components are explained and elaborated on when these are introduced in the following sections. In Chapter 5.4.1, all sets and indices are introduced and explained, together with a brief introduction to the parameters and variables. Chapter 5.4.2 gives a more thorough introduction to the parameters and variables through a detailed explanation of the objective function and all of the constraints.

5.4.1 Sets, indices, parameters and variables

Let T^S be the set of time periods in the strategic time horizon. T^S is defined as $T^S = \{1, 2, ..., n\}$, where n is the amount of periods in the strategic horizon. A strategic time step, or period, is indexed by t. Related to each strategic period t is a set of operational periods, T_t^O. The operational periods are indexed by o. Expressed mathematically, we have that $o \in T_t^O \; \forall \; t \in T^S$. Additionally, $T_t^O = \{1, 2, ..., h\}$, where h is the number of periods in the operational horizon. The length of each strategic period is given in years, while the length of each operational period is given in hours.

The problem is subject to operational uncertainty, represented by a set of predefined scenarios. The set S^O is defined as the set of operational scenarios, indexed by s. If there are k operational scenarios related to each operating horizon, then $S = \{1, 2, ..., k\}$. The sets T^S, T_t^O and S^O are used to index parameters and variables related to a certain operational period o in a given scenario s for a particular strategic period t.

The five remaining sets represent the components included in the model. First, let E be the

set of all available diesel generators, PV-panels and battery units. E is defined as a set of subsets, $E = \{E^G, E^P, E^B\}$, and is indexed by e. The subset E^G is the set of all available diesel generator types, E^B is the set of all available battery units, and E^P is the set of all available PV-panel types. The set of different power sources included in the model is defined as E^{En}, where $E^{En} = \{P, G, B^+, B^-\}$. E^{En} is indexed by i, and is related to the performance of the chosen units from E for each source. P relates to the energy produced by the PV-panels, and G relates to the energy produced by the diesel generator. The energy from the battery unit is split in discharging (B^+) and charging (B^-). All sets and indices are summarized in Table 5.3 and Table 5.4.

Table 5.3: Sets

Set		**Description**
T^S	-	Set of strategic periods
T_t^O	-	Set of operational periods, under strategic period t
S^O	-	Set of operational scenarios
E^{En}	-	Set of power sources = $\{G, P, B^+, B^-\}$
E	-	Set of possible PV-units, generator units and battery units
E^G	-	Set of possible generator units
E^P	-	Set of possible PV-panel units
E^B	-	Set of possible battery units

Table 5.4: Indices

Index		**Description**
t	-	in set T^S
o	-	in set T_t^O
s	-	in set S^O
i	-	in set E^{En}
e	-	in sets E, E^G, E^P and E^B

All parameters and variables that are used in the model are listed in Table 5.5 and 5.6. Parameters are defined as uppercase letters, while variables are given as lowercase letters. The indices relating the parameters and the variables to the different sets are added as subscripts. Superscripts are used to increase the legibility of the model.

Table 5.5: Parameters

Parameter		Description
δ_t	-	Discount factor in strategic period $t \in T^S$
D_{os}	-	Load demand in period $o \in T_t^O$ in scenario $s \in S^O$ [kWh]
I_{os}	-	Irradiation in period $o \in T_t^O$ in scenario $s \in S^O$ [kW/m^2]
$\bar{R}^G$	-	Maximum share of energy produced from the diesel generator [%]
O_e^{PV}	-	Surface area of PV-unit $e \in E^P$ [m^2]
η_e^{PV}	-	Efficiency of PV-unit $e \in E^P$
C_e	-	Cost per unit $e \in E$ [$]
C^L	-	Value of lost load (VOLL) [$/kWh]
C^F	-	Cost per unit of fuel consumed by generator [$/l]
θ^{oc}	-	Scaling factor for operational costs in the objective function
$\bar{P}_e^G$	-	Maximum power rating of generator $e \in E^G$ [$]
G^{min}	-	Minimum ramping of the diesel generator [%]
A^F	-	Marginal fuel consumption coefficient - diesel generator [l/kWh]
B^F	-	Fixed fuel consumption coefficient - diesel generator [l/h]
π_s	-	Probability of scenario $s \in S^O$
H	-	Length of operating period [hours]
η^+, η^-	-	Conversion efficiency for discharging and charging battery, respectively
$\bar{P}^{B+}$	-	Maximum discharging power rating of the battery unit [kW]
$\bar{P}^{B-}$	-	Maximum charging power rating of the battery unit [kW]
$\bar{E}_e^B$	-	Maximum rated energy capacity of battery unit $e \in E^B$ [kWh]
L^B	-	Total Battery lifetime given in number of cycles
M^B	-	Big-M value related to battery reinvestment

Table 5.6: Variables

Variable		Description
x_e	-	1, if invest in a unit $e \in E \backslash \{E^P\}$
	-	0, otherwise
x_e	-	Integer variable denoting number of PV-panel unit $e \in E^P$ that are invested in
x_{et}^B	-	1, if reinvestment in battery unit $e \in E^B$ is necessary in $t \in T^S$,
	-	0, otherwise
p_{itos}	-	Aggregate power from/to source $i \in E^{En}$ in operating period $t \in T^S$, $o \in T_t^O$ in scenario $s \in S^O$ [kW]
f_{tos}	-	Amount of fuel used in operating period $t \in T^S$, $o \in T_t^O$ in scenario $s \in S^O$ [l/h]
β_{etos}^G	-	1, if generator $e \in E^G$ running in operating period $t \in T^S$, $o \in T_t^O$ in scenario $s \in S^O$,
	-	0, otherwise
n_{tos}^L	-	Load not covered in operating period $t \in T^S$, $o \in T_t^O$ in scenario $s \in S^O$ [kW]
s_{tos}^B	-	Total SOC in operating period $t \in T^S$, $o \in T_t^O$ in scenario $s \in S^O$ [kWh]
l_t	-	Expected total energy charged to the battery unit from the time of investment until the end of $t \in T^S$ [kWh]

5.4.2 Multi-horizon stochastic model formulation

In this section, we present the multi-horizon stochastic model formulation of the MISSMDP based on the already presented sets, indices, parameters and variables. Included is an explanation of the objective function and all constraints related to their area of application. The areas of application are defined as operational constraints, generator constraints, PV-system constraints, battery constraints, battery lifetime constraints, first stage variable constraints, and variable definitions. A summary of the mathematical model is included in Appendix A.

Objective function

The main objective of the MISSMDP, referring to Equation (1a), is to minimize the total lifetime cost of investing in and operating a microgrid.

The first term of the objective function relates to the investment costs in the first strategic period. For all generator and battery units $e \in E \backslash \{E^P\}$, where $E = \{E^G, E^P, E^B\}$, the variable x_e is a binary first-stage decision variable. x_e takes the value 1 if an investment is made in a particular unit/type of equipment, otherwise the variable takes the value 0. For the subsets E^G and E^B, it is at most invested in one unit from each set. For all PV-units $e \in E^P$, x_e is a non-negative integer variable counting the number of PV-panels of type e that are invested in, in the first stage.

Associated with each unit type e is the unit cost of purchasing said equipment, C_e. Accordingly, the first term of the objective function determines the initial investment costs by taking the sum of $C_e x_e$ for all available units e.

$$\min z = \sum_{e \in E} C_e x_e + \sum_{t \in T^S} \delta_t \sum_{e \in E^B} C_e x^B_{et} + H \sum_{t \in T^S} \delta_t \sum_{s \in S^O} \pi_s \sum_{o \in T^O_t} \theta^{oc} \left(C^F f_{tos} + C^L n^L_{tos} \right) \tag{1a}$$

The second term of the objective function is related to the cost of possible reinvestment in batteries for the strategic periods. The cost C_e is assumed constant throughout the planning horizon. The second term is rendered below.

$$\sum_{t \in T^S} \delta_t \sum_{e \in E^B} C_e x^B_{te}$$

x^B_{te} is a binary variable denoting whether it is necessary to reinvest in the battery in a strategic period t. x^B_{te} takes the value 1 if a reinvestment is made, and is otherwise equal to 0. The cost of reinvesting in batteries, $C_e x^B_{te}$, is discounted in each strategic period t with the discounting factor δ_t, in order to determine the present value of future costs.

The cost of the operational decisions in the MISSMDP, is related to fuel consumption by the diesel generator and the cost of not covering load. The operational costs are found in the third term of the objective function:

$$H \sum_{t \in T^S} \delta_t \sum_{s \in S^O} \pi_s \sum_{o \in T^O_t} \theta^{oc} \left(C^F f_{tos} + C^L n^L_{tos} \right)$$

Fuel consumption, denoted f_{tos}, is a continuous variable related to the consumption of fuel for an operational period o of a given scenario s, in a strategic period t. C^F is the cost per unit of fuel consumed. The total operational costs from the generator is found by taking the sum of $HC^F f_{tos}$, where H is the length of each operating period in hours.

n^L_{tos} is a continuous variable related to the load not covered in strategic period t, operational period o, and scenario s. C^L is the cost of load not covered. This cost is often referred to as a rationing cost, or the value of lost load (VOLL). Accordingly, the cost of load not covered is the sum of $HC^L n^L_{tos}$, where H is the length of each operating period in hours.

The recourse is weighted with the probability of realizing each operating scenario s, given as π_s. As each scenario might be shorter than one full year, the operational costs are multiplied with the scaling factor θ^{oc}. Finally, the sum is discounted in each strategic period t with the discounting factor δ_t.

An operational period o, in scenario s and strategic period t, is hereafter referred to as operating period (t, o, s).

Operational constraints

The energy balance of the system, Constraints (2a), are defined for every operating period (t, o, s). The constraints ensure that the sum of power produced from all energy sources, less power charged to the battery, is equal to the load demand less load not covered. p_{itos} is the aggregate power produced by source $i \in E^{En}$, while n^L_{tos} is load not covered. H is the parameter defining the length of each operational period in hours, and D_{os} is the load demand for operating

period o in scenario s. The first term of the energy balance is the sum of energy delivered from all sources $i \in E^{En} \backslash \{B^-\}$, and the second term is the energy charged to the battery.

$$\sum_{i \in E^{En} \backslash \{B^-\}} (Hp_{itos}) - Hp_{B^-tos} = D_{os} - Hn^L_{tos} \qquad ,t \in T^S, o \in T^O_t, s \in S^O \tag{2a}$$

Constraints (3) restrict the amount of energy produced from the diesel generator, by defining a specific target on the share of renewables in the energy mix. This target is enforced by a maximum limit on the share of energy from the diesel generator dispatched to cover load throughout the operating horizon for each strategic period t and operational scenario s. p_{Gtos} refers to the power delivered from the generator, where the index G refers to the source G in the set of possible power sources E^{En}. D_{os} is the load demand, and $\bar{R}^G$ is the maximum limit on the share of energy from the diesel generator.

$$H \left(\frac{\sum_{o \in T^O_t} p_{Gtos}}{\sum_{o \in T^O_t} D_{os}} \right) \leq \bar{R}^G \qquad ,t \in T^S, s \in S^O \tag{3}$$

Generator constraints

Constraints (4a) state that the continuous variable denoting power output of the diesel generator, p_{Gtos}, can only be greater than zero when β^G_{etos} is 1. β^G_{etos} is a binary variable that takes the value 1 if diesel generator $e \in E^G$ is running in operating period (t, o, s). Constraints (4a) also ensures that when β^G_{etos} is 1 and the generator is running, the maximum power output in the operational period is constrained by the maximum power output of the chosen generator, $\bar{P}^G_e$.

$$p_{Gtos} \leq \sum_{e \in E^G} \bar{P}^G_e \beta^G_{etos} \qquad ,t \in T^S, o \in T^O_t, s \in S^O \tag{4a}$$

Constraints (5) say that β^G_{etos} can only take the value 1 if a specific generator has been purchased in the first stage, i.e. if x_e is 1, for any generator unit $e \in E^G$.

$$\beta^G_{etos} \leq x_e \qquad ,e \in E^G, t \in T^S, o \in T^O_t, s \in S^O \tag{5}$$

It is common practice to comply with a minimum ramping limit when operating a diesel generator. Constraints (6) force p_{Gtos} to be greater than or equal to a predefined minimum percentage

of the maximum power rating of the generator, $\bar{P}_e^G$. The minimum percentage is given as G^{min}. For the constraints to be active only when the generator is running, the right hand side is multiplied by β_{etos}^G.

$$p_{Gtos} \geq \sum_{e \in E^G} \left(G^{min} \bar{P}_e^G \beta_{etos}^G \right) \qquad ,t \in T^S, o \in T_t^O, s \in S^O \tag{6}$$

In Constraints (7), the fuel consumption, f_{tos}, is calculated based on the power produced from the generator, p_{Gtos}, where the index G denotes that the power produced comes form the source generator, and the indexes (t,o,s) refer to the operating period. The fuel consumption is a linear relationship between power production and fuel consumption. The parameter A^F is the marginal fuel consumption coefficient for the generator (slope), and B^F is the intercept coefficient.

$$f_{tos} - (A^F p_{Gtos} + B^F \sum_{e \in E^G} \beta_{etos}^G) \geq 0 \qquad ,t \in T^S, o \in T_t^O, s \in S^O \tag{7}$$

Figure 5.3 illustrates a linear fuel consumption relationship, where A^F is 1 and B^F is 3. The value of the coefficients are not realistic, and the figure is purely meant to be illustrative. In the sum $\sum_{e \in E^G} B^F \beta_{etos}^G$ in Constraints (7), β_{etos}^G is multiplied with the intercept coefficient in order to ensure that fuel consumption is zero if the generator is not producing power.

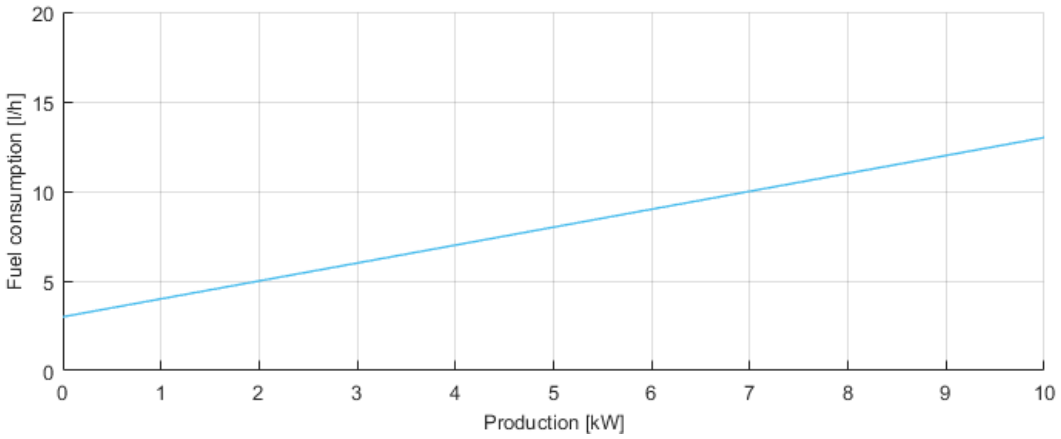

Figure 5.3: Linear fuel consumption relationship for diesel generator

PV-system constraints

The power produced by the PV-system, p_{Ptos}, in operational period o, is restricted by how many PV-panels of type e that are invested in, x_e, their surface area O_e^{PV}, its manufacturer rated efficiency η_e^{PV}, and the irradiation I_{os}. In order to ensure intra-hour stability of the system in the situation where the irradiation suddenly spikes, and the load and maximum charging capacity of the battery cannot absorb the subsequent rise in instantaneous PV power production, it is assumed that the PoE control system is able to limit the power output of the PV-panels. Constraints (8) therefore define power produced as less than or equal to maximum available power production.

$$p_{Ptos} \leq I_{os} \sum_{e \in E^P} \eta_e^{PV} O_e^{PV} x_e \qquad ,t \in T^S, o \in T_t^O, s \in S^O \tag{8}$$

Battery constraints

Constraints (9) update the SOC (energy stored in the battery), s_{tos}^B, which is a continuous variable defined at the end of each operating period (t,o,s). s_{tos}^B is updated given the SOC at the end of the previous operational period, $s_{t,o-1,s}^B$, less power discharged from the battery, p_{B^+tos}, plus the power charged to the battery, p_{B^-tos}. The power charged to and discharged from the battery is multiplied by the time-scale of the operating period in hours, H, providing the equivalent energy in kWh. The efficiency parameters η^{B-} and η^{B+}, are included in order to account for efficiency losses when charging and discharging the battery, respectively.

$$s_{tos}^B = s_{t,o-1,s}^B + H(\eta^- p_{B^-tos} - \eta^+ p_{B^+tos}) \qquad ,t \in T^S, o \in T_t^O \backslash \{1\}, s \in S^O \tag{9}$$

The SOC is assumed to be zero in the beginning of each operational horizon. As the SOC is defined for the end of an operational period, Constraints 10 ensure that the SOC at the end of the first operational period for all scenarios s and strategic periods t, s_{t1s}^B, is equal to the energy charged to the battery in that period, $\eta^- H p_{B^-t1s}$. This implies that the battery has to be empty at the beginning of the operational horizon.

$$s_{t1s}^B = \eta^- H p_{B^-t1s} \qquad ,t \in T^S, s \in S^O \tag{10}$$

Constraints (11) connect the energy stored in the battery to the physical limits of the battery. They ensure that s^B_{tos} is restricted by the maximum rated energy capacity of the battery unit, $\bar{E}^B_e$. As the maximum rated energy capacity is different for each battery unit, the right hand side of the constraints are a sum of the capacity rating multiplied with x_e in order to provide the correct limit for the battery unit that it is invested in, in the first stage. Recall that x_e is a binary variable that is equal to 1 if it is invested in a specific battery unit.

$$s^B_{tos} \leq \sum_{e \in E^B} \bar{E}^B_e x_e \qquad ,t \in T^S, o \in T^O_t, s \in S^O \tag{11}$$

The maximum amount of energy that can be discharged from the battery in an operational period is restricted by the available amount of energy stored in the battery at the end of the previous operational period, $s^B_{t,o-1,s}$. Correspondingly, the maximum amount of energy that can be charged to the battery in an operational period is restricted by the unused capacity of the battery. The maximum energy charging and discharging limits of the battery are managed by Constraints (9) in combination with Constraints (11). These constraints define the SOC-balance in the system, while ensuring that the SOC is below its maximum limit. For these constraints to hold, the energy charged to the battery can never exceed the unused capacity, and the energy discharged can never exceed the available amount of energy stored in the battery. Accordingly, the maximum charging and discharging capacity of the battery is accounted for.

In addition to being restricted by the amount of energy stored in the battery at the beginning of the operational period, the charging and discharging power, p_{B+tos} and p_{B-tos}, is restricted by the maximum charging and discharging power rating of the battery. Constraints (12) and (13) enforce the instantaneous charging and discharging limits on the battery, given maximum power rating, $\bar{P}^{B-}$ and $\bar{P}^{B+}$, for charging and discharging respectively.

$$p_{B^+tos} \leq \bar{P}^{B+} \qquad ,t \in T^S, o \in T^O_t, s \in S^O \tag{12}$$

$$p_{B^-tos} \leq \bar{P}^{B-} \qquad ,t \in T^S, o \in T^O_t, s \in S^O \tag{13}$$

Constraints (14) ensure that the power discharged from the battery in the first operational period in all strategic periods t and scenarios s is equal to zero. This is in compliance with assuming the SOC to be zero at the beginning of each operational horizon (assumption 10).

$$p_{B^+t1s} \leq 0 \qquad ,t \in T^S, s \in S^O \tag{14}$$

Battery lifetime constraints

For battery lifetime considerations, we suggest a model based on average energy throughput of the battery. The continuous variable l_t is a measure of expected aggregated energy throughput in the battery unit from the time of investment until the end of strategic period t. l_t is updated for each strategic period based on the expected total energy charged to the battery in the operational horizon. Furthermore, l_t is limited by an upper limit defined in Constraints (17). If that upper limit is reached, a reinvestment in the battery unit is performed (a replacement), and l_t is reduced to zero.

Constraints (15) update the energy throughput of the battery in strategic period t. The previous value, l_{t-1}, is added to the expected total energy charged to the battery unit during the operational horizon of strategic period t. The continuous variable p_{B^-tos} is the power charged to the battery and H is the time scale of each operational period in hours. The total energy charged into the battery in every operating period o, of a scenario s, is weighted with the probability of each scenario, π_s, in order to find the expected value of total energy charged to the battery. The big-M formulation with the binary variable x^B_{te} ensures that the aggregated energy throughput to the battery, l_t, is reduced to zero if a reinvestment is made. x^B_{et} is 1 when a reinvestment is made, and 0 otherwise. The actual value of the big-M parameter is discussed and defined later in this chapter.

$$l_t \geq l_{t-1} + H \sum_{s \in S^O} \pi_s \sum_{o \in T^O_t} p_{B^-tos} - M^B \sum_{e \in E^B} x^B_{et} \qquad ,t \in T^S \backslash \{1\} \tag{15}$$

In order to ensure that l_t takes the right value for the first strategic period, as well as for any strategic period where a reinvestment has been made, Constraints (16) are included. As reinvestments happen at the beginning of a strategic period, and l_t is defined at the end of each strategic period, the variable will always be greater than or equal to the expected energy throughput in the current strategic period. The same logic applies to the first strategic period, where l_t is greater than or equal to the total expected energy throughput. Constraints (16) enforce this limit.

$$l_t \geq H \sum_{s \in S^O} \pi_s \sum_{o \in T^O_t} p_{B^-tos} \qquad ,t \in T^S \tag{16}$$

Constraints (17) limit l_t to its maximum value. The upper limit of l_t is defined as the maximum aggregated amount of energy throughput to the battery before it is replaced. As the MISS-MDP is a strategic decision tool, an approximate of the value is constructed by multiplying the manufacturer specified minimum amount of full cycles (from 0% - 100% SOC) that the battery should endure, L^B, with the maximum rated energy capacity, $\bar{E}^B_e$, for a specific battery type $e \in E^B$. Together with Constraints (15), Constraints (17) ensure that when l_t reaches its maximum allowed value, x^B_{te} takes the value 1 and a reinvestment is performed.

$$l_t \leq \sum_{e \in E^B} L^B \bar{E}^B_e x_e \qquad ,t \in T^S \backslash \{1\} \tag{17}$$

The model only allows reinvestments in the same battery type as the one chosen in the first strategic period. I.e. x^B_{te} will only be able to take a value other than 0 if x_e is 1. Constraints (18) connect these two variables and ensure the relationship between them.

$$x^B_{et} \leq x_e \qquad ,e \in E^B, t \in T^S \tag{18}$$

First stage variable constraints

The first stage variables, x_e, are defined as binary variables for subset E^B and E^G deciding which generator and battery units to invest in. As the DM can only invest in one battery and one diesel generator, the sum of x_e over all $e \in E^B$ and over all $e \in E^G$ is less than or equal to one. These relationships are enforced in Constraints (19) and (20).

$$\sum_{e \in E^G} x_e \leq 1 \tag{19}$$

$$\sum_{e \in E^B} x_e \leq 1 \tag{20}$$

Variable definitions

Constraints (21) - (27) are variable definitions. p_{itos}, f_{tos}, s^B_{tos}, n^L_{tos} and l_t are continuous variables restricted to positive values, and Constraints (21) - (23) are their non-negativity constraints.

$$p_{itos} \geq 0 \qquad ,i \in E^{En}, t \in T^S, o \in T^O_t, s \in S^O \tag{21}$$

$$f_{tos}, \quad s^B_{tos}, \quad n^L_{tos} \geq 0 \qquad ,t \in T^S, o \in T^O_t, s \in S^O \tag{22}$$

$$l_t \geq 0 \qquad ,t \in T^S \tag{23}$$

Finally, the mathematical formulation is dependent upon four different binary variables and one integer variable. Constraints (24) - (26) restrict the binary variables to take the value of either 0 or 1, while Constraints (27) ensure integer values for x_e when $e \in E^P$.

$$x_e \in \{0,1\} \qquad ,e \in E \backslash \{E^P\} \tag{24}$$

$$x^B_{et} \in \{0,1\} \qquad ,e \in E^B, t \in T^S \tag{25}$$

$$\beta^G_{etos} \in \{0,1\} \qquad ,e \in E^G, t \in T^S, o \in T^O_t, s \in S^O \tag{26}$$

$$x_e \in \mathbb{Z}^+ \qquad ,e \in E^P \tag{27}$$

5.5 Continuous diesel generator formulation

As discussed in Chapter 5.3, an excessive amount of computation time is spent branching on the binary variable associated with the generator. In this section, we present an alternative to the original generator formulation in Constraints (4a)-(7). The alternative formulation is a simple continuous diesel generator model. The fuel consumption is modelled based on a constant relationship between power production and cost, obtained by producing an approximated fuel consumption curve intercepting at zero. I.e. the intercept coefficient B^F is equal to zero, and the marginal fuel consumption coefficient for the generator, A^F, is adjusted to fit the approximated curve.

In an effort to construct the approximated curve without imposing severe under- or overestimations, we have tested a variety of approaches. We refer to Chapter 6 for an explanation of how we calculate the new slope A^F for the approximated curve. Figure 5.4 provides an illustration of the approximated curve together with the original linear fit. The numbers in the figure are arbitrarily chosen.

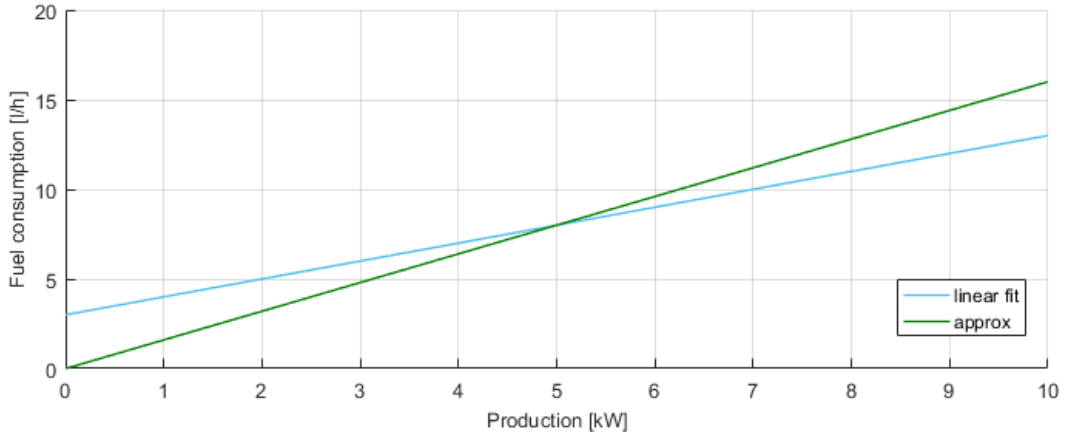

Figure 5.4: Example of approximated fuel consumption curve for the diesel generator

Based on Figure 5.4, fuel consumption is given by the relationship in Equation (5.1).

$$f_{tos} \geq A^F p_{Gtos} \tag{5.1}$$

Due to the costs related to fuel consumption, Equation (5.1) will in all practical applications be given by equality. If we define total fuel costs as TFC, we find that

$$TFC = HC^F f_{tos} = HC^F A^F p_{Gtos} \tag{5.2}$$

By introducing the following definition:

$$C^F A^F = C^G \tag{5.3}$$

we observe that the fuel consumption Constraints (7) are superfluous, and replace $HC^F f_{tos}$ with $HC^G p_{Gtos}$ in the objective function. Furthermore, having removed β^G_{etos} from the model, we are no longer able to enforce a minimum limit on the ramping of the generator, nor model if it is running or not. Consequently, Constraints (6) and (5) are removed from the model. This leaves us with Constraints (4a). A slight modification of the constraints, replacing β^G_{etos} with $x_e, \forall e \in E^G$, results in Constraints (4b), rendered below.

$$p_{Gtos} - \sum_{e \in E^G} \bar{P}^G_e x_e \leq 0 \qquad ,t \in T^S, o \in T^O_t, s \in S^O \tag{4b}$$

Constraints (4b) state that the continuous variable denoting power output of the generator, p_{Gtos}, can only be greater than zero if a generator has been purchased, i.e. when x_e is equal to 1. If a generator has been purchased, the maximum power output in each operational period is constrained by the maximum rated power output of the chosen generator, $\bar{P}^G_e$. These are the only constraints needed in the simple continuous diesel generator formulation.

The new parameter of the model, C^G, is included in Table 5.7 below. In addition to removing the binary variable β^G_{tos}, the continuous variable f_{tos} is no longer needed explicitly in the modelling when using the simple continuous diesel generator formulation. The entire new objective function is found in Equation (1b), and the resulting constraints modelling the generator are given as Constraints (4b).

Table 5.7: New notation for continuous diesel generator formulation

Parameter		Description
C^G	-	Cost per unit kWh produced by generator

$$\min z = \sum_{e \in E} C_e x_e + \sum_{t \in T^S} \delta_t \sum_{e \in E^B} C_e x^B_{et} + H \sum_{t \in T^S} \delta_t \sum_{s \in S^O} \pi_s \sum_{o \in T^O_t} \theta^{oc} \left(C^G p_{Gtos} + C^L n^L_{tos} \right) \tag{1b}$$

5.6 Extensions to the model

We propose three extensions to the model that was suggested as further research in Arnesen and Borgen (2016). First, we present a simple extension allowing the DM to specify a maximum total area for PV-panels, followed by an extension that includes the considerations of the degradation of battery capacity. The final extension that we present, is a modelling of power from wind turbines.

5.6.1 Maximum PV-panel surface area

In some situations, there might be an actual limit on the total area that can be covered by PV-panels. In order to introduce a constraint on the maximum available surface area, we introduce the parameter found in Table 5.8

Table 5.8: New notation for limiting PV-panel surface area

Parameters		Description
O^{max}	-	Maximum total surface area of PV-panels [m^2]

The new constraint limiting the total surface area covered by PV-panels is rendered below. They take the sum of the area of each PV-panel unit $e \in E^{PV}$ multiplied with the number of panels bought of each type, x_e. This sum is then forced to be less than or equal to a predefined maximum surface area, O^{max}.

$$\sum_{e \in E^{PV}} O_e^{PV} x_e \leq O^{max} \tag{P1}$$

5.6.2 Degradation of battery capacity

When a battery unit is charged and discharged over time, it will slowly experience a degradation of storage capacity. Being able to model this degradation is valuable as decreasing storage capacity could influence the timing of the reinvestment decision. In the literature review, we introduce several articles considering the degradation of battery capacity. However, most of these formulations are either far too complex for our strategic model or not applicable to component specific parameters.

As existing approaches are not applicable to our base model, we propose a novel approach to battery capacity degradation considerations. The approach is based on the energy throughput calculations represented by the l_t-variable, which counts total energy throughput in each strategic period, and manufacturer specified properties of the battery. Before the mathematical formulation is presented, we introduce two new parameters found in Table 5.9.

Table 5.9: New notation for battery degradation

Paramters		**Description**
R^B	-	Total allowed degradation of battery units [%]
M^{BS}	-	Big-M value related to degradation of battery

For utility battery units, manufacturers specify a level of capacity degradation at which the battery is considered to have exceeded its lifetime. In our capacity degradation formulation, we assume that the maximum degradation of the battery coincides with the maximum energy throughput. Equation (5.4) illustrates the linear relationship between battery degradation, and the total consumption of the maximum energy throughput. BD_e refers to the battery degradation of battery unit e.

$$BD_e = \frac{l_{(t-1)}}{L^B \bar{E}^B_e} \bar{E}^B_e R^B \tag{5.4}$$

The highest possible value that can be taken by the variable l_t is equal to the maximum number of cycles L^B multiplied by the energy capacity of the battery, $\bar{E}^B_e$. The fraction in Equation (5.4) is therefore a number between 0 and 1, defining how much of the total energy throughput that has been consumed up until the current strategic period. This share is then multiplied with total degradation of the battery unit, R^B, to find the equivalent percentage decrease in battery energy capacity. Multiplying this percentage with the manufacturer rated energy capacity of the battery, provides the decrease in kWh. Equation (5.4) can easily be simplified to Equation (5.5).

$$BD_e = \frac{l_{(t-1)}}{L^B} R^B \tag{5.5}$$

Based on the definition in Equation (5.5), we have formulated Constraints (E1) relating the maximum battery state of charge to the available capacity in each strategic horizon.

$$s^B_{tos} \leq \bar{E}^B_e x_e - \frac{R^B l_{(t-1)}}{L^B} + (1 - x_e) M^{BS} \qquad ,e \in E^B, t \in T^S \backslash \{1\}, o \in T^O_t, s \in S^O \tag{E1}$$

Constraints (E1) state that battery state of charge, s^B_{tos}, has to be less than or equal to the maximum energy capacity of the chosen battery, $\bar{E}^B_e$, less the degradation of the battery based on total energy throughput up until the current strategic period. The last expression in Constrains (E1), is included to ensure that the constraints are only binding for the unit e where x_e is equal to 1. M^{BS} is a big-M value related to battery degradation, and is defined in Chapter 5.7.

As we want to utilize full battery capacity in the first strategic period, Constraints (E2) are defined for $t = 1$. They are similar to the original maximum SOC constraints (Constraints 11).

$$s^B_{1os} \leq \sum_{e \in E^B} \bar{E}^B_e x_e \qquad ,o \in T^O_t, s \in S^O \tag{E2}$$

5.6.3 Wind turbines

The inclusion of wind turbines as a possible RES in the MISSMDP is of high interest as it complements PV-panels and may increase the reliability of the system. There exists a large amount of literature modeling the power output of a wind turbine as a function of the wind speed in various ways, most commonly resulting in linear, quadratic or cubic relationships. In a long-term strategic model such as ours, the power output of a wind turbine, P_w, can be sufficiently modelled as a piecewise linear function of wind speed, $V(t)$. The piecewise linear function is rendered in Equation (5.6), and considers the turbine specific cut-in and cut-off wind speed, V^{cin} and V^{cof}, rated wind speed V^R and rated power production $\bar{P}^R$.

$$P_w = \left\{ \begin{array}{ll} \bar{P}^R \frac{V(t)-V^{cin}}{V^R-V^{cin}} & \text{if } V^{cin} \leq V(t) \leq V^R \\ \bar{P}^R & \text{if } V^R \leq V(t) \leq V^{cof} \\ 0 & \text{otherwise} \end{array} \right\} \tag{5.6}$$

Equation (5.6) is a linear approximation of the non-linear power output of the wind turbine when wind speed is above cut-in wind speed and below rated wind speed, $V^{cin} \leq V(t) \leq V^R$. All turbine specific parameters used ($V^{cin}, V^{cof}, V^R, \bar{P}^R$) are available from the manufacturer. To include the option of investing in different wind turbines, some additional notation is required. We expand the set E to also include the subset E^W, denoting potential wind turbines that the DM can invest in. Then, we define the first-stage investment variable x_e as integer $\forall e \in E^W$. Wind turbines also have O&M costs that have to be accounted for in the objective function. C^{om}, which is an estimated marginal O&M cost, is multiplied with the power produced, p_{etos}, in order to represent the incurred costs in the objective function (in addition to what follows

from the expansion of set E). p_{etos} is the continuous variable defining the power produced by wind turbine $e \in E^W$ in operating period (t,o,s). Equation (5.7) shows the O&M costs added to the objective function.

$$\sum_{t \in T^S} \delta_t \sum_{s \in S^O} \pi_s \sum_{o \in T_t^O} \sum_{e \in E^W} C^{om} H p_{etos} \tag{5.7}$$

In order to include the relationship from Equation (5.6) in the mathematical program, a MIP representation is necessary. The quantities introduced in Equation (5.6) needs some additional indexes, and we introduce an auxiliary variable γ^W_{etos}. First, The power output from wind turbines, p_{etos}, is defined differently than for other sources, which have the source as index (p_{itos}). This difference is due to ease of modeling of the wind production. The cut-in and cut-off wind speed, rated wind speed and rated power production depend on the type of turbine, and will gain an index $e \in E^W$; $\bar{P}^R_e, V^{cin}_e, V^{cof}_e, V^R_e$. The wind speed in each operating period will gain two indexes, $o \in T_t^O$ and $s \in S^O$, and is an input parameter represented as V_{os}. The auxiliary variable γ^W_{etos} is a binary variable used to force the power production to zero when the wind speed is too high or too low. Finally, we introduce three big-M parameters needed to model the wind production. Their numerical values are discussed later in this chapter. An overview of the new notation is found in Table 5.10.

Table 5.10: New notation for wind turbines

Set		**Description**
E^W	-	Set of potential wind turbine types
E	-	Set of possible units $= \{E^G, E^P, E^B, E^W\}$
Variables		**Description**
x_e	-	Integer variable denoting number of unit $e \in E^P \cup E^W$
p_{etos}	-	Power produced by unit $e \in E^W$ in period $t \in T^S, o \in T_t^O, s \in S^O$
γ^W_{etos}	-	1, if $V_{os} \leq V^{cin}_e$ or $V_{os} \geq V^{cof}_e$
	-	0, otherwise, for unit $e \in E^W$ in period $t \in T^S, o \in T_t^O, s \in S^O$
Parameters		**Description**
$\bar{P}^R_e$	-	Rated power output of wind turbine $e \in E^W$ at rated wind speed
V^{cin}_e	-	Cut-in wind speed of wind turbine $e \in E^W$
V^{cof}_e	-	Cut-off wind speed of wind turbine $e \in E^W$
V^R_e	-	Rated wind speed of wind turbine $e \in E^W$
V_{os}	-	Wind speed in operational time period $o \in T_t^O$ for scenario $s \in S^O$
M^{V1}_e	-	Big-M for setting γ^W_{etos} equal to 1 if wind speed is out of bounds
M^{V2}_e	-	Big-M for setting γ^W_{etos} equal to 1 if wind speed is out of bounds
M^W	-	Big-M for not restricting p_{etos} when wind speed is within bounds

The first set of new Constraints, (W1), models the approximated linear relationship when $V^{cin}_e \leq V_{os} \leq V^R_e$. When this is the case, γ^W_{etos} is zero, and p_{etos} is constrained by the linear relationship

relating the actual wind speed to the cut-in and rated wind speed. When wind speed is below cut-in wind speed, γ^W_{etos} will take the value 1, and the Big-M parameter M^W is added to the right hand side of the constraints. The big-M formulation is included in order to maintain a positive upper limit on p_{etos} when $V_{os} < V^{cin}_e$.

$$p_{etos} \leq \bar{P}^R_e x_e \frac{V_{os} - V^{cin}_e}{V^R_e - V^{cin}_e} + \gamma^W_{etos} M^W \qquad ,e \in E^W, t \in T^S, o \in T^O_t, s \in S^O \qquad \text{(W1)}$$

Constraints (W2) restrict the power produced by the wind turbines $e \in E^W$ to their maximum rated power production, and becomes the binding constraints when $V^R_e \leq V_{os} \leq V^{cof}_e$.

$$p_{etos} \leq \bar{P}^R_e x_e \qquad ,e \in E^W, t \in T^S, o \in T^O_t, s \in S^O \qquad \text{(W2)}$$

Constraints (W3) and (W4) ensure that γ^W_{etos} is equal to 1 when wind speed is out of bounds for a given turbine type $e \in E^W$. In Constraints (W3), γ^W_{etos} is forced to 1 when $V_{os} > V^{cof}_e$. The big-M (M^{V1}_e) is sufficiently large to maintain feasibility for the program when γ^W_{etos} is equal to 1. A Similar big-M formulation with M^{V2}_e in Constraints (W4) force γ^W_{etos} to 1 when $V_{os} < V^{cin}_e$.

$$V_{os} \leq V^{cof}_e + \gamma^W_{etos} M^{V1}_e \qquad ,e \in E^W, t \in T^S, o \in T^O_t, s \in S^O \qquad \text{(W3)}$$

$$V_{os} \geq V^{cin}_e - \gamma^W_{etos} M^{V2}_e \qquad ,e \in E^W, t \in T^S, o \in T^O_t, s \in S^O \qquad \text{(W4)}$$

The final constraints in the wind model are Constraints (W5), which force the power produced by wind turbine $e \in E^W$ to be zero when the wind speed is out of bounds. Allthough M^W is used in Constraints (W1), it is defined for Constraints (W5) for not restricting p_{etos} when wind speed is within bounds.

$$p_{etos} \leq M^W (1 - \gamma^W_{etos}) \qquad ,e \in E^W, t \in T^S, o \in T^O_t, s \in S^O \qquad \text{(W5)}$$

Constraints P1, E1 and E2, and W1 - W5 are included in the full mathematical model enclosed in Appendix B.

5.7 Strengthening the Big-M formulations

With the base model, and the suggested extensions in Chapter 5.6, we have a total of five big-M parameters that have to be assigned a value. These are; M^B related to the reinvestment variable x^B_{te} in Constraints (15), M^{BS} related to the maximum SOC limit in Constraints (E1), M^{V1}_e and M^{V2}_e used to assign γ^W_{etos} the value 1 if the wind speed is out of bounds, and M^W that is used in Constraints (W5) to allow p_{etos} to take a value when the wind speed is within its bounds.

For each constructed instance, the big-M's should be made as tight as possible in order to provide a strong MIP formulation. If the big-M's are not appropriately defined, their size could have a negative effect on the performance of the program. This section is therefore dedicated to defining the numerical value of each of the big-M parameters.

We begin with M^B. For purpose of reference, Constraints (15) are rendered below, together with Constraints (17). Constraints (17) define the maximum value for l_t as the maximum energy throughput.

$$l_t \geq l_{t-1} + H \sum_{s \in S^O} \pi_s \sum_{o \in T^O_t} p_{B-tos} - M^B \sum_{e \in E^B} x^B_{te} \qquad ,t \in T^S \backslash \{1\} \tag{15}$$

$$l_t \leq \sum_{e \in E^B} L^B \bar{E}^B_e x_e \qquad ,t \in T^S \tag{17}$$

A big-M parameter has to account for the worst case situation. In the situations where $(l_{t-1} + H \sum_{s \in S^O} \pi_s \sum_{o \in T^O_t} p_{B-tos})$ of Constraints (15) result in a l_t that violates Constraints (17), x^B_{te} is assigned the value 1. M^B should then reduce l_t to zero. The worst case situation that M^B has to account for is defined as the highest possibly allowed value of l_t. This situation occurs if the first stage decision provides an investment in the battery unit with the highest capacity. Accordingly, M^B should be defined as:

$$M^B = \max_{e \in E^B} \left\{ L^B \bar{E}^B_e \right\} \tag{5.8}$$

However, l_{t-1} could be close to this value without having violated Constraints (17) in the previous strategic period. The right hand side of Constraints (15) could therefore increase above the big-M value due to the term related to the increase in l_t in the current strategic period. As the battery is assumed to be fully discharged at the beginning of each strategic period (assumption

10 in Table 5.2), the maximum theoretical amount of operational periods, in which the battery can be charging, is half of the defined length of the operational horizon. I.e. if the operational horizon consists of 100 periods, the battery can be charging at maximum instantaneous capacity $\bar{P}^{B-}$ in at most 50 of the periods for it to be able to discharge the same amount of power. The accordingly adjusted definition of M^B given in Equation (5.9) is suggested in Arnesen and Borgen (2016), and is the M^B that is applied in this thesis.

$$M^B = \max_{e \in E^B} \left\{ L^B \bar{E}_e^B + \frac{|T_t^O| \, \bar{P}^{B-}}{2} \right\} \tag{5.9}$$

The function of M^{BS} is to ensure that Constraints (E1) are binding only if x_e is equal to 1. If x_e is equal to 0, Constraints (E1) should allow s_{tos}^B to be less than or equal to a value that is greater than or equal to the maximum rated energy capacity of the batter that is invested in, $\sum_{e \in E^B} \bar{E}_e^B x_e$. M^{BS} thus has to be equal to the energy capacity of the largest available battery unit, plus the maximum amount of energy that a battery can be degraded. Equation (5.10) defines the value of M^{BS}.

$$M^{BS} = \max_{e \in E^B} \left\{ (1 + R^B) \bar{E}_e^B \right\} \tag{5.10}$$

M_e^{V1} and M_e^{V2} are used to assign γ_{etos}^W the value 1 if the wind speed is out of bounds. M_e^{V1} appears in Constraints (W3) which assign a value to γ_{etos}^W when $V_{os} > V_e^{cof}$. If $V_{os} > V_e^{cof}$, γ_{etos}^W will be equal to 1 and M_e^{V1} should be greater than or equal to $V_{os} - V_e^{cof}$ for the problem to stay feasible. M_e^{V1} has to account for the worst case being the highest value of V_{os}. Accordingly, Equation (5.11) defines the value of M_e^{V1} as:

$$M_e^{V1} = \max_{o,s} \{V_{os}\} - V_e^{cof} \tag{5.11}$$

M_e^{V2} appears in Constraints (W4), where γ_{etos}^W takes a value if $V_{os} < V_e^{cin}$. In that case, M_e^{V2} should be greater than or equal to $V_e^{cin} - V_{os}$. Accounting for the worst case, where V_{os} is equal to 0, Equation (5.12) defines the value of M_e^{V2}

$$M_e^{V2} = V_e^{cin} \tag{5.12}$$

Finally, M^W is related to Constraints (W1) and (W5). We define the value of M^W based on Constraints (W5), which provide an upper limit on p_{etos}. When γ_{etos}^W is equal to 1, p_{etos} is

forced to zero, and when γ^W_{etos} is equal to 0, p_{etos} has to be less than a maximum theoretical total production, M^W. This value is difficult to define without knowing how many turbines the DM invests in. For each wind turbine type $e \in E^W$, total production has to be less than the maximum rated capacity of the turbine, $\bar{P}^R_e$, multiplied with the amount of turbines it is invested in, x_e.

We suggest that the DM defines a maximum realistic number of each turbine that it could be invested in, and treat this value as an input parameter, N^W. Accordingly, when accounting for the wind turbine with the highest rated capacity, M^W is defined in Equation (5.13).

$$M^W = N^W \max_{e \in E^W} \{\bar{P}^R_e\} \tag{5.13}$$

A slightly tighter formulation could be provided by introducing a M^W for each specific $e \in E^W$. As the formulation in any case is quite poor, there is little value to be added by increasing the number of input parameters in this way.

As already mentioned, M^W is also included in Constraints (W1). The function of M^W is here to prevent the constraints from imposing a negative upper limit on p_{etos} when $V_{os} < V^{cin}$.

5.8 Challenges with solution procedure

The strategic microgrid design problem, in its simplest form, bears resemblance to the classical capacitated lot sizing problem (CLSP), which is proven to be $\mathscr{NP}$-hard. This implies that when scaling up the instances in terms of scenarios, strategic periods and operational periods, the size of the problem and computation time, grows exponentially. Our problem formulation introduce integer and binary variables in the first stage, binary second stage variables related to the modelling of the diesel generator and wind production, as well as calculations of expected total battery life spent, further complicating the structure of the program. The capability of traditional solvers to find solutions for the program within reasonable time has proven to be poor (Arnesen and Borgen, 2016), and we find that there is a need to implement and test alternative formulations and solution methods if aiming at solving realistically sized instances of the problem.

Several techniques and solution methods can be applied to the MISSMDP in order to decrease problem size and solution time. Clever scenario generation techniques, and the definition of representative scenarios can decrease the size of the scenario tree and speed up the solution process, while still providing stable solutions. Exploiting the structure of the MISSMDP, and

its known resemblance to the CLSP, suggests that problem specific heuristics or mathematical programming based heuristics could increase computational performance even further. Additionally, decomposition methods can prove to be a powerful tool in solving complex stochastic programs.

As proven by Birge and Louveaux (2011), the expected recourse function of a stochastic integer program is in general lower semi-continuous, non-convex and discontinuous, implying lacking performance of known decomposition methods for stochastic two-stage programs (Parija et al., 2004). The application of decomposition methods to integer stochastic programs is however not uncharted landscape, and Kuznia et al. (2013) successfully apply a Benders' decomposition to a stochastic mixed integer power system design program, bearing resemblance to the MISSMDP. However, the problem solved in Kuznia et al. (2013) was solved for a one year period, and with less complex battery modelling and information structure than for the MISSMDP.

In an effort to overcome the challenges imposed by the complex formulations in the MSSMDP, the implementation of a nested Benders' decomposition algorithm was evaluated. However, the algorithm was considered to be very complicated and time consuming to implement, and without a guarantee of improvements in execution time. This is due to the high number of subproblems that would need to communicate with each other, and the many ways in which one could iterate between these.

It is therefore immediately of a higher interest to study simpler and faster ways to decrease solution time, suggested based on the characteristics of the program and the structure of the solution process. Methods for increasing computational performance that will be studied in this thesis are therefore alternative formulations and the definition of representative scenarios, improved implementations, and simple heuristic solution methods.

Chapter 6

Data analysis

This chapter begins with a review of how we obtained the operational data used when generating scenarios, and how we have analyzed and manipulated these data sets. The data is related to the archipelago Froan, being one of the cases provided by Trønder Energi. We have chosen to study Froan as this is the first location considered for constructing a microgrid pilot in the Island Project. We then elaborate on the choice of scenario generation method, before we present a discussion on the remaining input parameters. Most of the input parameters are provided by Trønder Energi, in particular data concerning component costs and performance.

6.1 About the operational data

Before we use the historical operational data to generate scenario trees and test the MISSMDP, we have to evaluate the quality of the data sets, and perform analysis and manipulations where it is deemed necessary.

6.1.1 Analyzing the weather data

Two of the most important input parameters in order to predict the intermittent behavior of RES, is hourly means of wind speed and irradiance. Fortunately, weather data is usually quite easily obtained, and well-observed in most countries. Hourly time series of mean wind speed for the last hour, for the years 2012-2016, were obtained through the Norwegian Meteorological Institute's publicly available web portal [1]. The wind data analyzed was measured at the Sula

[1] Website: www.eklima.no

weather station (latitude: 63.8467, longitude: 8,4667), which has station number 65940. This is the closest weather station to our case study location, Froan, and it has similar topological conditions; a flat island in an archipelago in the open sea. Figure 6.1 shows the daily means of the 5 years of wind speed observations. The observations show a clear seasonality that is important to preserve in a scenario generation algorithm. The wind data was cleaned by linear interpolation if less than five consecutive data points were missing. If more than five and less than ten consecutive data points were missing, we sampled values from a normal distribution where the mean and standard deviation is set equal to the mean and standard deviation of the eight data points before and after the missing section. This last method was only used twice for all the historic data, and we observed no occurrences of more than ten missing data points. The wind data was found to have a Weibull probability distribution.

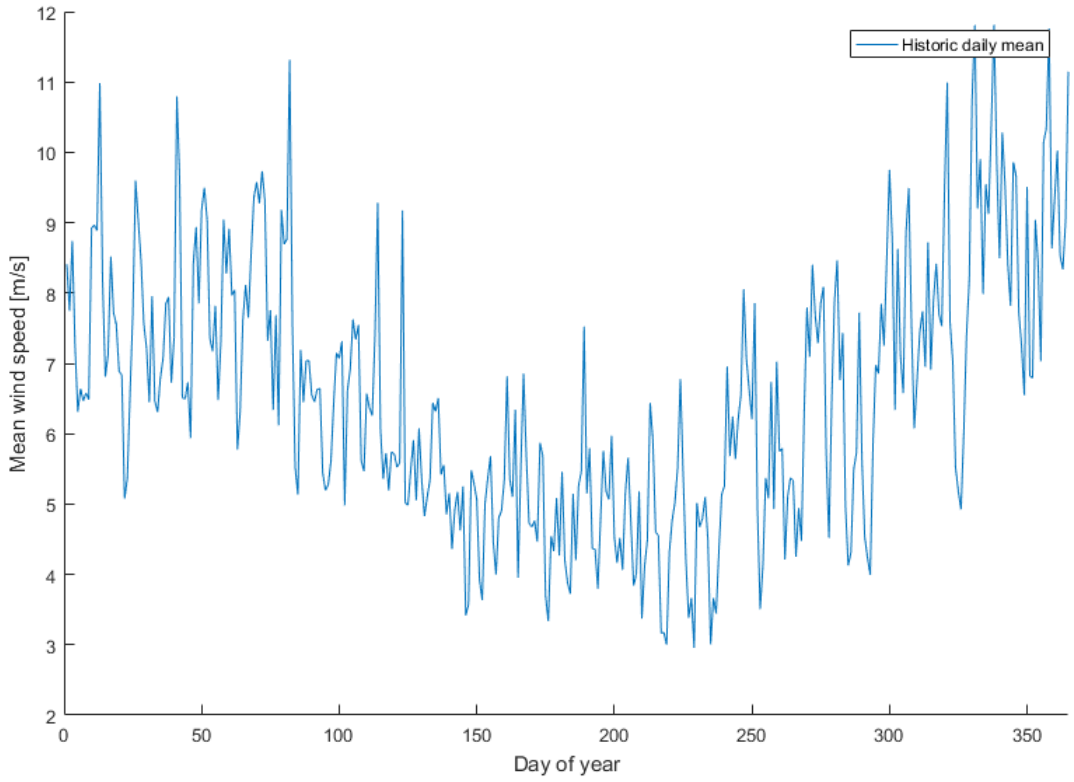

Figure 6.1: Historic daily means of wind speed throughout the year

Hourly time series of irradiance for the years 2012-2016 were obtained from the publicly available online service of Agrometeorology Norway[2]. They provide hourly time series data from 52 measurement stations in Norway, located around the country. This source was chosen because of easy access, and relatively high quality data. The location of the closest measurement station is Rissa (latitude: 63.58569, longitude: 9.97007), which has more or less the same latitude as our case study location. Figure 6.2 shows a plot of mean hourly values throughout the day for

[2]Website: lmt.nibio.no

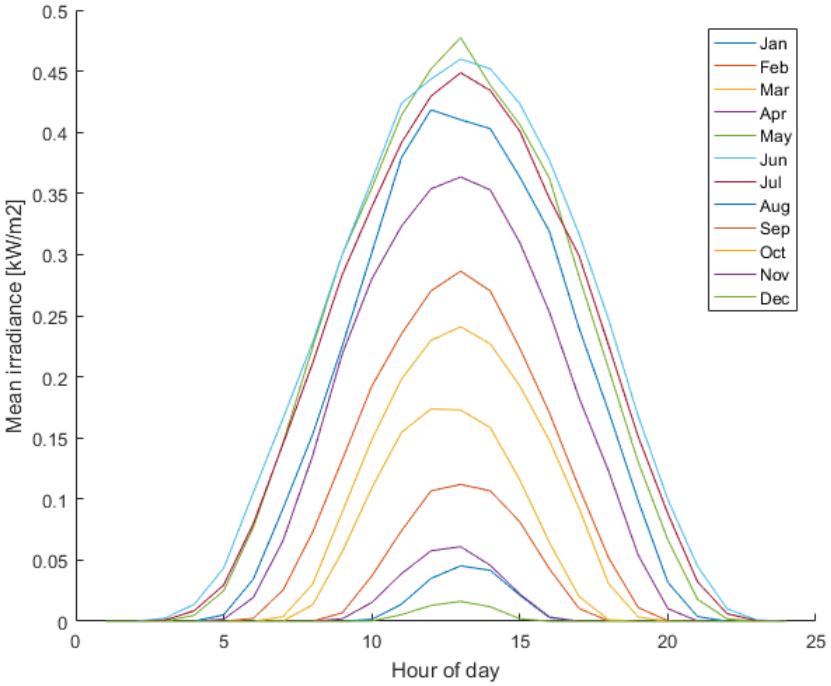

Figure 6.2: Historic hourly mean irradiance throughout the day for every month

every month of the year based on the historical data. As expected, this plot shows, in addition to a clear seasonality, a clear daily profile in the data set that needs to be preserved in the scenario generation routine. The data set was cleaned with linear interpolation. If night-time data entries were missing, zero-entries were inserted for the same amount of hours as the day before and after.

Irradiance observations are unfortunately not as common as wind speed observations. If no nearby observations can be found, a report produced by Multiconsult on behalf of Enova states that for irradiation estimation in northern countries, such as Norway, the commercial software Meteonorm is the best choice for obtaining irradiation data (Multiconsult, 2013).

6.1.2 Analyzing the load data

Trønder Energi has provided one full year of hourly measured load demand data from three substations located at Froan and Gjessingen. Before the measurement instruments were deployed, the only available load data was estimated consumption based on customer reporting. The substation with the most complete measurements was the station located at Sørburøy. Additionally, Sørburøy is the most populated island, and has a relatively stable load throughout the year. As shown in Table 6.1, it has the lowest variance for the full year, which facilitates the generation

of meaningful scenarios. Gjessingen, with its very few permanent residents and high number of vacation homes is prone to irregular sudden load spikes, creating the high variance shown. This is harder to replicate in a scenario generation routine. Therefore, we chose to use the load data from Sørburøy substation in the following analysis.

Table 6.1: Variance in load data

Substation	**Variance [kWh]**
Sørburøy (NS29050)	5.74
Nordøya (NS29060)	6.67
Gjessingen (NS29040)	8.28

The load data measurements were cleaned using the same method as for wind. Additionally, for the first month of measuring, the instruments experienced a malfunction due to wrong settings, and measured values on the wrong scale. By inspection we saw that by upscaling these values by a factor of 50, they were on the same level as the rest of the measurements, and had a comparable standard deviation to the consecutive month.

6.2 Scenario generation

We begin this section by providing a review of scenario generation techniques and examples from literature that are relevant for our problem, serving as motivation for our choice of method. We then explain the scenario generation algorithm used in this thesis, and conclude this section with a discussion regarding the resulting scenario generation algorithm.

6.2.1 Choice of scenario generation method

The stochastic elements in our model, being wind speed, irradiation and load, are all given in the form of large data sets. Being able to generate high quality scenarios that realistically represent the underlying stochastic processes, is key to our model providing valuable and practically viable solutions. As we are considering weather and load data, several decisions have to be made when choosing scenario generation method. We have to define how to replicate the stochastic processes in the most representative way without making the model too complex. We also have to account for dependencies between the different stochastic processes in the constructed scenarios. Other considerations are how to account for auto-correlations between consecutive data points, how to represent seasonal variations, and whether to create fitted distributions for the stochastic processes, or sample directly from the historical data.

Kaut et al. (2013) suggests ways to evaluate different scenario generation methods for stochastic problems, and provide a minimal requirement for approving a given method. But even when having chosen a good method, the resulting scenario tree might not perform as expected. For sampling methods, this is often due to poor sampling or too few scenarios. Too many scenarios, on the other hand, could lead to a significant increase in computation time.

In terms of sampling methods, one can either sample directly from historical data, or from a fitted distribution. Wind speed is often assumed to have a Weibull distribution (Nogueira et al., 2014; Li et al., 2012; Tina et al., 2006), while different distributions are fitted to irradiation as different sites may have different characteristics. Abdulkarim et al. (2015) concludes that in most cases, a beta distribution is preferable for irradiation, followed by a gamma distribution providing the second best fit. A normal distribution is the preferred distribution used to fit historical load data in most literature, among others in Kuznia et al. (2013) and Balachandra and Chandru (1999).

Generally, it can be argued that the quality of samples drawn from a fitted distribution is highly dependent on valid assumptions about the underlying historical data. Sampling from a fitted distribution might also not be appropriate when there is clear auto-correlations within the data, and correlation between different data sets. Sampling directly from the historical data, on the other hand, implies the assumption that data from the past represents the future. Both approaches require a high number of observations to ensure good representation of the underlying stochastic processes, but it is considered to be more crucial when sampling from historical data. If the data set is considered to be representative of both the stochastic process and the future, sampling from historical data eliminates the risk of making wrong assumptions of the distribution. An alternative to sampling is forecasting methods. Arabali et al. (2014) creates an ARMA model based on ten years of historical data in order to forecast a time series of wind, irradiation and load data.

Of the literature studied in this thesis, those presenting deterministic models pay significance to the creation of good representative load profiles. Sachs and Sawodny (2016a) split load measurements into days and use a k-means clustering algorithm to find the minimum amount of representative daily load profiles that still accurately estimates the behaviour of the system. Many articles discussing scenario generation for wind and load data use a similar line of reasoning, dividing a year into seasons described by days, or series of days, sampled from historical data or fitted distributions. Kuznia et al. (2013) use 12 seasons, one per month. They generate their load scenarios based on samples from a normal distribution fitted to historical data, while they create wind speed scenarios by multiplying observed historical wind speed with a random factor drawn from a triangular distribution.

As mentioned in the beginning of the chapter, it is important for us to define representative profiles, and a partition into seasons is therefore an interesting approach. Allowing each scenario to be related to a specific season, and consisting of a specified number of consecutive days, has proven to be a good way to create representative weather and load profiles without resulting in computationally intractable scenario trees. However, in the method used by Kuznia et al. (2013), each hour is drawn randomly from a fitted distribution representing the entire season, leading to difficulties when trying to account for the dependencies between wind speed, irradiation and demand. This challenge can be overcome by applying a moment matching algorithm based on subjective beliefs of the marginal distributions and correlations between the different hours in each season in the data sets (Høyland et al., 2003). But even with moment matching, there is no guarantee that the auto-correlation within each data set is reflected in the generated scenarios. As we consider it important to reflect the auto-correlation within each data set as well as the correlation between them in the scenarios that we generate, we have chosen to apply a variation of the method used in Seljom and Tomasgard (2015) and Skar et al. (2016).

Similar to Kuznia et al. (2013), Seljom and Tomasgard (2015) and Skar et al. (2016) divide the year into seasons, and sample scenarios as daily profiles from each season. This ensures that potential seasonality in the underlying data is preserved in the scenario generation method. Seljom and Tomasgard (2015) sample profiles from historical data, avoiding incorrect assumption about the distributions of the underlying stochastic processes. Furthermore, sampling from historical data takes into account the hourly correlation between the different profiles, while preserving the auto-correlation within each profile and scenario. This approach is considered appropriate, by the assumption that historical weather and load data is representative for the future. Furthermore, a sufficiently high number of observations are usually available when discussing weather data.

When sampling from historical data, a scenario is sampled by randomly selecting a day within the season, and the same day is sampled for all of the profiles (wind speed, irradiation and load). It is unlikely that the exact same realizations will occur in the future, but together with several other scenarios they can be used as representative days. A scenario tree is constructed from a set number of scenarios from each season. In order to ensure that the scenario trees reflect the characteristics of the underlying historical data in a satisfying manner, several trees are created and evaluated against the moments of the historical data. Using an approach similar to this, we are able to create scenario trees that preserves the characteristics of the historical data, while accounting for the auto-correlation within each generated scenario. The specifics of the scenario generation algorithm applied in this thesis is presented in the following section.

6.2.2 The scenario generation algorithm

For the purpose of generating scenarios trees, we propose an iterative random sampling method, as described in Algorithm 1. The input data is the pre-processed wind, irradiance and load data, partitioned into monthly sets.

Algorithm 1: Scenario generation

Data: Pre-processed historicaldata

Result: A scenario tree matching the underlying historical data

1. Calculate the four first moments (see Appendix E) for the stochastic parameters wind speed and irradiance for every hour of the day (1-24) in every month of the historical data;

for *U scenario trees* **do**
  for *M months* **do**
    for *S scenarios* **do**
      2. Randomly sample $|T_t^O|$ consecutive hours from the historical data time series;
    end
    3. Calculate the four first moments for the stochastic parameters for every hour;
  end
end

4. Create a final scenario tree by combining parts of the trees that have the lowest absolute deviation in statistical moments from the underlying data for every month (see Appendix E for details);
5. Include in scenario tree the load demand data from the same time periods of the year as is used to represent the wind and irradiance, and verify that mean and variance for load is acceptable;
6. Verify that scenarios follow same distribution as historical data.

In item 2 of the scenario generation algorithm, a starting hour is sampled from a population consisting of all hour 1's (00:00-01:00) from a given month in the historical data. Then, the $|T_t^O|$ consecutive hours after that hour is sampled into the scenario tree. By starting the sample only from the first hour of the day, we avoid unintended start and end effects that arise due to the cyclic nature of irradiance data. It also makes the moment comparison less complicated as the first entry in every scenario will always be an hour 1 entry.

As there is a large discrepancy in the amount of historical data obtained for the load demand and the weather data, a simple way of including load data in the scenario tree, as shown in item 5, is conducted. It is deemed likely that obtaining load data in general is considerably more difficult than obtaining weather data, and that this is a common challenge met when attempting to solve the MISSMDP. As there is no way of accurately gaining historical data that has not been measured, and we have only one year of historical load data to sample from, the true correlation between weather data and load data is impossible to account for. However, an attempt to capture at least some of the seasonal correlation is done by sampling from the same month of the year. This is an obvious weakness of the scenario generation method, but with the data available it is

necessary to assume that only accounting for the seasonal correlation between load and weather data is sufficient.

Finally, in item 6 of the algorithm, we verify that the generated scenarios follow a similar distribution as the historical data. This is done by fitting a distribution to both the historical data sets, and to the generated scenarios, and then comparing the parameters. Figures 6.4-6.5 show an example of verification of the distribution of wind speed, irradiance and load, for a scenario tree with 30 scenarios and 72 operational periods. From the figures, and from inspection of the fitted distribution parameters, it is evident that the scenario generation method is able to produce probability distributions that match the probability distributions of the historical data.

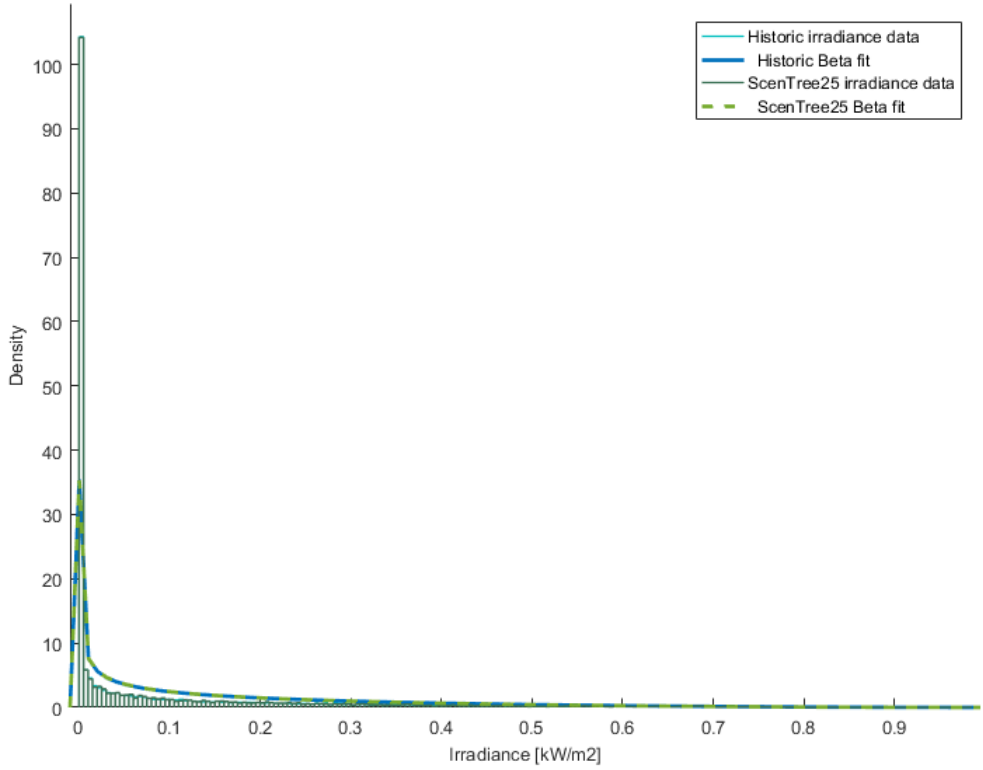

Figure 6.3: Probability distribution of historical irradiation data and a generated scenario tree

The scenarios contained within each scenario tree, constitutes the representative days of operation for the system. The number of scenarios, S, that are needed, depends on the underlying model and data set. With too few scenarios, the solution we obtain when solving the model may depend on the scenario representation, where each sample provides a different solution or objective value. This is unfavourable, as the model should rather be depending on the underlying stochastic data. If a stochastic model depends on the scenario representation it is said to be unstable. It is, however, desirable to use as few scenarios as possible, considering computational

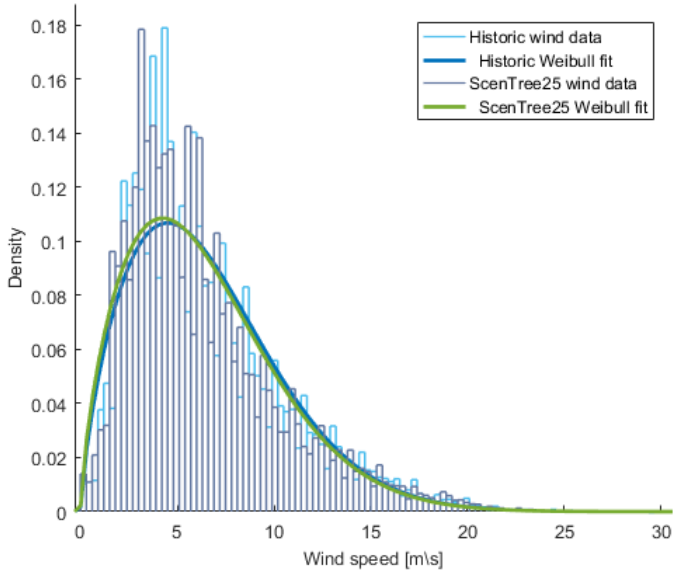

Figure 6.4: Probability distribution of historical wind data and a generated scenario tree

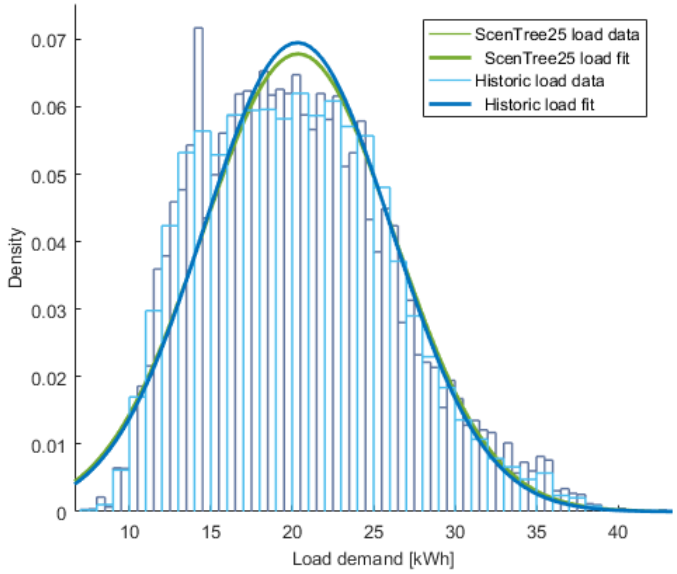

Figure 6.5: Probability distribution of historical load data and a generated scenario tree

intractability, as long as the stability requirements are satisfied (Seljom and Tomasgard, 2015). To determine how many scenarios the scenario tree should consist of, and to evaluate if the proposed scenario generation method results in stable solutions, in-sample and out-of-sample stability testing (Kaut et al., 2013) is performed in Chapter 7.4.

6.3 Evaluation of input parameters

The input parameters are related to the instances we define for the MISSMDP. These instances are defined in Chapter 7, and each instance consists of parameters related to a set of production technologies available for the DM. For the case we test the MISSMDP on (Sørburøy), the technical parameters are equal, and the only difference between the instances is the length of the strategic horizon. The numeric values for the technical parameters are found in Appendix D, while the rest of this section elaborates on how the input parameters have been obtained and manipulated to fit the MISSMDP.

6.3.1 Scaling Factor

As we create scenario trees consisting of representative scenarios, each scenario will contain only a few days of actual operation. Thus, for several of the considerations in the model, an adjustment is necessary in order to represent the full year of operation. A scaling factor is therefore defined in Equation (6.1), where $|T_t^O|$ is the amount of operating periods in each scenario.

$$\theta^{oc} = \frac{8760h}{|T_t^O|} \tag{6.1}$$

First of all, this scaling factor is used in the objective function to upscale the recourse costs in the model, making them realistic and comparable to the first-stage costs. The scaling factor is also included in the definition of maximum cycles for the Li-ion battery systems, elaborated on in the next section.

6.3.2 Battery Parameters

In Equation (5.9), from Chapter 5.7, the value of the big-M parameter M^B, used to reset the battery lifetime variable, is dependent on the defined maximum cycles of the battery, L^B. According to the product warranties of several manufacturers of Li-ion batteries, a battery should be able to perform 10 000 full cycles over the duration of its lifetime (Saft SA, 2014; sonnen, 2016). The scaling factor, defined in Chapter 6.3.1, is used to downscale the maximum amount of cycles from 10 000, to a number that can be compared to the representative operational scenarios. Our definition of L^B is then given as

$$L^B = \frac{10000}{\theta^{oc}} \tag{6.2}$$

Another important battery parameter is the total allowed capacity degradation throughout its lifetime, R^B. Tesla, Inc., sonnen, Inc. and Saft SA, which are all large manufacturers of Li-ion batteries, warrants that their batteries retains 70% of its initial energy storage capacity during the warranty period (Saft SA, 2014; sonnen, 2016; Tesla, 2017). Accordingly, we assign the total degradation of the battery unit during its lifetime, R^B, to be 30%.

All remaining technical parameters and costs related to the battery units are provided by Trønder Energi. Investments costs include both installation and transportation. In accordance with assumption 2, maximum charging and discharging power of the battery unit ($\bar{P}^{B+}$ and $\bar{P}^{B-}$) are defined as equal to maximum recorded historical load measurement.

6.3.3 Diesel generator parameters

As mentioned in Chapter 5, the fuel consumption of the diesel generator in l/h is dependent on the power produced in kW and the size of the generator. In other words, a low capacity generator might use less fuel per hour at 10 kW than a high capacity generator. Some examples of fuel consumption relationships for different sized generators are found in Figure 6.6. We have obtained data on fuel consumption for generators based on the load level at which it is operating from technical product information provided by manufacturers.

For the plots in Figure 6.6, linear regression models provide good approximations for the fuel consumption. Based on this observation, we aggregated the fuel consumption data for all generators included in our instance, resulting in the scatter plot in Figure 6.7. If we apply a linear regression model, we get a good linear fit for the scatter plot with an acceptable R-squared value. I.e. it seems that the effects of size on the fuel consumed at different production levels is small. The linear fit in Figure 6.7 is the fuel consumption curve used in the original diesel generator formulation, with A^F, B^F and binary variable β^G_{etos}.

In an effort to remove the binary variable from the formulation, we suggested an alternative diesel generator model in Chapter 5.5. This model relies on a linear relationship between power production and fuel consumption where the intercept coefficient B^F is equal to zero. We have tested a variety of methods approximating the linear fit without either overestimating or underestimating the fuel consumption, and we find that the following method resulted in a good approximation, preserving the characteristics of the original linear fit.

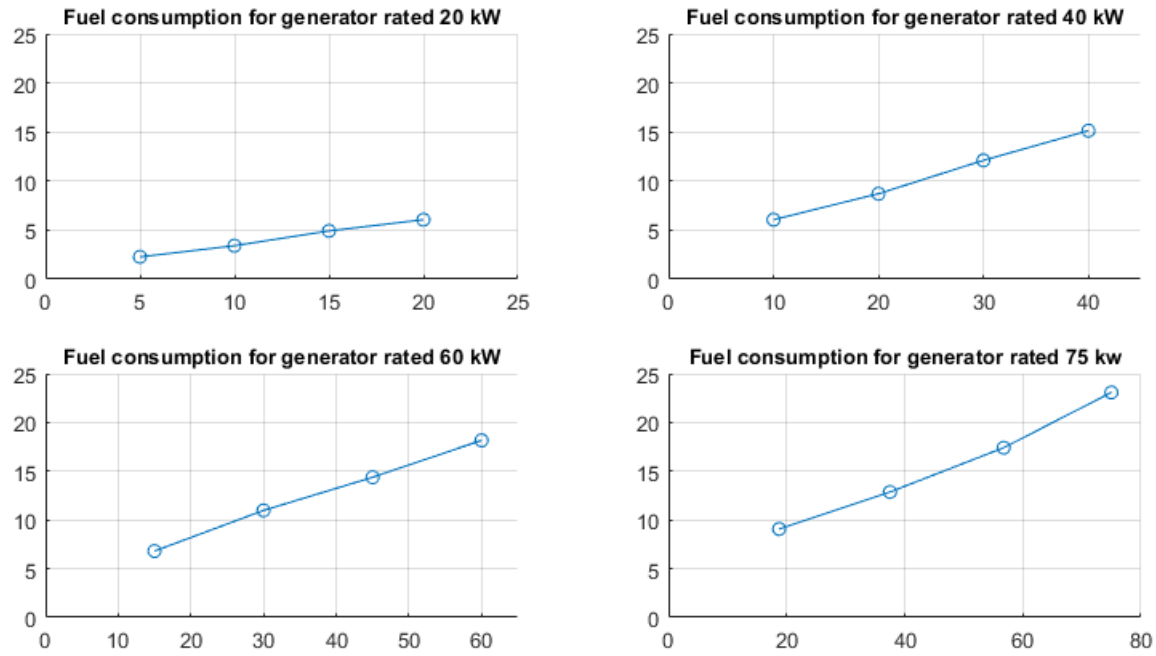

Figure 6.6: Fuel consumption curves for generators of different sizes; production in kW on x-axis; consumption in l/h on y-axis

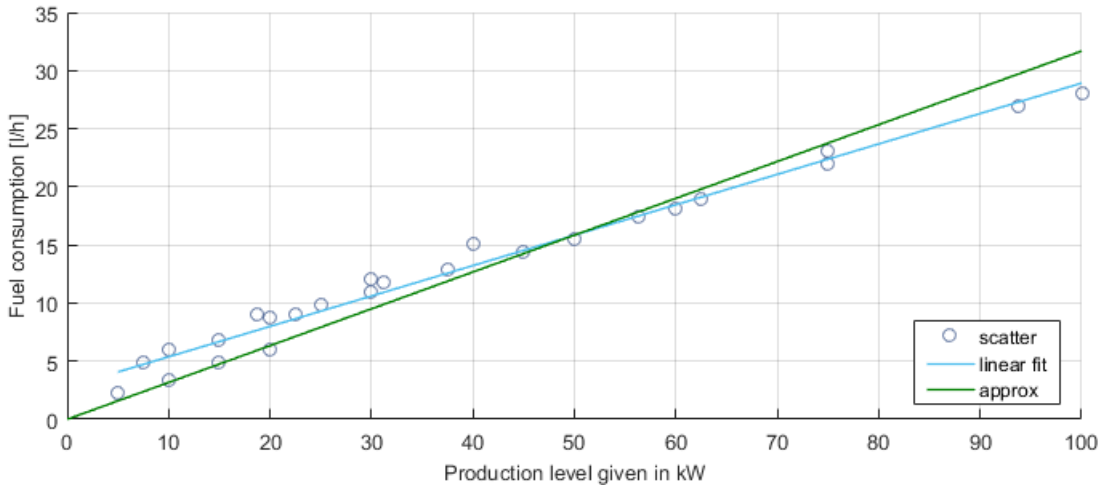

Figure 6.7: Aggregated fuel consumption scatter plot for diesel generator with linear regression and approximated fit

We construct a curve that intercepts with the linear fit to the scatter plot at the center of the observed range of power production, i.e the centre of the range on the x-axis. The slope of this curve is found by the following relationship:

$$A^{F,new} = \frac{(B^F + A^F P^{max}/2)2}{P^{max}} \tag{6.3}$$

The constructed curve is referred to as *approx* in Figure 6.7. For lower production levels, the curve slightly underestimates the fuel consumption, while it represents an overestimation for higher production levels.

Regarding the remaining parameters for the diesel generator, the maximum share of production allowed from the diesel generator within one strategic period, $\bar{R}^G$, as well as fuel costs, C^F, are defined by Trønder Energi. All other technical parameters and the investments costs for the diesel generators are based on estimates. The investment costs include installation costs, but not transportation costs as they are considered fixed and of little consequence to the final investment decision.

6.3.4 Wind Parameters

Parameters regarding wind turbines are provided by Trønder Energi, based on a selection of wind turbines deemed relevant for the case study. Investment costs include installation and a 100 000 NOK estimate for transportation costs, as transportation costs can be considered a marginal cost directly related to each wind turbine.

6.3.5 PV parameters

Parameters regarding PV-panels are also provided by Trønder Energi and include installation and inverter cost. An additional 15 000 NOK in fixed transportation costs is expected. As transportation costs are fixed and not directly proportional to amount of PV-panels, it is overlooked in the optimization procedure itself as we assume that PV-panels will be installed. Transportation costs may simply be added to the objective function after a solution is found.

6.3.6 Value of lost load

In Chapter 5.4, we assign a cost to not covering load in the objective function of the MISSMDP. This cost, C^L, is referred to as the value of lost load (VOLL), or a rationing cost. The actual numeric value of this cost is not clearly defined, and difficult to determine, especially for an

islanded microgrid. Recall that in Chapter 2.2, it is specified that for Trønder Energi and the Island Project, there is an obligation to supply the same level of security in terms of equal or lower LOLP than what citizens on the islands are currently experiencing. Defining a VOLL leading to the desired LOLP for the island project requires a comprehensive analysis that is beyond the scope of this thesis. Instead, we assume that the choice of not covering load should not be a realistic one in the model, and define the VOLL accordingly. The numeric value of the VOLL is therefore set artificially high at $1000.

Chapter 7

Computational study

This chapter describes the different tests that are carried out in order to evaluate the performance of the MISSMDP. The chapter begins with an introduction to the hardware and software used when running the different test instances, before the test instances themselves are introduced and described. The rest of the chapter includes a technical analysis focusing on the computational performance of the program, followed by a consideration and evaluation of the practical performance of the program.

The technical analysis begins with a discussion of the two suggested diesel generator formulations. This discussion is partially practical, but it is the technical performance that is tested. Next, we test the stability of the scenario generation algorithm, i.e. in-sample stability and out-of-sample stability. The stability testing allows us to evaluate the quality of the generated scenario trees for the MISSMDP, and provides a conclusion on the configuration of the parameters in the algorithm. We then move on to suggest and study some improved implementations, including simple heuristics and speed-up strategies.

The practical evaluation consists of two parts. The first part being Chapter 7.6, where the value of information and the stochastic modelling is evaluated, as well as the value of a more detailed battery formulation. The last part of the computational study provides a discussion of the actual practical performance of the solutions to the MISSMDP. All values of computation time are given in seconds, and all costs are given in USD.

7.1 Hardware and software

The computational study is performed on Solstorm HPC on an Intel® E5-2643v3–6 Core™ CPU processor at 3.40 GHz and 512 GB RAM. The software used is FICO® Xpress Optimization Suite, with Xpress Optimization Suite versjon 8.0.4, subsequently referred to as Xpress. All tests are executed directly from the mentioned software. All details are listed in Table 7.1.

Table 7.1: Details of computer and solver used in computational study

Console	Lenovo Nextscale nx360 M5
Processor	CPU: 2 x 3.40 GHz Intel® E5-2643v3–6 Core™
RAM	512 GB
Disk	120 GB SATA SSD
Operating system	Linux 2.6.32-642.el6.x86_64 (x86_64)
Xpress Optimization Suite version	8.0.4
Maximum computation time	200 000 seconds
Optimality gap tolerance	0.7%

The relative optimality gap tolerance is defined at 0.7% as any lower gap results in increased computation time and has a negligible effect on the optimal first-stage decisions. As the MISS-MDP is a strategic planning tool, there are no pressing arguments for stopping the solution process before optimality is reached. It is considered to be more interesting to study the results after having reached the desired optimality gap, rather than how well the model performs given a predefined limitation on maximum computation time. Accordingly, the maximum computation time is defined as 200 000 seconds.

7.2 Test Instances

The computational study focuses on the case of Sørburøy. We have defined four instances with varying length of the strategic horizon. The technical parameters described in Chapter 6 are common for all instances. All tests are performed on the full model found in Appendix B, including all extensions proposed in Chapter 5.6, unless otherwise stated.

Instance number 1 and 2 have the shortest strategic horizons, and are employed for studies where there is no need to analyze the full strategic horizon, or in preliminary studies to provide a basis for further computational studies. Instance 1 and 2 are also utilized in some of the speed-up strategies and heuristics suggested later in this chapter.

Instance number 3 and 4 have longer strategic horizons, and are the instances that a DM realistically would study. These are used for both the technical and the practical analysis. All instances are listed in Table 7.2

Table 7.2: Instances

Instance	Substation	Strategic periods
1	Sørburøy (NS29050)	5
2	Sørburøy (NS29050)	10
3	Sørburøy (NS29050)	20
4	Sørburøy (NS29050)	30

7.3 Diesel generator formulations

In Chapter 5, we presented two different diesel generator formulations, one based on the binary variable β^G_{etos}, and one simplified continuous formulation. The motivation for suggesting the continuous formulation was the realization that a disproportionate amount of the computation time was spent branching on the generator binary variable. In this section, we test both formulations, to determine if the simplified continuous formulation is a good approximation of the original generator model.

In the following discussion, we refer to the binary formulation as *GEN1*, and the continuous formulation as *GEN2*. Both formulations are tested on a scenario tree with 72 operational periods, and 30 scenarios in each season (a total of 360 scenarios), on instance 1 and 2 (5 and 10 strategic periods). Computation time, first stage decisions, generator behaviour and objective value are the different factors that we analyze.

Table 7.3: Results from testing the different generator formulations, $\Delta\%_{RC}$ is the relative change in computation time, $\Delta \mathbf{z}^*$ is the absolute difference in objective values, and $\Delta \mathbf{z}^*_{RC}$ is the relative change from *GEN*1.

	Computation time			Objective value			
Instance	*GEN1*	*GEN2*	$\Delta\%_{RC}$	*GEN1*	*GEN2*	Δz^*	Δz^*_{RC}
1	53,723	1,994	-96.3%	8,568,154	8,542,262	-25,892	-0.30%
2	200,000	8,390	-95.2%	13,158,035	13,122,943	-35,092	-0.27%

From Table 7.3, we observe a distinct decrease in computation time from *GEN1* to *GEN2* for both instances, with relative improvements above 95%. The objective values are very similar

for both formulations, but we see that *GEN2* slightly underestimates the objective value compared to *GEN1*. However, the difference is small, and we record relative changes of less than 0.3%. For instance 2 and *GEN*1, the computation was interrupted when reaching maximum computation time. At this point, we observed an optimality gap of less than 3%, and a current best objective value similar to that recorded from the same instance on *GEN*2. Results from further testing on instance 1 for three additional scenario trees with similar properties are rendered in Table 7.4. These tests yielded similar results and conclusions as those drawn from the initial tests in Table 7.3, confirming the validity of these results. We will not comment on the stability of the scenario generation algorithm in this section, our only motivation for evaluating more trees is to strengthen our analysis of the difference between the performance of the two diesel generator formulations.

Table 7.4: Further results from testing *GEN*1 and *GEN*2 on instance 1.

		Computation time			**Objective value**			
Inst.	**Tree**	*GEN1*	*GEN2*	$\Delta\%_{RC}$	*GEN1*	*GEN2*	Δz^*	Δz^*_{RC}
1	1	53,723	1,994	-96.3%	8,568,154	8,542,262	25,892	-0.30%
1	2	38,835	1,314	-96.6%	9,234,216	9,209,763	24,454	-0.26%
1	3	11,970	1,226	-89.8%	8,974,604	8,968,268	6,336	-0.07%
1	4	67,888	1,289	-98.1%	8,447,001	8,444,974	2,027	-0.02%
Avg.		*43,104*	*1,456*	*95.2%*	*8,805,994*	*8,791,317*	*14,677*	*0.17%*

As the MISSMDP is a strategic model, we are inclined to accept simplifications that lead to different operational solutions, as long as we record a substantial improvement in computational performance together with stable strategic decisions (first-stage investment decisions). We have commented on the clear computational benefits of *GEN*2, and proved that the objective value is stable. Inspecting the value of the decision variables, we find that for both instances and all scenario trees, there are few differences in the first-stage decisions between the two formulations. In Figure 7.1, the division of cost between investment decisions and operational decisions for the four runs on instance 1 is shown explicitly, confirming the stability of the first-stage solutions.

Inspection of the operational solutions obtained when testing *GEN*1 and *GEN*2 on the MISSMDP, revealed that the diesel generator is operated in very few of the operational periods. This is due to the maximum limit on energy produced from the diesel generator enforced in Constraints (3). Within the periods where the generator is running, we did however record a high share of occurrences where the diesel generator was found running below minimum limits for *GEN*2. For instance 1 and tree 1, the generator was below 20% of capacity in 21% of the periods where it was running, and below 30% in 42% of the periods. For instance 2, the generator was below 20% of capacity in 22% of the periods, and below 30% in 43%.

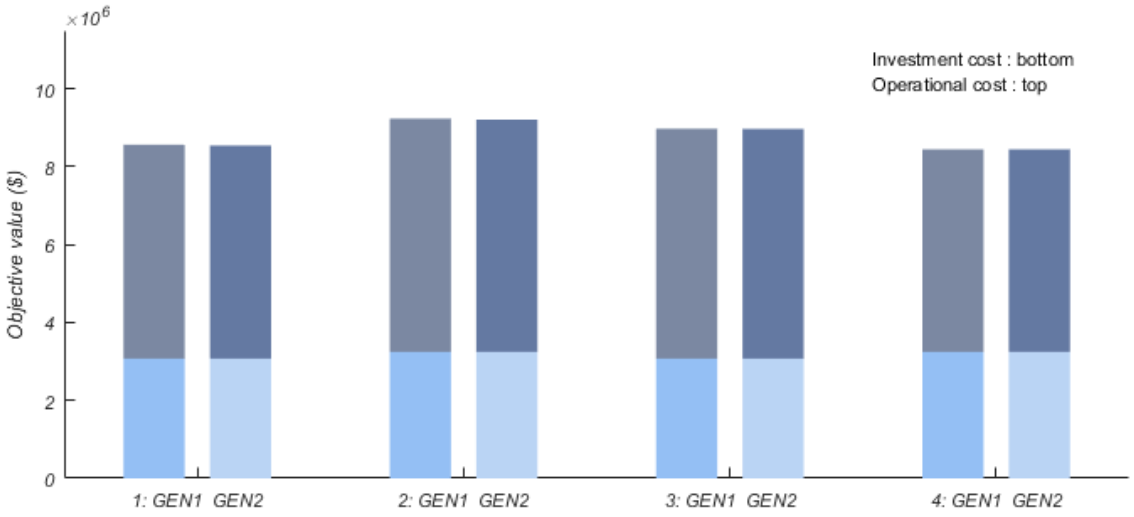

Figure 7.1: Objective values for *GEN*1 and *GEN*2 on all four tests on instance 1. Bottom parts are investment costs, top parts are operational costs.

It is clear that the lack of restriction on minimum ramping in the continuous formulation (*GEN*2), leads to less realistic operational solutions. However, the objective value and the strategic decisions are barely affected by the simplification. As the MISSMDP is a strategic model that is not recommended for operational planning, we consider the number of occasions where the generator is running at low values to be acceptable and of little consequence. Furthermore, the significant gain in computational performance is immensely important in overcoming the computational intractability of the binary formulation, especially if aiming at solving the more realistically sized instances (3 and 4). Based on these arguments, the diesel generator formulation chosen and used in the rest of the computational study is *GEN*2.

7.4 Stability testing

The major goal of scenario generation is to obtain a small optimality gap. By optimality gap, we refer to the difference between the value obtained with the true objective function at the optimal solutions of the true and the approximated problem (Kaut and Wallace, 2003). It is however not always possible to estimate the optimality gap, as it requires solving the problem with the true random vector. Solving the problem with the true random vector is rarely doable for most practical cases. In these cases, other weaker requirements such as "stability" can be used to evaluate the fitness of a given scenario generation method. In this section, we first provide some theory on evaluation of a scenario generation method, before we introduce the stability tests that we will use to evaluate our scenario generation algorithm for the MISSMDP. In order

to present both theory and tests, we begin by introducing some notation. The notation is similar to that used in Kaut and Wallace (2003), and the theory presented here is based on their work.

First, "true" random variables are denoted as $\tilde{\xi}$, random variables connected to a scenario tree as $\hat{\xi}$, and single realizations being sample points or scenarios as ξ. In testing a scenario generation method, we are less concerned with how well the method approximates the underlying stochastic processes, and more concerned with if it is able to produce stable solutions. Equation (7.1) defines the error of approximating a random vector $\tilde{\xi}$ by $\hat{\xi}$ mathematically, where F is the true objective function, $\hat{\mathbf{x}}^*$ is the optimal solution of the approximated problem, and z^* is the optimal objective of the true problem.

$$e(F,\hat{F}) = \ldots = F(\hat{\mathbf{x}}^*) - z^* \tag{7.1}$$

As it is not doable to solve our problem with the true random vector, we evaluate our scenario generation algorithm by testing different requirements of stability. Kaut and Wallace (2003) present two types of stability tests that we apply to the MISSMDP, being out-of-sample stability and in-sample stability testing.

It is important to notice that in evaluating the optimality gap, or in our case the stability measures, we compare the values of the objective function, not the actual optimal solutions. Kaut and Wallace (2003) stress that, as there typically exists different solutions leading to similar objective values for a stochastic programming problem, it is not thought wise to consider different solutions leading to similar objective values as a sign of instability.

7.4.1 In-sample stability

In-sample-stability refers to stability when evaluating the solutions on the scenario tree that they came from. If a scenario generation method has in-sample stability, it means that regardless of what scenario tree we use, generated based on the same data and with the same settings, the optimal objective value reported by the model itself should be the same (or approximately the same).

In order to test in-sample stability, one first has to generate a number of scenario trees K by running the scenario generation algorithm several times on the same input and with the same settings. For each scenario tree $\hat{\xi}_k$, the optimization problem is solved and the optimal solution $\hat{\mathbf{x}}_k^*$ is obtained. The stability requirement as defined by Kaut and Wallace (2003) is then given as

$$\hat{F}_k(\hat{\mathbf{x}}_k^*) \approx \hat{F}_l(\hat{\mathbf{x}}_l^*) \tag{7.2}$$

Having in-sample stability ensures that each time we run the scenario generation algorithm, and then solve the optimization program, we obtain objective values that are approximately the same and therefore stable. Without in-sample stability, we produce random results, and we may get good solutions without being able to verify their quality.

7.4.2 Out-of-sample stability

The term out-of-sample stability refers to judging the stability of a solution on a different scenario tree than what was used to obtain it. If we can prove that we have out-of-sample stability, we know that the real performance of a solution $\hat{\mathbf{x}}_k^*$ does not depend on which scenario tree $\hat{\xi}_k$ we choose. Kaut and Wallace (2003) state the requirement of out-of-sample stability in the following way: *"If we generate several scenario trees (discretizations $\hat{\xi}$) for a given random vector $\tilde{\xi}$, and solve the stochastic programming problem with each tree, we should get approximately the same value of the true objective function."* This relationship is given mathematically in equation (7.3).

$$F(\hat{\mathbf{x}}_k^*) \approx F(\hat{\mathbf{x}}_l^*) \tag{7.3}$$

Again, we notice that we are only able to test this stability measure if we are able to evaluate the true objective $F(\mathbf{x})$. For our problem, this is not possible. There does however exist a weaker form of out-of-sample stability that can be tested for the MISSMDP, given as

$$\hat{F}_k(\hat{\mathbf{x}}_k^*) \approx \hat{F}_k(\hat{\mathbf{x}}_l^*) \tag{7.4}$$

$$\hat{F}_l(\hat{\mathbf{x}}_l^*) \approx \hat{F}_l(\hat{\mathbf{x}}_k^*) \tag{7.5}$$

and accordingly

$$\hat{F}_k(\hat{\mathbf{x}}_l^*) \approx \hat{F}_l(\hat{\mathbf{x}}_k^*) \tag{7.6}$$

If we have out-of-sample stability without in-sample stability, we will not know how good our solutions really are. If we have in-sample stability without out-of-sample stability, our solutions might depend on the scenario tree. We will therefore test the MISSMDP for both types of stability, beginning with in-sample.

7.4.3 Testing the stability of the MISSMDP

Before we begin the stability testing of the MISSMDP, we introduce a proposition that arose in discussions prior to conducting the stability tests. The proposition is related to the multi-horizon information structure in the MISSMPD, more specifically to the uncertainty of the problem being isolated to the operational horizon.

Proposition 7.1. *The in-sample stability of a multi-horizon optimization program with operational uncertainty deteriorates with increasing number of strategic periods.*

The validity of proposition 7.1 depends on the structure of the decision variables and their related costs. In the MISSMDP, a high investment cost incurs in the first strategic period. In the consecutive strategic periods, costs are related to the operational decisions, and the odd reinvestment in batteries. The reasoning behind proposition 7.1 is that due to high investment costs, the relative increase in average total costs by adding a strategic period to the problem is smaller than the relative increase in total error. This reasoning also implies that as strategic periods are added to the problem, the initial investment cost becomes less dominating, and the effect of proposition 7.1 will gradually diminish. Proposition 7.1 should therefore be evaluated and understood in relation to proposition 7.2.

Proposition 7.2. *The effect proposed in proposition 7.1 diminishes with increasing number of strategic periods.*

How fast the effect of proposition 7.1 diminishes will depend on how dominating the cost of the initial investment is. The validity of both propositions for the MISSMDP is discussed after having obtained the results from the stability tests. The concern is that if the effect of proposition 1 proves to be dominating, the stability tests might not be a good measure of the fitness of a scenario generation method for the multi-horizon problem formulation, and other measures should be considered.

In-sample stability testing

In testing the in-sample stability of the MISSMDP, we wish to quantify how the scenario generation algorithm performs on all relevant instances. Additionally, we want to determine the numerical value of two parameters; number of scenarios in the scenario tree, and the length of the operational horizon. For the purpose of determining an appropriate number of scenarios and operational periods, we have tested the combinations of operational horizons and number of scenarios listed in Table 7.5. The combinations are tested on a low number of strategic periods for computational simplicity. This is considered sufficient for determining the parameters because of the multi-horizon structure of the problem, as it simply reiterates the same scenario tree during the strategic horizon. To verify this claim, the tests have been performed on both 5 and 10 strategic periods (instance 1 and 2). If the claim holds, the results from all combinations with instance 1 should yield the same decisions with respect to operational horizon and number of scenarios as the results from all combinations with instance 2. After deciding on number of scenarios and operational periods, further testing is performed on the chosen configuration for the remaining instances.

Table 7.5: Combinations tested for deciding parameters in in-sample stability testing

Combination	Instance	Strategic	Operational	Scenarios
A	1	5	48	10, 20, 30, 40, 50
B	2	10	48	10, 20, 30, 40, 50
C	1	5	72	10, 20, 30, 40, 50
D	2	10	72	10, 20, 30, 40, 50
E	1	5	96	10, 20, 30, 40, 50
F	2	10	96	10, 20, 30, 40, 50

The selection of operational horizons was chosen based on the characteristics of our problem, especially considering that each operational scenario has to be sufficiently long to capture the behaviour of the battery. As the battery rarely performs more than one full cycle within 24 hours, it is preferable to study 48 hours or more. Too long operational horizons, however, leads to increased computation time. In accordance with this line of reasoning, we have tested horizons of 48 hours, 72 hours and 96 hours (two, three and four days). For all horizons, we have tested from 10 up to 50 scenarios, with increments of ten. The given number of scenarios refers to number of scenarios per month. I.e. 30 scenarios implies that the tree itself consists of $30 \times 12 = 360$ scenarios.

For all combinations in Table 7.5, we create ten scenario trees using the scenario generation procedure explained in Chapter 6. Each tree is chosen from 10 000 randomly sampled trees based on statistical fit with the underlying historical data. The objective value, $\hat{F}_k(\hat{\mathbf{x}}_k^*)$, is recorded

from each run. For the ten runs on the same combination from Table 7.5 and a specific number of scenarios, we calculate the average objective value, the standard deviation, and subsequently the coefficient of variation (CV). The CV provides a measure of the extent of variability in relation to the mean, more precisely a measure of the precision and repeatability of the results obtained from different scenario trees. It is therefore the CV that is evaluated in order to determine if $\hat{F}_k(\hat{\mathbf{x}}_k^*) \approx \hat{F}_l(\hat{\mathbf{x}}_l^*)$. The results from the tests are portrayed in Figure 7.2, where the x-axis is number of scenarios, and the y-axis is the CV (%). Each curve represents the development of CV for a combination in Table 7.5.

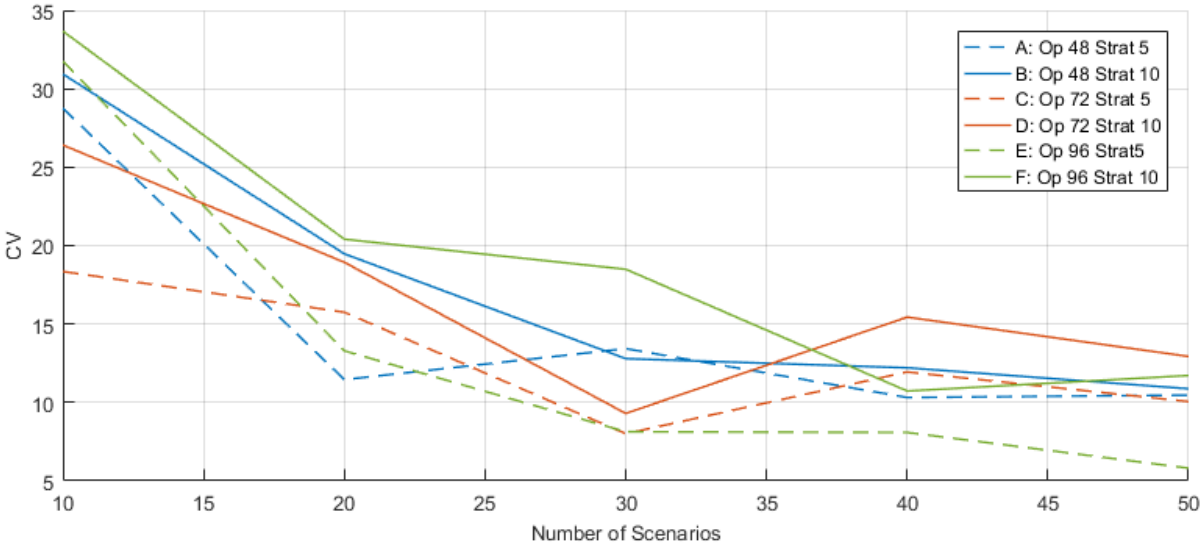

Figure 7.2: Average Coefficient of Variation [%] from in-sample stability tests on instance 1 and 2

The plots in Figure 7.2 show that the CV experiences a distinct improvement from 10 to 20 scenarios for all combinations, and a slight improvement from 20 to 30 scenarios for most combinations. After 30 scenarios there are only small improvements of the CV for some combinations, and slight aggravation for others. At 30 scenarios, the CV stabilizes around 10-15%, suggesting that increasing the number of scenarios will not necessarily improve the in-sample stability of the MISSMDP. Furthermore, there are only small deviations in the first-stage solutions obtained for each individual scenario tree at 30 scenarios. These arguments suggest that the in-sample stability of the MISSMDP is satisfactory at 30 scenarios for the purpose of strategic planning. A final conclusion on 30 scenarios is supported by the plots in figure 7.3. We observe that by increasing the number of scenarios above 30, the computation time rises for all combinations. While the impact of increasing the number of scenarios above 30 is small and inconclusive on the CV, it is clear on computation time, and we conclude that the in-sample stability of the model is satisfactory at 30 scenarios.

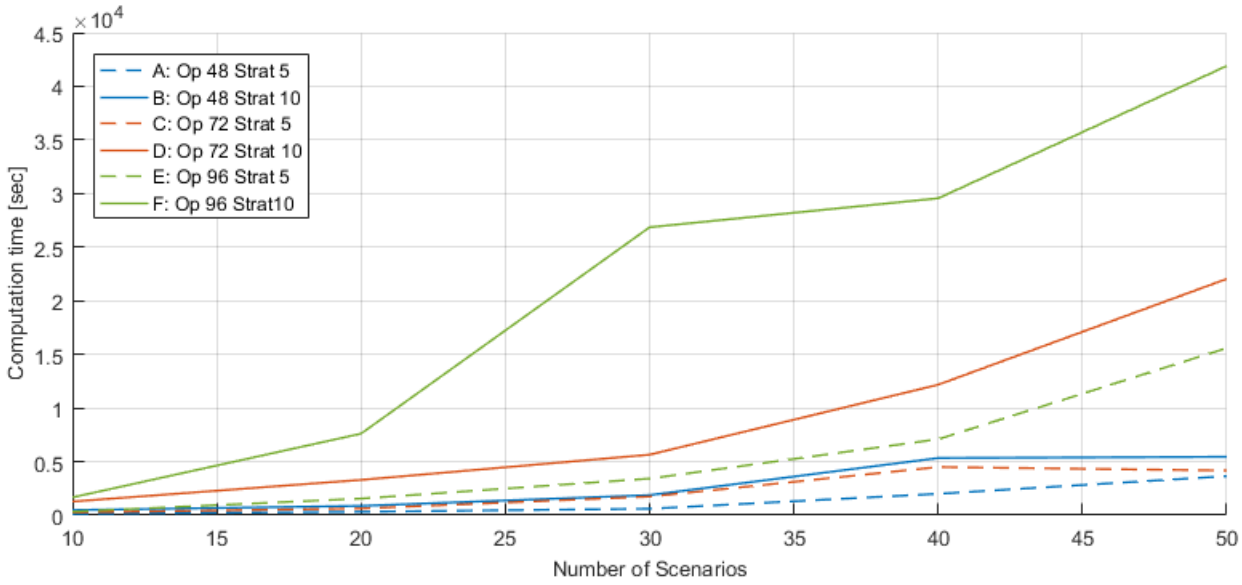

Figure 7.3: Average computation time for in-sample Stability tests on instance 1 and 2

Solving the model on 5 and 10 strategic periods (instance 1 and 2) suggest similar trends for the development of in-sample stability. This confirms our assumption of the validity of testing in-sample stability on shorter strategic horizons for the purpose of determining the operational horizon and number of scenarios. In accordance with proposition 1, we also observe that the CV in general is worse for instance 2 for a given combination of scenarios and operational periods.

Studying the development of average computation time for the combinations in Table 7.5 (Figure 7.3), we see that the combinations with a higher number of operational and strategic periods are the most computationally demanding. There is also a clear trend that for the higher number of operational periods, the difference in computational time between instance 1 and 2 is drastically larger for all number of scenarios. Thus, by choosing a number of operational periods higher than 72, one stands to gain little in terms of scenario tree stability, while gaining a substantial amount of computation time. Based on overall performance, on both computational time and CV, we have therefore chosen to proceed with 72 operational periods and 30 scenarios for further testing.

Finalizing the in-sample stability testing, we test instance 3 and 4 on 72 operational periods and 30 scenarios. The procedure is the same as for the initial tests, and the results for all instances are presented in Table 7.6. The final in-sample stability tests, support the conclusion that 30 scenarios and 72 operational periods produce results that are stable enough for further testing of the model; the stability is maintained for a realistic number of strategic periods, and the in-sample stability does not seem to give conclusive indication of improvement with increasing number of neither operational periods nor scenarios.

Table 7.6: Results from in-sample stability testing. CV is calculated over ten runs, $^{\Delta CV}/_{\Delta|T^S|}$ is the change in CV relative to increase in strategic periods.

Instance	**1**	**2**	**3**	**4**
Strategic periods	5	10	20	30
CV	*8.0%*	*9.3%*	*10.6%*	*11.0%*
ΔCV	-	1.3%	1.3%	0.4%
$\Delta\|T^S\|$	-	5	10	10
$^{\Delta CV}/_{\Delta\|T^S\|}$	-	*0.26%*	*0.13%*	*0.04%*

Earlier in this chapter, we proposed that the in-sample stability of the MISSMDP would deteriorate with increasing number of strategic periods (proposition 1), but that this effect would be diminishing for a problem with similar cost structure to the MISSMDP (proposition 2). In Table 7.6, the change in CV relative to the increase in strategic periods ($^{\Delta CV}/_{\Delta|T^S|}$) is included in the last row, providing proof of proposition 1 as all values are positive. In accordance with proposition 2, the effect of proposition 1 is diminishing with increasing number of scenarios. As the effect of proposition 1 is small to begin with, and fast diminishing, we find that the stability tests remain a good measure of the fitness of the scenario generation algorithm for our model.

The multi-horizon structure provides the possibility of performing stability tests on fewer strategic periods than a DM would realistically consider. However, if this advantage is to be exploited, we think it wise to bear in mind proposition 1, as it might prove to have an effect on the results of the tests. I.e. one should expect the measure of in-sample stability to increase with increasing length of the strategic horizon, and therefore lower the threshold at which a model is considered to be stable.

Out-of-sample stability testing

The out-of-sample stability tests are performed on a scenario tree with 72 operational periods and 30 scenarios, which is run on 20 and 30 strategic periods (instance 3 and 4). To test for out-of sample stability, we reuse the optimal first-stage solution $\hat{\mathbf{x}}_k^*$ produced by using scenario tree k, as fixed input in another scenario tree l, and vice versa. We then record the objective values $\hat{F}_k(\hat{\mathbf{x}}_l^*)$ and $\hat{F}_l(\hat{\mathbf{x}}_k^*)$. This procedure is repeated for 5 unique pairs, allowing us to evaluate the relationships given in Equations (7.4) - (7.6). For each pair, we have calculated the relative difference for all three equations as the absolute deviation between the objective values divided by the average objective value. Equation (7.7) shows how the relative difference for Equation (7.6) is calculated for a given pair.

$$\frac{|\hat{F}_k(\hat{\mathbf{x}}_l^*) - \hat{F}_l(\hat{\mathbf{x}}_k^*)|}{(\hat{F}_k(\hat{\mathbf{x}}_l^*) + \hat{F}_l(\hat{\mathbf{x}}_k^*))/2} \tag{7.7}$$

All results from the out-of-sample stability tests, together with the average relative difference is recorded in Table 7.7. A stable scenario generation procedure should produce as small deviations as possible.

Table 7.7: Relative difference in out-of-sample stability testing

	Instance 3			**Instance 4**		
Pair	Eq. (7.4)	Eq. (7.5)	(Eq. 7.6)	Eq. (7.4)	Eq. (7.5)	Eq. (7.6)
1	3.15%	1.41%	8.76%	2.77%	1.81%	11.37%
2	1.07%	1.24%	7.96%	4.11%	1.59%	6.30%
3	0.86%	0.10%	12.28%	0.07%	0.12%	14.03%
4	0.01%	0.36%	26.93%	0.01%	0.83%	28.87%
5	2.47%	0.59%	8.63%	0.31%	0.25%	11.94%
Avg.	*1.51%*	*0.74%*	*12.91%*	*1.62%*	*0.94%*	*11.44%*

The largest relative differences are recorded for the relationship in Equation (7.6) for both instances and all pairs. These values are more similar to those obtained in the in-sample testing. For the relationships in Equations (7.4) and (7.5), we observe low relative differences. Recall that we observed similar first-stage decisions for almost all runs, which could explain why these values are so low. The results in Table 7.7 show that the MISSMDP is also out-of-sample stable for the proposed configuration of the scenario generation algorithm.

The computational studies in Chapter 7.5 are performed on four scenario trees generated with the proposed configuration; 30 scenarios for each season and 72 operational periods in each scenario. In evaluating the impact of different strategies on computation time, we want to determine the overall performance of the strategy, not the performance for a specific instance. As we have recorded large deviation in computation time on different trees from the stability testing, we have chosen to study multiple trees to gain a more comprehensive understanding of the obtained results. In order to provide consistency in the overall presentation of results from the computational study, the remaining analysis in Chapters 7.6 and 7.7 are performed on the same four scenario trees. In these chapters, we are more concerned with the actual results than computational performance, and the need to evaluate multiple trees is less pressing. However, as we have shown an acceptable level of stability for the MISSMDP, evaluating average values should not influence the analysis compared to evaluating a single tree.

7.5 Improved implementation

In Chapter 5.8, we commented on the lacking capability of traditional solvers to find optimal solutions to the MISSMDP within reasonable time. So far, we have increased the computational performance of the program by generating scenario trees based on representative profiles and seasons, defining a trade-off between the size of the scenario tree and the stability of the algorithm, and by replacing the binary generator formulation with a simpler continuous model. Although having improved the performance of the MISSMDP, the computation time remains high for the more realistically sized instances if solving to optimality.

In this chapter, we suggest various ways of speeding up the solution process of the problem. First, we discuss the application of heuristics, and try the application of a matheuristic. We then test how the addition of a lower bound on the objective value affects the computational performance. Finally, a customization of the solution algorithm in Xpress, developed based on insight gained from inspection of the solution process, is implemented and tested.

7.5.1 Heuristics

As mentioned in Chapter 5.8, the solution time and complexity of the problem grows exponentially with size of the problem instance. A common way of overcoming this issue is by developing problem specific heuristics that facilitate the solution process in the solver software, often at the cost of exact solution of the problem.

There are several ways to classify heuristics. Some common classes of heuristics are constructive heuristics, local search heuristics, and matheuristics (Lundgren et al., 2010). Based on the problem structure, it could be interesting to explore a local search heuristics that takes advantage of the binary and integer first stage variables of the problem. A local search heuristic is based on iteratively improving the solutions by searching in a defined neighbourhood. If no improved solution can be found, the current solution is chosen as a local optimum (Lundgren et al., 2010). Preliminary testing of simple neighbourhood searches did however not prove to be very promising, given the size of the resulting operational problem that needs to be optimized. By applying smart constructive heuristics for defining the first feasible solution of the local search, the heuristic could prove to be more valuable in terms of improved computation time and solution quality. However, the construction heuristic would be dependent on the technical input data in each individual case, leading to difficulties in defining a general solution algorithm for the MISSMDP. We find it more interesting to study less comprehensive strategies for improving the computational performance rather than developing a case specific heuristic.

Another class of heuristics that could be interesting for the MISSMDP is matheuristics. Recall from Chapter 5.8 that the MISSMDP bears resemblance to the classical CLSP, and that mathematical programming based heuristics have proven to be capable of improving the computational performance for such problems.

Matheuristics

A matheuristic refers to a heuristic that takes advantage of mathematical programming techniques in order to improve the computation time of a problem (Boschetti et al., 2009). A class of simple matheuristics applicable for MIPs is based on solving the program with exact mathematical programming techniques, but accepting a solution without having proven optimality. This could either be performed by defining a maximum computation time, a maximum number of nodes visited in a branch-and-bound search, stopping the search after having found a number of integer solutions, or termination at a specified optimality gap tolerance.

When solving the MISSMDP for the realistically sized instances, it was observed that a substantial amount of computation time was spent on improving the relative gap between the primal and the dual solution from a 2-5% gap to below the predefined tolerance gap at 0.7%. Additionally, it was observed that for the majority of the time spent in closing this gap, it is the lower bound on the optimal solution that is improving. In most cases, the objective value barely changes after the first and second integer solution. These observations suggest that applying one of the matheuristics suggested in the above paragraph could lead to enhanced computational performance, without compromising too much accuracy in the solution.

Based on the characteristics of the solution process, termination at a specified optimality gap tolerance shows promising potential in providing close to optimal solutions, and should speed up the computation time for the MISSMDP. In order to test this heuristic, we define the optimality gap tolerance to be 5%. The heuristic is tested on instance 3 and 4, being the most computationally demanding instances, and the more realistically sized ones at 20 and 30 strategic periods. Table 7.8 shows average computation time and objective values for instance 3 and 4 for a 0.7% tolerance gap, and a 5% tolerance gap.

Table 7.8: Average computation time and objective value with 0.7% and 5% tolerance gap, and the relative change.

	Avg objective value		**Avg computation time [s]**		**Relative change**	
Instance	0.7%	5.0%	0.7%	5.0%	Obj	Time
3	20,620,908	20,630,190	53,124.25	26,334.28	+0.045%	-50.4%
4	25,535,050	25,766,097	91,863.68	56,512.63	+0.90%	-38.5%

The results in Table 7.8 show a clear improvement in average computation time for the MISSMDP when implementing a 5% tolerance on the relative gap between primal and dual solution. As we expected, the relative change in objective value is negligible, and the heuristic shows great potential in providing good solutions. The average improvement in computation time obtained at a 5% tolerance gap compared to the 0.7% tolerance gap is 50.4% for instance 3, and 38.5% for instance 4. The best improvement is as high as 88.3% for instance 3 and 65.2% for instance 4. The individual results from each run can be found in Appendix G. As a conclusion to the testing of matheuristics, these results clearly show that the solution structure of the MISSMDP is such that solving with a high tolerance gap leads to large gains in computation time combined with an insignificant loss in accuracy.

7.5.2 Pre-processing for a lower bound

The second speed-up strategy that we propose relates to finding a lower bound of the objective value. As we have observed that the solution time increases drastically with increasing number of strategic periods, it could prove to be beneficial to limit the feasible region with a lower bound when solving the model for a higher number of strategic periods.

Due to the multi-horizon structure of our problem, we are able to exploit the fact that solving the problem on a low number of strategic periods will relatively quickly provide a reasonable lower bound for the problem solved on a higher number of strategic periods. This is due to the fact that with increasing number of strategic periods, the first-stage solution still only occurs once, while the operational costs of another ten strategic periods is substantial.

To verify that pre-processing for a lower bound based on shorter strategic horizons is a feasible approach, Figure 7.4 shows the objective values of ten different scenario trees run on 5, 10, 20 and 30 strategic periods. From this figure, we can clearly see that the objective values of a shorter strategic horizon can be used as a lower bound when solving for a higher number of strategic periods, without cutting off optimal solutions. Our approach for evaluating the effect of pre-processing for a lower bound is as follows: first, we run the MISSMDP on instance 1, having a strategic horizon of 5 years. The objective value obtained when solving this problem is recorded and added as a cut on the objective function when running the MISSMDP on instance 2. The same procedure is repeated for instance 2 and 3, where instance 3 is solved with a cut from instance 2.

The results from testing lower bounds are presented in Table 7.9. The total time quoted includes the computation time spent finding the lower bound. Based on the results in Table 7.9,

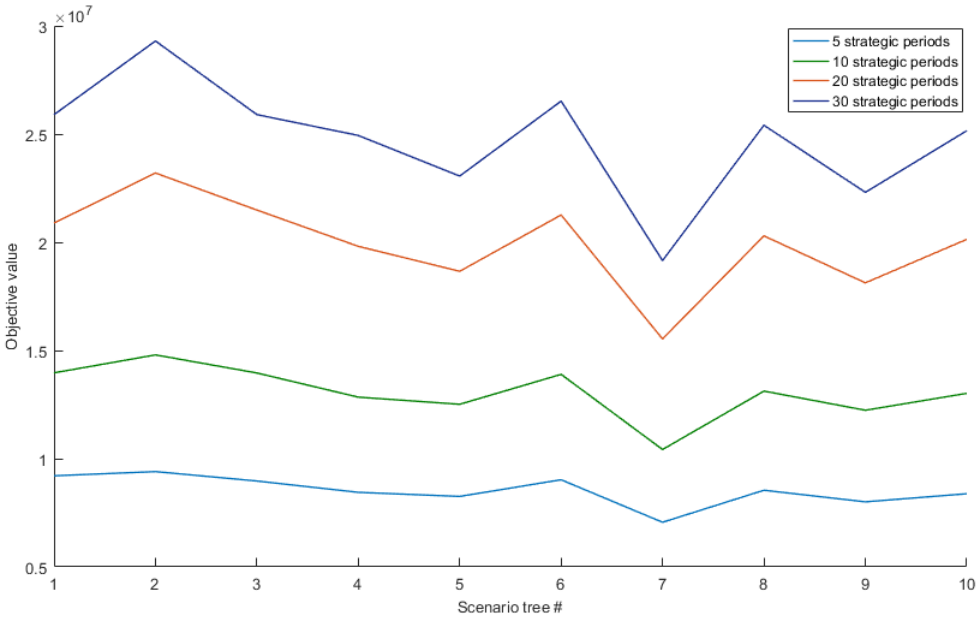

Figure 7.4: Objective values of solving the MISSMDP on ten different scenario trees with 72 operational horizons and 30 scenarios, run on instance 1-4 (5, 10, 20 and 30 strategic periods)

pre-processing for a lower bound based on shorter strategic horizons shows little promise as a speed-up strategy, and is therefore not investigated further on instance 4. Without exception, the results state that including a lower bound in this manner, rather than decreasing, actually increases the total computation time. This could be related to the increased complexity added by implementing a cut that involves all decision variables present in the original objective function.

Table 7.9: Average objective value and computation time from including a lower bound, found by solving the MISSMDP for a lower number number of strategic periods, together with the relative change in computation time.

	Avg objective value		**Avg computation time [s]**			
		With		With	Total with	
Instance	Default	lower bound	Default	lower bound	lower bound	Diff [%]
2	13,473,120	13,473,120	4911.19	7,155.98	8478.44	+72.6%
3	20,620,908	20,620,908	53,124.25	52,389.90	57,301.10	+7.9%

7.5.3 Solver Settings

A final approach for improving the computational performance is to explore combinations of various algorithms and branching strategies in Xpress. This approach may have great potential, as we have observed that excessive computation time is spent on the LP-relaxations and root cutting for the MISSMDP.

For most users of commercial optimization software, the default behaviour of the Optimizer will be sufficient. However, in large and time consuming problems such as the one presented in this

thesis, there is potential gain in customizing the solution procedure. Xpress provides its users with the possibility to customize which algorithm to use when solving the LP relaxation. It is also possible to define which algorithm to use when the Optimizer solves the node relaxation problems during the branch and bound search. In the solution process and structure observed for the MISSMDP, we observe that very little, if any, computation time is spent on performing a branch and bound tree-search. This suggest that there is little to gain by customizing branching strategies, and that the real potential is in customizing the LP relaxation algorithm and tuning the root cutting and heuristics procedure that is done prior to the actual branch and bound tree-search.

For the LP relaxation algorithm one may choose between the *primal simplex*, *dual simplex* and *Newton-Barrier* algorithm. By default, Xpress solves the LP relaxation with all three algorithms, until one of them reaches optimality. For the *dual* and *primal simplex*, the number of iterations required to reach optimality increases with increasing model size. For the *Newton Barrier* algorithm, although it is only able to find an approximated optimal solution, the number of necessary iterations is more dependent on the required proximity of the optimal value than the number of decision variables. This is related to how the algorithms iterate through the feasible region. The *primal* and *dual simplex* iterate through vertices of the feasible region, while the *Newton Barrier* iterates through solutions that are not strictly on the boundary of the feasible region. When considering large scale instances as those studied in this thesis, with a very high number of decision variables, it might be beneficial to choose the *Newton-Barrier* algorithm, excluding the remaining two from the solution procedure. This approach could potentially speed up the solution process by decreasing the number of iterations undertaken in the LP-relaxation. Another potential benefit with choosing only one LP-relaxation algorithm is that you eliminate the extra computations necessary when solving the LP relaxation with three different algorithms at once. We therefore test the impact of solving the LP-relaxation of the MISSMDP with the *Newton-Barrier* algorithm and compare it to the default settings of the solver.

When using the *Newton-Barrier* algorithm, there is a choice of performing a procedure called "crossover" towards the end of the iterations. This procedure is a part of the default settings of the solver, and is performed in an effort to obtain a true optimal solution by performing some simplex iterations towards the end. The crossover procedure may be time consuming, and the benefit of finding a true optimal LP solution as a starting point for the root cutting and heuristics for the MISSMDP has proven to be small. Accordingly, the crossover procedure is turned off for the tests performed with the *Newton-Barrier* algorithm. The relative change in average computation time by applying the *Newton-Barrier* algorithm without crossover to instance 2 and 3 is presented in column 4 of Table 7.10.

There are several other parameters that can be changed in order to further customize the solution procedure of the solver. Many of these were tested, but showed little potential for improvements from the default settings. In addition to specifying the LP-relaxation algorithm and removing the crossover procedure, the only parameter seen to have an effect on the performance was customization of the cut strategy used by the solver. The effect of customizing the cut strategy might relate to the excessive computation time spent on root cutting for the MISSMDP. The cut strategy is by default automatically selected by the solver, and we want to test the impact of specifying an aggressive cut strategy.

An aggressive cut strategy will generate a greater number of cuts in each node, but may in turn result in fewer nodes being explored by the algorithm. I.e. there is a trade off between the number of nodes being visited, and the number of cuts generated in each node. As we have observed that very few nodes are explored in solving the MISSMDP, an aggressive cut strategy could prove feasible for improving computational performance. The aggressive cut strategy is tested in combination with the *Newton-Barrier* algorithm without crossover, and compared to the default computation time. The relative change in average computation time by applying the *Newton-Barrier* algorithm without crossover and an aggressive cut strategy to instance 2 and 3 is presented in column 6 of Table 7.10. The relative difference in objective value was observed to be less than 0.01 % for all instances and combinations, and is therefore not included in the table.

Table 7.10: Average computation time by default, with the *Newton-Barrier* (N-B) LP-relaxation algorithm and with the N-B and an aggressive cut strategy (cut-str), as well as the respective relative change (Rel chng)

Instance	**Default [s]**	**N-B [s]**	**Rel chng**	**N-B + Cut str [s]**	**Rel chng**
2	4,911.2	12,127.7	+146.9%	5,938.3	+20.9%
3	53,124.3	38,089.8	-28.3%	20,052.6	-62.3%

Table 7.10 shows that customizing the solution procedure in Xpress by customizing the LP-relaxation algorithm and cut strategy becomes beneficial when solving large instances of the MISSMDP. However, when applying the customization to solve a smaller instance (instance 2), the computation time increases. This is valuable insight that should be noted when attempting to solve the MISSMDP on large instances for planning purposes in the future, and these settings will also be applied in the practical analysis in Chapter 7.7.

To sum up the improved implementation section, we have seen that applying a simple matheuristic, as well as customizing the solution algorithm for the larger instances, produce promising results with regards to reduction in computation time without a significant reduction in accuracy. The *Newton-Barrier* algorithm and an aggressive cut strategy may be applied to the program for all practical purposes, and the matheuristic could be applied when solving with a small optimality gap tolerance yields too long computation times.

7.6 Value of information and the stochastic solution

As stochastic programs have a tendency to be more computationally challenging than their deterministic counterpart (the expected value problem), it is valuable to discuss the real value of solving the more difficult program. I.e. determine if simpler programs such as the deterministic one provide optimal solutions, or if they are inaccurate and under-performing compared to the stochastic program.

In order to compare the solutions obtained from the stochastic program with simpler deterministic alternatives, two tests are commonly applied: the *expected value of perfect information* (*EVPI*) and the *value of the stochastic solution* (*VSS*) (Birge and Louveaux, 2011). The former is an estimate of the maximum amount a DM would pay for more accurate forecasts of the weather data and the load profiles in our problem. As both weather data and load profiles are subject to external uncertainty that is difficult to eliminate, the *EVPI* is less relevant to our problem. Accordingly, we will not provide a numeric value for the *EVPI*, but rather a discussion of its relevance for the MISSMDP. The *VSS*, on the other hand, is very relevant for the MISSMDP, being a measure of the expected value of planning with uncertainty, compared to the deterministic counterpart (Birge and Louveaux, 2011). In addition to discussing the *EVPI* and evaluating the *VSS*, we want to quantify the value of considering battery lifetime, and the value of considering degradation of battery capacity. This is referred to as the *expected value of planning with battery lifetime and degradation* (*EVPBD*).

7.6.1 The expected value of perfect information and the value of the stochastic solution

As defined by Kall et al. (1994), the expected value of perfect information is the difference between the wait-and-see solution (*WS*) and the stochastic solution (*RP*):

$$EVPI = RP - WS \tag{7.8}$$

RP, is the objective value of the recourse problem (the stochastic program), while *WS* is the objective value of the wait-and-see problem. The wait-and-see problem is the expected value when we solve all scenarios as independent deterministic problems (Birge and Louveaux, 2011).

Solving all scenarios as independent deterministic problems is challenging for the MISSMDP, due to the multi-horizon information structure. One way of evaluating the *WS* is to solve individual problems with the same operational scenario embedded under each strategic node. This is however not a realistic realization of future conditions, and a combination of different scenarios is preferred. Testing all possible combinations of 360 scenarios over 30 years is comprehensive work, and could be computationally demanding. Furthermore, our scenarios are related to specific seasons, leading to complicated evaluations in combining scenarios.

As pointed out in the introduction to this section, the *EVPI* is less relevant to our problem as both weather data and load profiles are subject to external uncertainty that is difficult to eliminate. Considering the lack of value added for a DM by knowing the *EVPI*, and the uncertain elements in determining how to evaluate the *WS*, we have chosen not to analyze the *EVPI* for the MISSMDP.

Birge and Louveaux (2011) define the value of the stochastic solution as the difference between the *expected result of using the expected value solution* (*EEV*) and the objective value of the recourse problem (*RP*).

$$VSS = EEV - RP \tag{7.9}$$

The expected result of using the expected value (*EV*) solution, is defined mathematically as

$$EEV = E_{\xi}(EV) \tag{7.10}$$

where the *EV* is the problem obtained when all random variables in the stochastic program is replaced by their expected values. The *EEV* is thus the objective value obtained when the first stage solution from the *EV* is evaluated in the stochastic program.

7.6.2 The expected value of planning with battery lifetime and degradation

In addition to evaluating the value of the stochastic program, we want to study how considering lifetime and battery degradation add value to the program. We consider one measure in order to quantify the value of information, being the *EVPBD*.

First, we stress that when we refer to the *RP* in this chapter, we refer to the solution of the MISSMDP. The *EVPBD* is defined as the difference between the objective value obtained when solving the *RP*, and the objective value obtained when solving the *fixed reinvestment problem* (*FRP*). The *FRP* is the problem where battery lifetime and degradation is not modelled, and a reinvestment in the battery unit is included at fixed intervals. The interval is set at 10 years, as this is the warranty period provided by manufacturers (Saft SA, 2014; Tesla, 2017). All other modelling considerations and representation of uncertain parameters are the same as for the MISSMDP. Equation (7.11) describes the *EVPBD* mathematically.

$$EVPBD = FRP - RP \tag{7.11}$$

7.6.3 The vaule of the MISSMDP

The *VSS* and the *EVPBD* is calculated for the MISSMDP on instance 3 and 4, and the results are collected in Table 7.11. For each instance, we have evaluated the measures on four different scenario trees, and calculated the average values. The arguments for evaluating multiple trees are provided in Chapter 7.4. The individual solutions obtained for each tree and instance is enclosed in Appendix F.

In calculating the *EEV*, we first have to solve the *EV* problem. As the MISSMDP has a multi-horizon information structure, the process of replacing the random variables with their expected values requires some explanation. Recall from earlier in this chapter that we create scenario trees with 12 seasons, 30 scenarios in each season, and 72 operational periods in each scenario. A duplicate of this tree is embedded under each strategic decision node in the MISSMDP.

If we calculate the expected value for each operational period from all scenarios, creating one single expected value scenario under each strategic node, we lose the seasonality in the historical data. Due to the information structure, the full year would be represented by three consecutive average days. In order to calculate meaningful expected values for the *EV*, we have to account for the assumptions behind the information structure of the MISSMDP. Accordingly, we calculate the expected value of each operational period within each season, resulting in 12 scenarios with 72 operational periods. Each scenario represents the expected value for a specific season. When solving the *EV* problem, we are thus solving the problem with the expected value scenario for each month embedded under each strategic node.

Table 7.11: Average VSS and EVPBD for all combinations with instance 3 and 4 for the MISSMDP, % refers to the average relative change in objective value compared to the *EEV* and the FRP.

Inst	**Strat**	***RP***	***EEV***	***FRP***	***VSS***	**%**	***EVPBD***	**%**
3	20	20,620,908	467,039,443	20,891,856	*446,418,535*	*-95.6%*	*270,948*	*-1.30%*
4	30	25,535,050	627,842,744	26,064,626	*602,307,693*	*-95.9%*	*529,576*	*-2.03%*

The average *EEV* recorded in Table 7.11 is significantly larger than the *RP*, leading to high values for the resulting *VSS*. This is true for both instances. When planning for the expected value scenario, the extreme situations in the historical data are not adequately represented, and a tendency to invest in far less components than when solving the *RP* is observed. Accordingly, fixing the first-stage decisions in the *RP* to those obtained from the *EV* (solving the *EEV*), leads to a situation where a lot of the realized load is not met. The resulting *VSS* recorded for the MISSMDP does therefore assume noticeably high values. The average improvement in objective value from the stochastic program compared to the expected value solution is as great as 95.6% for instance 3 and 95.9% for instance 4. These results indicates that for the trees we have evaluated, the stochastic solution is equally valuable for 20 and 30 strategic periods.

As discussed in Chapter 6.3.6 the VOLL is defined artificially high at $1000 based on the assumption that the choice of not covering load should not be a realistic one. The definition of the VOLL strongly affects the *VSS*, as the resulting cost of not covering load in the *EEV* becomes dominating. With a VOLL defined to provoke the correct level of LOLP, the gain of planning with uncertainty is expected to be less distinct. Again, as discussed in Chapter 6.3.6, correct definition of the VOLL is beyond the scope of this thesis. The VOLL would however be defined at such a level that the cost of not covering load is still dominating compared to investment costs, and the *VSS* is expected to show clear evidence of the value of planning with uncertainty. In an effort to provide some perspective on the *VSS*, it is evaluated on instance 1 on tree number 4 for a VOLL at $100. This resulted in a *VSS* of $41,748,228, or an improvement in objective value of 89.9% from using the *RP* compared to the *EEV*.

The average *EVPBD* reveales that the improvement from planning with battery lifetime and degradation compared to the *FRP* is 1.30% for instance 3 and 2.03% for instance 4. The value of planning with battery lifetime and degradation is relatively small, and the first stage decisions obtained when solving the *FRP* are quite similar to those obtained for the *RP*. It is worth noticing that of the technical components considered in the defined instances for this computational study, it is with no exception the largest battery unit that is chosen. A better resolution in storage capacity for the battery units, or larger units included in the list of components, could affect the *EVPBD*. The effect of assumptions in input parameters on the *EVPBD* is however unclear without studying instances for comparable cases to that of Sørburøy.

As a conclusion to the evaluation of the value of the MISSMDP, it is clear that there is a great value of planning with uncertainty across all instances and trees. The impact of considering battery lifetime and degradation is less clear due to the unknown effect of assumptions in input data. For the case of Sørburøy we find that the added value from increasing the level of information in the battery formulation is inconclusive. Planning with battery lifetime and degradation proves valuable for some of the instances and trees evaluated in this thesis, but in most cases there is little additional value.

7.7 Practical analysis

In this section of the computational study, we analyze the practical performance of the MISSMDP given the design choices in the modelling chapter. More specifically, we study the practical implications of some of the main assumptions made in Chapter 5.1 and 5.2, assumptions related to the modelling of the battery, and assumptions related to the scenario generation algorithm. The first-stage solutions is not commented on explicitly, as they are partly based on estimated values, and the objective of this thesis is to develop and evaluate the overall performance of the MISSMDP.

7.7.1 Battery

From the second-stage solutions and the reinvestment decision variables of various instances we observe that with the current parameters, the model will not reinvest in a battery unit. There are several possible reasons for the battery behaving in this way, and the lack of reinvestment is likely to be caused by a combination of these. First of all, our assumption that battery lifetime considerations can be sufficiently approximated based on energy throughput could be false for the case we are studying. Secondly, the structure of the scenario trees generated, may not capture the full energy throughput of the battery. This is related to assumption 10 in Table 5.2 stating that SOC is zero at the beginning of each operating horizon, in combination with the use of representative days in the scenario tree. Thirdly, the newest battery technology available, which is what most of the relevant parameters are based on, may not need a reinvestment at all for the strategic horizons we are studying. However, as the fraction of actual spent battery lifetime and capacity degradation through 20-30 strategic periods is observed to be very small, it is unlikely that this number is realistic and that the lack of reinvestment is caused by the parameters being based on the newest battery technology alone.

Upon inspection of the end-values of SOC on the battery unit in each individual scenario, we notice several occasions where the battery still contains energy in the last operational period of a scenario that will simply be left unused. However, as the battery lifetime considerations are based on power charged to the battery, this observation suggests that the battery lifetime depletion is overestimated. This is the opposite of what we have observed regarding the battery lifetime estimations, and it is apparent that assumption 10 does not have a substantial impact on the battery lifetime calculations.

A final aspect that may have an impact on the validity of the battery lifetime calculations, is the actual case study itself. Our case study location experiences an exceptionally steady presence of relatively high velocity wind. The historically recorded wind speeds are high enough to produce wind power in over 80% of the hours throughout the year, with very few occurrences of wind speeds above the cut-off speed for the majority of available wind turbines. Therefore, this location will be dominated by wind, and rely heavily on the availability of this RES. A microgrid in this location will not be as dependent on the battery unit for energy storage as a microgrid in a less wind-dominated location would. In a different case study, where solar plays a more dominant role, the battery unit is expected to experience more energy throughput, and the lifetime calculations modelled in the MISSMDP may yield more correct results. An indication of this effect can be shown by removing the option to invest in wind for the MISSMDP, and relax the constraint on maximum PV-panels. In this case, we observe a higher energy throughput leading to more accurate battery lifetime calculation and degradation. Accordingly, the current model is more likely to yield correct decisions regarding reinvestment in areas that are dominated by solar power production, than in areas where that are dominated by wind. This implies that the appropriateness of applying the simple lifetime calculations presented in this thesis, should be evaluated on a case-by-case basis. In our case, we consider it likely that the simple battery lifetime calculations performed here, do not sufficiently represent the lifetime and capacity degradation of the unit.

7.7.2 Changing future prices

According to assumption 4 in Table 5.2, the future costs of fuel and components are kept constant throughout the planning horizon. The costs are assumed to stay at today's level. This is an assumption that may have large implications for the investment decision today, and the objective value of the MISSMDP. To analyze the impact of assumption 4, we test the practical implications for the results obtained from the MISSMDP by solving it for a set of expected future prices given as input.

The prices for batteries are expected to decrease in the future, but as we currently do not experience any reinvestments in battery units, this decrease is expected to have little effect. Therefore, changing prices for the battery is not further analyzed. For the fuel price analysis, we perform three tests on instance 3 (20 strategic periods). The first test evaluates a fuel price experiencing a yearly increase of 5%, the second test evaluates a yearly increase of 10% and the third test considers a yearly decrease of 5% for the fuel price. For all tests, we compare the first stage solutions and objective values, in order to gain some understanding of the impact of the potential future price development on optimal first-stage solutions.

The first-stage solutions obtained are identical for all tests. The objective values are slightly increased when testing an increase in fuel prices, and there is an opposite effect when the fuel price decreases. However, the changes in the objective values are considered to be small. The objective values obtained are presented in Table 7.12. It is interesting to emphasize that even when increasing the fuel price by 10% every year, resulting in a fuel price that is almost 7 times higher in year 20 than in year 1, we still observe the same first-stage solutions, and only a slight increase in objective value.

Table 7.12: Objective values of the MISSMDP when solving with constant fuel cost, or an increasing/decreasing fuel cost, with either 5% or 10% yearly increase, or 5% yearly decrease.

	Objective value with fuel price			
Instance	Constant	5% increase	10% increase	5% decrease
3	20,886,735	20,896,857	20,915,103	20,880,213

As the MISSMDP already limits the use of the diesel generator by enforcing a renewable energy fraction ensuring a predefined proportion of energy provided by RES, the stochastic program will provide solutions with limited use of the generator. In the case of Sørburøy, the allowed fraction of energy supplied by the generator is set to 5%, explaining why the general effect of increasing and decreasing fuel cost is observed to be minor. In conclusion, the MISSMDP is not heavily dependent on the future outlook of fuel prices when a renewable fraction is included in the formulation, and the practical implication of assumption 4 is shown to be small.

7.7.3 Changing load demand

A potential, and likely, future development, is that the microgrid will experience significant changes in load demand, challenging one of the assumptions behind the scenario generation method. This assumption relates to historical load demand being representative for the future. However, the long-term development of load demand in a potential microgrid location is dif-

ficult to predict. It could for instance be increasing, due to a gradual increase in the use of power-intensive applications. In the extreme opposite direction, there could be a complete collapse of load demand due to a sudden relocation of all the inhabitants, leaving the island with no permanent residents. There is a lot of uncertainty related to planning for a horizon of 20-30 years, and making claims of how load demand actually will develop, is beyond the scope of this thesis. Instead we perform a simple analysis of how a steady 2.5% increase or a steady 2.5% decrease of the load demand may impact the first stage solutions. This analysis allows us to evaluate the sensitivity of the first stage solutions towards changes in load demand.

Table 7.13: Objective values of the MISSMDP when solving with stable future load demand, a 2.5% yearly increase, and a 2.5% yearly decrease.

	Objective value with future load demand		
Instance	Stable	2.5% increase	2.5% decrease
3	20,886,736	43,099,104	11,890,758

The objective values obtained are presented in Table 7.14. The first-stage solutions differed substantially for the different tests, leading to a clear difference in the objective values. In Table 7.14, we observe an approximate doubling of the objective value with increasing load demand, and corresponding halving when load is decreased. It is evident that the optimal objective value and the realization of the first-stage decision variables for the MISSMDP has a clear dependency on the development of future load demand. This is important knowledge to bear in mind for a DM in a strategic planning phase, and suggests that spending time and resources on eliminating uncertainty in future load demand may be of high value.

7.7.4 Comparing cost per kW/kWh - approach to the MISSMDP

An effortless way of designing a microgrid, is to simply pick the components with the lowest cost per kW for generating units, and lowest cost per kWh for storage units. By studying the first-stage solutions obtained from running the MISSMDP, we see that the model generally does not follow this rule, and picks components based on much more complex considerations. In order to quantify the added value of planning with the MISSMDP compared to the simpler approach, we solve the model for the situation where only the "cheapest" (in cost per kW/kWh) components are available. This means that, in effect, the battery and generator decision will be fixed, while the PV-panels and wind turbines will be restricted to choosing the amount to

invest in of a pre-specified component. The results, presented in Table 7.14, clearly show that basing the planning of a microgrid on the cheapest component in cost per kW/kWh leads to a significantly more expensive microgrid than what one is able to design when accounting for more complex considerations in the MISSMDP.

Table 7.14: Objective value of MISSMDP considering all components and considering only the "cheapest" components

	Objective value with	
Instance	All components	"Cheapest" components
3	20,886,735	120,028,624

Chapter 8

Future research and concluding remarks

8.1 Future research

In this section we summarize the various topics that we consider to be of interest in future research. There are three main directions that we find it interesting to pursue; strategic uncertainty, component modelling and solution methods.

A possible area of future research, exploiting the potential that lies in the multi-horizon information structure of the MISSMDP, is to include uncertainty on the strategic level. The strategic uncertainty can be related to fuel prices, component costs, future load demand, and climate. As discussed in Chapter 7.7.3, the most apparent weakness in our model is the prediction of future load data, and this might be the most interesting parameter to consider when including strategic uncertainty. By including strategic uncertainty in future development of component prices and fuel costs, one would be able to revise assumption 4 in Table 5.2, and ideally it follows that the model should also allow for reinvestment in all available components throughout the strategic horizon, thereby removing assumption 6 in Table 5.2. The resulting model with increased level of information could provide a better tool for DM's in the planning phase of a microgrid project. It is however important to bear in mind that there is a trade-off between increased level of uncertainty and information, and the computational performance of a mathematical program.

This thesis makes an attempt to take into account battery lifetime calculations in the strategic planning of a microgrid. However, battery lifetime calculations are in reality highly non-linear and complex. Accordingly one of the suggestions for further research is to explore the possibility of incorporating a probabilistic approach to battery lifetime considerations. This could possibly tackle the observed weaknesses in the current assumption that battery lifetime calculations are sufficiently approximated based on energy throughput and a maximum amount of

cycles endured.

We further suggest that it could be interesting to study the effect of adding temperature as an uncertain parameter to the model. By adding this uncertain element, one is able to explore the known effect temperature has on PV-power output, in order to get a more accurate representation of the available PV-power. Additionally, it is interesting to investigate the possible correlation between load and temperature, and the effect this may have on the optimal solution.

For the MISSMDP to evolve into a more comprehensive decision making tool for strategic planners, a natural extension of the model is to include the possibility to invest in other storage technologies, such as hydrogen fuel cells, other RES, such as wave power plants and even the possibility of investing in transmission capacity. This will provide a more holistic picture of the possible energy supply solutions for a given area.

Although the computational performance of the MISSMDP was improved substantially in this thesis, it is still quite computationally burdensome. Therefore, further research into solution methods is suggested. Motivation for pursuing this goal is to facilitate the inclusion of longer operational horizons, and more realistic (and therefore also complex) component modelling. Including longer operational horizons may capture more of the uncertainty in each season, and allow for energy storage across several days and weeks. Exploring the possibilities that lie in Bender's decomposition, applied to a multi-horizon model structure could be a very interesting approach. More specifically, the idea of using a nested Bender's algorithm could be worth exploring, decomposing the problem into more easily solvable sub-problems while maintaining the multi-horizon structure. In a Bender's decomposition solution method one could also take advantage of the benefits of parallel computing of the sub-problems, in order to solve larger and more complex operational problems. This concludes our suggested areas for future research.

8.2 Concluding remarks

The problem of identifying the optimal size of components in a stand-alone microgrid is challenging. This is because the short-term operational considerations combined with long-term strategic decisions, result in very large and computationally burdensome mathematical programs. The problem becomes even more challenging when considering uncertainty in operational input parameters.

In this thesis we have developed a novel mathematical model for the strategic microgrid design problem, taking into account the stochastic nature of the operational input parameters. The proposed mathematical model is referred to as the mixed integer stochastic strategic microgrid design problem (MISSMDP), and is applied to a case study location. The MISSMDP aims to provide decision makers with valuable insights in the strategic planning phase of a microgrid project. For the case studied in this thesis, the MISSMDP evaluates investments in battery units, solar photovoltaic panels, fuel based generators and wind turbines. Additionally, the model accounts for battery lifetime calculations and degradation of battery performance.

When considering the operational performance and costs of today's investments over the lifetime of the system, the size of the resulting stochastic program quickly becomes intractable for commercial solvers. In an effort to improve the computational tractability of the MISSMDP, we have applied a multi-horizon information structure that to our knowledge has never previously been applied to a strategic microgrid design problem. We show that this information structure is applicable to the MISSMDP, and capable of handling the strategic dependencies arising in the mathematical modelling. Consequently, we are able to decrease the size of the stochastic program drastically. After this, we provide a thorough discussion on the level of detail necessary in the modelling of the components, and an analysis of the impact of various model formulations on computational and practical performance of the model.

In order to represent the uncertainty in the operational input parameters for the MISSMDP, we have performed an analysis of the underlying stochastic processes in historic weather and load data at our case study location. The results from this analysis are used in the development of the scenario generation algorithm that we propose for the MISSMDP. The scenario generation algorithm proposed relies on seasonal scenarios sampled from historical data. In combination with the multi-horizon information structure, the scenario generation algorithm constitutes an essential step towards improving the computational performance of the stochastic program. Extensive stability testing of the MISSMDP has validated the performance of the defined scenario generation algorithm, and led to the identification of the smallest possible scenario tree, that still yields stable solutions and represents the underlying stochastic processes adequately.

Through the technical and practical analysis in the computational study, a variety of strategies applied to improve the computational tractability of the MISSMDP are shown to give promising results. In the technical analysis we first elaborated further on an alternative diesel generator formulation, and its impact on computation time. By making use of our experience with the problem and solution structure of the MISSMDP, we were able to propose a formulation that preserves the quality of the program, while decreasing the computational complexity. These considerations resulted in an improved implementation of the diesel generator formulation for the MISSMDP. Further improvements of computation time were achieved by applying a simple matheuristic, and a customization of the LP-relaxation algorithm in the solver.

By evaluating the value of the stochastic model, we have found that there is great value to be added by applying stochastic programming to the strategic microgrid design problem, whereas the value of increased information by adding battery lifetime calculations is inconclusive. Finally, we have evaluated the practical performance of the program, and exposed some weaknesses in the model related to battery lifetime calculations and sensitivity towards future load demand. Even so, the model has proved to be able to identify the optimal size of components within acceptable time, and provide valuable insights for decision makers in the strategic planning phase of a microgrid project. Based on the work presented in this thesis, we conclude that the potential gains from considering uncertainty in strategic microgrid projects are significant, and that there is value to be added by applying stochastic modelling approaches to the strategic microgrid design problem.

Bibliography

Abbey, C. and Joos, G. (2009). A stochastic optimization approach to rating of energy storage systems in wind-diesel isolated grids. *IEEE Transactions on Power Systems*, 24(1):418–426.

Abdulkarim, A., Abdelkader, S. M., and Morrow, D. J. (2015). Statistical analyses of wind and solar energy resources for the development of hybrid microgrid. In *2nd International Congress on Energy Efficiency and Energy Related Materials (ENEFM2014)*, pages 9–14. Springer.

Alsayed, M., Cacciato, M., Scarcella, G., and Scelba, G. (2014). Design of hybrid power generation systems based on multi criteria decision analysis. *Solar Energy*, 105:548–560.

Arabali, A., Ghofrani, M., Etezadi-Amoli, M., and Fadali, M. S. (2014). Stochastic performance assessment and sizing for a hybrid power system of solar/wind/energy storage. *IEEE Transactions on Sustainable Energy*, 5(2):363–371.

Arnesen, K. and Borgen, S. (2016). A stochastic programming approach to optimal component sizing for the strategic microgrid design problem. Unpublished project report at NTNU.

Askarzadeh, A. and dos Santos Coelho, L. (2015). A novel framework for optimization of a grid independent hybrid renewable energy system: A case study of iran. *Solar Energy*, 112:383–396.

Bahmani-Firouzi, B. and Azizipanah-Abarghooee, R. (2014). Optimal sizing of battery energy storage for micro-grid operation management using a new improved bat algorithm. *International Journal of Electrical Power and Energy Systems*, 56:42 – 54.

Balachandra, P. and Chandru, V. (1999). Modelling electricity demand with representative load curves. *Energy*, 24(3):219–230.

Bernal-Agustín, J. L. and Dufo-López, R. (2009). Simulation and optimization of stand-alone hybrid renewable energy systems. *Renewable and Sustainable Energy Reviews*, 13(8):2111 – 2118.

Birge, J. R. and Louveaux, F. (2011). *Introduction to stochastic programming*. Springer Science & Business Media.

Blanco, M. I. (2009). The economics of wind energy. *Renewable and Sustainable Energy Reviews*, 13(6–7):1372 – 1382.

Bordin, C., Anuta, H. O., Crossland, A., Gutierrez, I. L., Dent, C. J., and Vigo, D. (2017). A linear programming approach for battery degradation analysis and optimization in offgrid power systems with solar energy integration. *Renewable Energy*, 101:417 – 430.

Boschetti, M. A., Maniezzo, V., Roffilli, M., and Röhler, A. B. (2009). Matheuristics: Optimization, simulation and control. In *International Workshop on Hybrid Metaheuristics*, pages 171–177. Springer.

Brown, P. D., Lopes, J. P., and Matos, M. A. (2008). Optimization of pumped storage capacity in an isolated power system with large renewable penetration. *IEEE Transactions on Power systems*, 23(2):523–531.

Chauhan, A. and Saini, R. (2014). A review on integrated renewable energy system based power generation for stand-alone applications: Configurations, storage options, sizing methodologies and control. *Renewable and Sustainable Energy Reviews*, 38:99 – 120.

Chen, C., Duan, S., Cai, T., Liu, B., and Hu, G. (2011). Smart energy management system for optimal microgrid economic operation. *IET renewable power generation*, 5(3):258–267.

CIGRÉ (2010). Working group c6.22 microgrids evolution roadmap. *Microgrids 1: Engineering, Economics, and Experience*.

Dantzig, G. B. (1955). Linear programming under uncertainty. *Management science*, 1(3-4):197–206.

de Vries, H., Nguyen, T. T., and het Veld, B. O. (2015). Increasing the cycle life of lithium ion cells by partial state of charge cycling. *Microelectronics Reliability*, 55(11):2247 – 2253.

Doorman, G. L. (2016). *Course ELK15 - Hydro Power Scheduling*. Department of Electric Power Engineering, NTNU.

Downing, S. D. and Socie, D. (1982). Simple rainflow counting algorithms. *International journal of fatigue*, 4(1):31–40.

Dragičević, T., Pandžić, H., Škrlec, D., Kuzle, I., Guerrero, J. M., and Kirschen, D. S. (2014). Capacity optimization of renewable energy sources and battery storage in an autonomous telecommunication facility. *IEEE Transactions on Sustainable Energy*, 5(4):1367–1378.

Ekren, O. and Ekren, B. Y. (2010). Size optimization of a pv/wind hybrid energy conversion system with battery storage using simulated annealing. *Applied Energy*, 87(2):592 – 598.

Fossati, J. P., Galarza, A., Martín-Villate, A., and Fontán, L. (2015). A method for optimal sizing energy storage systems for microgrids. *Renewable Energy*, 77:539–549.

Gao, D. W. (2015). Chapter 5 - sizing of energy storage systems for microgrids. In Gao, D. W., editor, *Energy Storage for Sustainable Microgrid*, pages 125 – 142. Academic Press, Oxford.

Hassan, A., Saadawi, M., Kandil, M., and Saeed, M. (2015). Modified particle swarm optimisation technique for optimal design of small renewable energy system supplying a specific load at mansoura university. *IET Renewable Power Generation*, 9(5):474–483.

Hatziargyriou, N., Asano, H., Iravani, R., and Marnay, C. (2007). Microgrids. *IEEE power and energy magazine*, 5(4):78–94.

Hatziargyriou, N., Jenkins, N., Strbac, G., Lopes, J. P., Ruela, J., Engler, A., Oyarzabal, J., Kariniotakis, G., Amorim, A., et al. (2006). Microgrids–large scale integration of microgeneration to low voltage grids. *CIGRE C6-309*.

Hellemo, L., Midthun, K., Tomasgard, A., and Werner, A. (2013). Multi-stage stochastic programming for natural gas infrastructure design with a production perspective. In *Stochastic Programming: Applications in Finance, Energy, Planning and Logistics*, pages 259–288.

Higle, J. L. (2005). Stochastic programming: optimization when uncertainty matters. *Cole Smith J (ed) Tutorials in operations research*, pages 30–53.

Higle, J. L. and Wallace, S. W. (2003). Sensitivity analysis and uncertainty in linear programming. *Interfaces*, 33(4):53–60.

Høyland, K., Kaut, M., and Wallace, S. W. (2003). A heuristic for moment-matching scenario generation. *Computational optimization and applications*, 24(2):169–185.

IRENA (2015). Renewable power generation costs in 2014. *International Renewable Energy Agency*.

IRENA (2016). The power to change: Solar and wind cost reduction potential to 2025. *International Renewable Energy Agency*.

Jeyaprabha, S. B. and Selvakumar, A. I. (2015). Optimal sizing of photovoltaic/battery/diesel based hybrid system and optimal tilting of solar array using the artificial intelligence for remote houses in india. *Energy and Buildings*, 96:40–52.

Jordan, D. C. and Kurtz, S. R. (2013). Photovoltaic degradation rates—an analytical review. *Progress in Photovoltaics: Research and Applications*, 21(1):12–29.

Kall, P., Wallace, S. W., and Kall, P. (1994). *Stochastic programming*. Springer.

Karimi, B., Ghomi, S. F., and Wilson, J. (2003). The capacitated lot sizing problem: a review of models and algorithms. *Omega*, 31(5):365–378.

Katsigiannis, Y., Georgilakis, P., and Karapidakis, E. (2010). Multiobjective genetic algorithm solution to the optimum economic and environmental performance problem of small autonomous hybrid power systems with renewables. *IET Renewable Power Generation*, 4(5):404–419.

Katsigiannis, Y. A., Georgilakis, P. S., and Karapidakis, E. S. (2012). Hybrid simulated annealing 2013;tabu search method for optimal sizing of autonomous power systems with renewables. *IEEE Transactions on Sustainable Energy*, 3(3):330–338.

Kaut, M., Midthun, K. T., Werner, A. S., Tomasgard, A., Hellemo, L., and Fodstad, M. (2013). Multi-horizon stochastic programming. *Computational Management Science*, Online first.

Kaut, M. and Wallace, S. W. (2003). Evaluation of scenario-generation methods for stochastic programming.

King, A. J. and Wallace, S. W. (2012). Uncertainty in optimization. In *Modeling with Stochastic Programming*, pages 1–31. Springer.

Kishore, L. N. and Fernandez, E. (2011). Reliability well-being assessment of pv-wind hybrid system using monte carlo simulation. In *Emerging Trends in Electrical and Computer Technology (ICETECT), 2011 International Conference on*, pages 63–68.

Kolhe, M., Kolhe, S., and Joshi, J. (2002). Economic viability of stand-alone solar photovoltaic system in comparison with diesel-powered system for india. *Energy Economics*, 24(2):155 – 165.

Kuznia, L., Zeng, B., Centeno, G., and Miao, Z. (2013). Stochastic optimization for power system configuration with renewable energy in remote areas. *Annals of Operations Research*, 210(1):411–432.

Lasseter, R. H. (2002). Microgrids. In *Power Engineering Society Winter Meeting, 2002. IEEE*, volume 1, pages 305–308. IEEE.

Lasseter, R. H. and Paigi, P. (2004). Microgrid: a conceptual solution. In *Power Electronics Specialists Conference, 2004. PESC 04. 2004 IEEE 35th Annual*, volume 6, pages 4285–4290. IEEE.

Lee, T.-Y. and Chen, N. (1995). Determination of optimal contract capacities and optimal sizes of battery energy storage systems for time-of-use rates industrial customers. *IEEE Transactions on Energy Conversion*, 10(3):562–568.

Li, J., Wei, W., and Xiang, J. (2012). A simple sizing algorithm for stand-alone pv/wind/battery hybrid microgrids. *Energies*, 5(12):5307–5323.

Lundgren, J., Rönnqvist, M., and Värbrand, P. (2010). *Optimization*. Studentlitteratur.

Magnanti, T. L. and Wong, R. T. (1981). Accelerating benders decomposition: Algorithmic enhancement and model selection criteria. *Operations research*, 29(3):464–484.

Manwell, J. F. and McGowan, J. G. (1993). Lead acid battery storage model for hybrid energy systems. *Solar Energy*, 50(5):399 – 405.

McCormick, G. P. (1976). Computability of global solutions to factorable nonconvex programs: Part i — convex underestimating problems. *Mathematical Programming*, 10(1):147–175.

Multiconsult (2013). Kostnadsstudie, solkraft i norge 2013. Technical report, Enova.

Niknam, T., Azizipanah-Abarghooee, R., and Narimani, M. R. (2012). An efficient scenario-based stochastic programming framework for multi-objective optimal micro-grid operation. *Applied Energy*, 99:455 – 470.

Nogueira, C. E. C., Vidotto, M. L., Niedzialkoski, R. K., de Souza, S. N. M., Chaves, L. I., Edwiges, T., dos Santos, D. B., and Werncke, I. (2014). Sizing and simulation of a photovoltaic-wind energy system using batteries, applied for a small rural property located in the south of brazil. *Renewable and Sustainable Energy Reviews*, 29:151 – 157.

Ortega-Vazquez, M. A. and Kirschen, D. S. (2009). Estimating the spinning reserve requirements in systems with significant wind power generation penetration. *IEEE Transactions on Power Systems*, 24(1):114–124.

Paliwal, P., Patidar, N., and Nema, R. (2014). Determination of reliability constrained optimal resource mix for an autonomous hybrid power system using particle swarm optimization. *Renewable Energy*, 63:194 – 204.

Papavasiliou, A., Oren, S. S., and O'Neill, R. P. (2011). Reserve requirements for wind power integration: A scenario-based stochastic programming framework. *IEEE Transactions on Power Systems*, 26(4):2197–2206.

Parija, G. R., Ahmed, S., and King, A. J. (2004). On bridging the gap between stochastic integer programming and mip solver technologies. *INFORMS Journal on Computing*, 16(1):73–83.

Sachs, J. and Sawodny, O. (2016a). Multi-objective three stage design optimization for island microgrids. *Applied Energy*, 165:789–800.

Sachs, J. and Sawodny, O. (2016b). A two-stage model predictive control strategy for economic diesel-pv-battery island microgrid operation in rural areas. *IEEE Transactions on Sustainable Energy*, 7(3):903–913.

Saft SA (2014). Lithium-ion battery life. Technical Report 21893-2-0514, Saft batteries, 12 rue Sadi Carnot, 93170 Bagnolet - France.

Schwaegerl, C. and Tao, L. (2014). The microgrids concept. *Microgrids: Architectures and control*, pages 1–24.

Scioletti, M. S., Goodman, J. K., Kohl, P. A., and Newman, A. M. (2016). A physics-based integer-linear battery modeling paradigm. *Applied Energy*, 176:245–257.

Seljom, P. and Tomasgard, A. (2015). Short-term uncertainty in long-term energy system models—a case study of wind power in denmark. *Energy Economics*, 49:157–167.

Sharafi, M. and ElMekkawy, T. Y. (2014). Multi-objective optimal design of hybrid renewable energy systems using pso-simulation based approach. *Renewable Energy*, 68:67–79.

Shepherd, C. M. (1965). Design of primary and secondary cells ii. an equation describing battery discharge. *Journal of the Electrochemical Society*, 112(7):657–664.

Singh, S. and Kaushik, S. C. (2016). Optimal sizing of grid integrated hybrid pv-biomass energy system using artificial bee colony algorithm. *IET Renewable Power Generation*, 10(5):642–650.

Skar, C., Doorman, G. L., Pérez-Valdés, G. A., and Tomasgard, A. (2016). A multi-horizon stochastic programming model for the european power system. *CenSES Working paper*, 2016(2).

sonnen, I. (2016). Product factory warranty - sonnen, inc. Technical Report 03, sonnenBatterie, 10800 Burbank Blvd., Suite C, Los Angeles, CA, 91601.

Soshinskaya, M., Crijns-Graus, W. H., Guerrero, J. M., and Vasquez, J. C. (2014). Microgrids: Experiences, barriers and success factors. *Renewable and Sustainable Energy Reviews*, 40:659–672.

Tesla, I. (2017). Tesla powerwall limited warranty (usa). Technical Report 1.4, Tesla, Inc., 3500 Deer Creek Road, Palo Alto, California, 94304.

Tina, G., Gagliano, S., and Raiti, S. (2006). Hybrid solar/wind power system probabilistic modelling for long-term performance assessment. *Solar Energy*, 80(5):578 – 588.

Upadhyay, S. and Sharma, M. (2015). Development of hybrid energy system with cycle charging strategy using particle swarm optimization for a remote area in india. *Renewable Energy*, 77:586–598.

Vrettos, E. I. and Papathanassiou, S. A. (2011). Operating policy and optimal sizing of a high penetration res-bess system for small isolated grids. *IEEE Transactions on Energy Conversion*, 26(3):744–756.

Wallace, S. W. (2003). Decision making under uncertainty: The art of modeling. *Molde University College*, 15(03).

Wang, L. and Singh, C. (2009). Multicriteria design of hybrid power generation systems based on a modified particle swarm optimization algorithm. *IEEE Transactions on Energy Conversion*, 24(1):163–172.

Williams, H. P. (1993). *Model solving in mathematical programming*. Wiley.

Xu, B., Oudalov, A., Ulbig, A., Andersson, G., and Kirschen, D. (2016). Modeling of lithium-ion battery degradation for cell life assessment. *IEEE Transactions on Smart Grid*, PP(99):1–11.

Yang, H., Lu, L., and Zhou, W. (2007). A novel optimization sizing model for hybrid solar-wind power generation system. *Solar Energy*, 81(1):76 – 84.

Yang, H., Zhou, W., Lu, L., and Fang, Z. (2008). Optimal sizing method for stand-alone hybrid solar–wind system with {LPSP} technology by using genetic algorithm. *Solar Energy*, 82(4):354 – 367.

Zhao, B., Zhang, X., Chen, J., Wang, C., and Guo, L. (2013). Operation optimization of standalone microgrids considering lifetime characteristics of battery energy storage system. *IEEE Transactions on Sustainable Energy*, 4(4):934–943.

Appendix A

Mathematical Model - base

$$\min z = \sum_{e \in E} C_e x_e + \sum_{t \in T^S} \delta_t \sum_{e \in E^B} C_e x_{et}^B + H \sum_{t \in T^S} \delta_t \sum_{s \in S^O} \pi_s \sum_{o \in T_t^O} \theta^{oc} \left(C^F f_{tos} + C^L n_{tos}^L \right) \tag{1a}$$

$$s.t. \quad \sum_{i \in E^{En} \setminus \{B^-\}} H p_{itos} - H p_{B^- tos} + H n_{tos}^L = D_{os} \qquad ,t \in T^S, o \in T_t^O, s \in S^O \tag{2a}$$

$$H \left(\frac{\sum_{o \in T_t^O} p_{Gtos}}{\sum_{o \in T_t^O} D_{os}} \right) \leq \bar{R}^G \qquad ,t \in T^S, s \in S^O \tag{3}$$

$$p_{Gtos} - \sum_{e \in E^G} \bar{P}_e^G \beta_{etos}^G \leq 0 \qquad ,t \in T^S, o \in T_t^O, s \in S^O \tag{4a}$$

$$\beta_{etos}^G - x_e \leq 0 \qquad ,e \in E^G, t \in T^S, o \in T_t^O, s \in S^O \tag{5}$$

$$p_{Gtos} - \sum_{e \in E^G} \left(G^{min} \bar{P}_e^G \beta_{etos}^G \right) \geq 0 \qquad ,t \in T^S, o \in T_t^O, s \in S^O \tag{6}$$

$$f_{tos} - (A^F p_{Gtos} + B^F \sum_{e \in E^G} \beta_{etos}^G) \geq 0 \qquad ,t \in T^S, o \in T_t^O, s \in S^O \tag{7}$$

$$p_{Ptos} - I_{os} \sum_{e \in E^P} \eta_e^{PV} O_e^{PV} x_e \leq 0 \qquad ,t \in T^S, o \in T_t^O, s \in S^O \tag{8}$$

$$s_{tos}^B - s_{t,o-1,s}^B - H(\eta^- p_{B^- tos} - \eta^+ p_{B^+ tos}) = 0 \qquad ,t \in T^S, o \in T_t^O \setminus \{1\}, s \in S^O \tag{9}$$

$$s^B_{t1s} - H\eta^- p_{B^-t1s} = 0 \qquad ,t \in T^S, s \in S^O \tag{10}$$

$$s^B_{tos} - \sum_{e \in E^B} \bar{E}^B_e x_e \leq 0 \qquad ,t \in T^S, o \in T^O_t, s \in S^O \tag{11}$$

$$p_{B^+tos} - \bar{P}^{B+} \leq 0 \qquad ,t \in T^S, o \in T^O_t, s \in S^O \tag{12}$$

$$p_{B^-tos} - \bar{P}^{B-} \leq 0 \qquad ,t \in T^S, o \in T^O_t, s \in S^O \tag{13}$$

$$p_{B^+t1s} \leq 0 \qquad ,t \in T^S, s \in S^O \tag{14}$$

$$l_t - l_{t-1} - H \sum_{s \in S^O} \pi_s \sum_{o \in T^O_t} p_{B^-tos} + M^B \sum_{e \in E^B} x^B_{et} \geq 0 \qquad ,t \in T^S \backslash \{1\} \tag{15}$$

$$l_t - H \sum_{s \in S^O} \pi_s \sum_{o \in T^O_t} p_{B^-tos} \geq 0 \qquad ,t \in T^S \tag{16}$$

$$l_t - \sum_{e \in E^B} L^B \bar{E}^B_e x_e \leq 0 \qquad ,t \in T^S \tag{17}$$

$$x^B_{et} - x_e \leq 0 \qquad ,e \in E^B, t \in T^S \tag{18}$$

$$\sum_{e \in E^G} x_e \leq 1 \tag{19}$$

$$\sum_{e \in E^B} x_e \leq 1 \tag{20}$$

$$p_{itos} \geq 0 \qquad ,i \in E^{En}, t \in T^S, o \in T^O_t, s \in S^O \tag{21}$$

$$f_{tos}, \quad s^B_{tos}, \quad n^L_{tos} \geq 0 \qquad ,t \in T^S, o \in T^O_t, s \in S^O \tag{22}$$

$$l_t \geq 0 \qquad ,t \in T^S \tag{23}$$

$$x_e \in \{0,1\} \qquad ,e \in E \backslash \{E^P\} \tag{24}$$

$$x^B_{et} \in \{0,1\} \qquad ,e \in E^B, t \in T^S \tag{25}$$

$$\beta^G_{etos} \in \{0,1\} \qquad ,e \in E^G, t \in T^S, o \in T^O_t, s \in S^O \tag{26}$$

$$x_e \in \mathbb{Z}^+ \qquad ,e \in E^P \tag{27}$$

Appendix B

Mathematical Model - full

$$\min z = \sum_{e \in E} C_e x_e + \sum_{t \in T^S} \delta_t \sum_{e \in E^B} C_e x_{et}^B +$$
$$\sum_{t \in T^S} \delta_t \sum_{s \in S^O} \pi_s \sum_{o \in T_t^O} H \theta^{oc} \left(C^G p_{Gtos} + C^L n_{tos}^L + C^{om} \sum_{e \in E^W} p_{etos} \right) \tag{1c}$$

$$s.t. \quad \sum_{i \in E^{En} \setminus \{B^-\}} H p_{itos} + \sum_{e \in E^W} H p_{etos} - H p_{B^- tos} + H n_{tos}^L = D_{os} \qquad ,t \in T^S, o \in T_t^O, s \in S^O \tag{2c}$$

$$H \left(\frac{\sum_{o \in T_t^O} p_{Gtos}}{\sum_{o \in T_t^O} D_{os}} \right) \leq \bar{R}^G \qquad ,t \in T^S, s \in S^O \tag{3}$$

$$p_{Gtos} - \sum_{e \in E^G} \bar{P}_e^G x_e \leq 0 \qquad ,t \in T^S, o \in T_t^O, s \in S^O \tag{4b}$$

$$p_{Ptos} - I_{os} \sum_{e \in E^P} \eta_e^{PV} O_e^{PV} x_e \leq 0 \qquad ,t \in T^S, o \in T_t^O, s \in S^O \tag{8}$$

$$\sum_{e \in E^{PV}} O_e^{PV} x_e \leq O^{max} \tag{P1}$$

$$s_{tos}^B - s_{t,o-1,s}^B - H(\eta^- p_{B^-tos} - \eta^+ p_{B^+tos}) = 0 \qquad ,t \in T^S, o \in T_t^O \backslash \{1\}, s \in S^O \tag{9}$$

$$s_{t1s}^B - H\eta^- p_{B^-t1s} = 0 \qquad ,t \in T^S, s \in S^O \tag{10}$$

$$s_{tos}^B - \bar{E}_e^B x_e + \frac{R^B l_{t-1}}{L^B} - (1 - x_e) M^{BS} \leq 0 \qquad ,e \in E^B, t \in T^S \backslash \{1\}, o \in T_t^O, s \in S^O \tag{E1}$$

$$s_{1os}^B - \sum_{e \in E^B} \bar{E}_e^B x_e \leq 0 \qquad ,o \in T_1^O, s \in S^O \tag{E2}$$

$$p_{B^+tos} - \bar{P}^{B+} \leq 0 \qquad ,t \in T^S, o \in T_t^O, s \in S^O \tag{12}$$

$$p_{B^-tos} - \bar{P}^{B-} \leq 0 \qquad ,t \in T^S, o \in T_t^O, s \in S^O \tag{13}$$

$$p_{B^+t1s} \leq 0 \qquad ,t \in T^S, s \in S^O \tag{14}$$

$$l_t - l_{t-1} - H \sum_{s \in S^O} \pi_s \sum_{o \in T_t^O} p_{B^-tos} + M^B \sum_{e \in E^B} x_{et}^B \geq 0 \qquad ,t \in T^S \backslash \{1\} \tag{15}$$

$$l_t - H \sum_{s \in S^O} \pi_s \sum_{o \in T_t^O} p_{B^-tos} \geq 0 \qquad ,t \in T^S \tag{16}$$

$$l_t - \sum_{e \in E^B} L^B \bar{E}_e^B x_e \leq 0 \qquad ,t \in T^S \tag{17}$$

$$x_{et}^B - x_e \leq 0 \qquad ,e \in E^B, t \in T^S \tag{18}$$

$$p_{etos} \leq \bar{P}^R_e x_e \frac{V_{os} - V^{cin}_e}{V^R_e - V^{cin}_e} + \gamma^W_{etos} M^W \qquad ,e \in E^W, t \in T^S, o \in T^O_t, s \in S^O \tag{W1}$$

$$p_{etos} \leq \bar{P}^R_e x_e \qquad ,e \in E^W, t \in T^S, o \in T^O_t, s \in S^O \tag{W2}$$

$$V_{os} \leq V^{cof}_e + \gamma^W_{etos} M^{V1}_e \qquad ,e \in E^W, t \in T^S, o \in T^O_t, s \in S^O \tag{W3}$$

$$V_{os} \geq V^{cin}_e - \gamma^W_{etos} M^{V2}_e \qquad ,e \in E^W, t \in T^S, o \in T^O_t, s \in S^O \tag{W4}$$

$$p_{etos} \leq M^W (1 - \gamma^W_{etos}) \qquad ,e \in E^W, t \in T^S, o \in T^O_t, s \in S^O \tag{W5}$$

$$\sum_{e \in E^G} x_e \leq 1 \tag{19}$$

$$\sum_{e \in E^B} x_e \leq 1 \tag{20}$$

$$p_{itos} \geq 0 \qquad ,i \in E^{En}, t \in T^S, o \in T^O_t, s \in S^O \tag{21}$$

$$s^B_{tos}, \quad n^L_{tos} \geq 0 \qquad ,t \in T^S, o \in T^O_t, s \in S^O \tag{22}$$

$$p_{etos} \geq 0 \qquad ,e \in E^W, t \in T^S, o \in T^O_t, s \in S^O \tag{W6}$$

$$l_t \geq 0 \qquad ,t \in T^S \tag{23}$$

$$x_e \in \{0,1\} \qquad ,e \in E \backslash \{E^P E^W\} \tag{24}$$

$$x^B_{et} \in \{0,1\} \qquad ,e \in E^B, t \in T^S \tag{25}$$

$$\gamma^W_{etos} \in \{0,1\} \qquad ,e \in E^W, t \in T^S, o \in T^O_t, s \in S \tag{W7}$$

$$x_e \in \mathbb{Z}^+ \qquad ,e \in E^P \cup E^W \tag{27}$$

Appendix C

Notation - Full

Table C.1: Sets

Set		Description
T^S	-	Set of strategic periods
T_t^O	-	Set of operational periods, under strategic period t $in T^S$
S^O	-	Set of operational scenarios
E^{En}	-	Set of power sources = $\{G, P, B^+, B^-\}$
E	-	Set of possible PV-units, generator units, battery units and wind turbines
E^G	-	Set of possible generator units
E^P	-	Set of possible PV-panel units
E^B	-	Set of possible battery units
E^W	-	Set of possible wind turbine units

Table C.2: Indices

Index		Description
t	-	in set T^S
o	-	in set T_t^O
s	-	in set S^O
i	-	in set E^{En}
e	-	in sets E, E^G, E^W. E^P and E^B

Table C.3: Parameters

Parameter		Description
δ_t	-	Discount factor
D_{os}	-	Load demand in period $o \in T_t^O$, in scenario $s \in S^O$ [kWh]
I_{os}	-	Irradiation in period $o \in T_t^O$, in scenario $s \in S^O$ [kW/m^2]
$\bar{R}^G$	-	Maximum share of energy produced from the diesel generator [%]
O_e^{PV}	-	Surface area of PV-unit $e \in E^P$ [m^2]
O^{max}	-	Maximum total surface area of PV-panels [m^2]
η_e^{PV}	-	Efficiency of PV-unit $e \in E^P$
C_e	-	Cost per unit $e \in E$ [$]
C^F	-	Cost per kWh produced from diesel generator [$/kWh]
C^L	-	Value of lost load (VOLL) [$/kWh]
$\bar{P}_e^G$	-	Maximum power rating of generator $e \in E^G$ [kW]
π_s	-	Probability of scenario $s \in S^O$
H	-	Length of operating period [hours]
η^+, η^-	-	Conversion efficiency for discharging and charging battery, respectively
$\bar{P}^{B+}$	-	Maximum discharging power rating of battery $e \in E^B$ [kW]
$\bar{P}^{B-}$	-	Maximum charging power rating of battery $e \in E^B$ [kW]
$\bar{E}_e^B$	-	Maximum rated energy capacity of battery $e \in E^B$ [kWh]
R^B	-	Defined degradation at End of Life for battery unit [%]
L^B	-	Total Battery lifetime given in number of cycles
M^B	-	Big-M value related to battery reinvestment
M^{BS}	-	Big-M value related to degradation of battery
$\bar{P}_e^r$	-	Rated power output of wind turbine $e \in E^W$ [kW]
V_e^{cin}	-	Cut-in wind speed of wind turbine $e \in E^W$ [m/s]
V_e^{cof}	-	Cut-off wind speed of wind turbine $e \in E^W$ [m/s]
V_e^r	-	Rated wind speed of wind turbine $e \in E^W$ [m/s]
V_{os}	-	Wind speed in operational time period $o \in T_t^O$ for scenario $s \in S^O$ [m/s]
M_e^{V1}, M_e^{V2}	-	Big-M for setting wind γ_{etos} if wind speed is out of bounds
M^w	-	Big-M for not restricting p_{etos} when wind speed is within bounds

Table C.4: Variables

Variable		Description
x_e	-	1, if invest in a unit of type $e \in E \setminus \{E^P E^W\}$
	-	0, otherwise
x_e	-	integer variable denoting number of PV-panel or wind turbine model $e \in E^P \cup E^W$ are invested in
x^B_{et}	-	1, if reinvestment in battery $e \in E^B$ is necessary in $t \in T^S$,
	-	0, otherwise
γ^W_{etos}	-	1, if $V_{os} \leq V^{cin}_e$ or $V_{os} \geq V^{cof}_e$, for unit $e \in E^W$ in period $t \in T^S, o \in T^O_t, s \in S^O$
	-	0, otherwise
p_{itos}	-	Aggregate power from/to source $i \in E^{En}$ in operating period $t \in T^S$, $o \in T^O_t$ in scenario $s \in S^O$ [kW]
p_{etos}	-	Power produced by unit $e \in E^W$ in period $t \in T^S, o \in T^O_t, s \in S^O$ [kW]
n^L_{tos}	-	Load not covered in operating period $t \in T^S$, $o \in T^O_t$ in scenario $s \in S^O$ [kW]
s^B_{tos}	-	Total SOC in operating period $o \in T^O_t$, $t \in T^S$ in scenario $s \in S^O$ [kWh]
l_t	-	Expected total energy charged to the battery unit from the time of investment until the end of $t \in T^S$ [kWh]

Appendix D

Component data and input parameters

Table D.1: Input parameters for PV-panels

Model	Wp	Cost [$/unit]	Area [m^2]	Efficiency
PPAM Solar 6	230	316.6	1.655	13.9%
Qcellsq	250	268.5	1.645	15.2%
Centro Solar	255	371.4	1.723	14.8%
JA Solar	260	310.5	1.688	15.4%
Yingli Solar	270	324.6	1.646	16.4%
Sun PowerSun	327	624.8	1.721	19.0%

Table D.2: Input parameters for battery units

Size [kWh]	Technology	Cost [$]	Max charging [kW]	Max discharging [kW]	End of life
30	Li-ion	49 270	50	50	70%
50	Li-ion	82 117	50	50	70%
100	Li-ion	122 911	50	50	70%
180	Li-ion	188 382	50	50	70%
250	Li-ion	242 794	50	50	70%
500	Li-ion	434 324	50	50	70%

Table D.3: Input parameters for wind turbines

Rated Power [kW]	Cost [$/unit]	Rated wind speed [m/s]	Cut in [m/s]	Cut off [m/s]
10	63 099	9.0	3.0	25.0
15	71 801	10.0	3.0	25.0
20	145 955	10.0	3.0	26.0
50	176 471	11.0	3.0	26.0
200	423 529	15.0	4.5	27.0
250	857 353	15.0	3.0	28.0

Table D.4: Input parameters for diesel generators

Max power [kW]	**Cost [$]**	**Fuel consumption [l/kWh]**
12	5 000	0.3186
15	7 250	0.3186
20	11 000	0.3186
25	12 000	0.3186
30	13 000	0.3186
50	15 000	0.3186

Table D.5: General list of input parameters for the model

Parameter	**Explanation**	**Related to**	**Value**
$\bar{R}^G$	Maximum share	Diesel generator	5%
δ_t	Discount factor $(1/(1+rfr)^t)$	Cost calculations	$1/1.03^t$
C^L	VOLL	Load not covered	1000 $/kWh
C^G	Generation cost	Diesel generator	0.5978 $/kWh
η^+	Efficiency	Battery discharging	94%
η^-	Efficiency	Battery charging	94%
C^{om}	O&M costs	Wind turbines	0.01344 $/kWh
O^{max}	Max surface area	PV-panels	915 m^2
H	Length of operational period	Entire Problem	1h
L^B	Max cycles	Battery lifetime	82*
M^B	Big-M	Battery reinvestment	42 896*
M^{BS}	Big-M	Battery degradation	1000

Appendix E

Statistical property match calculations

After sampling $u = 1, .., U$ different scenario trees, one has to identify the tree u^* that is the best match with the underlying stochastic process. Because perfect knowledge of the underlying stochastic process is unobtainable, an approximation is necessary. Assuming that the past represents the future, historic data serves as a valid approximation. Therefore, as a measure of how well a sampled scenario tree represents the underlying stochastic process, we compare the four first statistical moments; expectation, variance, skewness and kurtosis, of every typical hour in every month of the scenario tree to that of the historic data.

This comparison is made by calculating the absolute deviation of the statistical moments. In the evaluation of the scenario trees, the deviation of the statistical moments are weighted equally, and summed in order to compare one part of a scenario tree to the corresponding historical data. The deviation calculations for the two stochastic parameters considered are done independently, and finally weighted equally when they are added in order to evaluate minimum total deviation.

The statistical properties of the historic data is obtained by pooling all data entries from each hour of the day of a specific month into one data set, and calculating the moments of these values. With five years of historic data, if we look at hour 1 (from 00:00 to 01:00) in January as an example, we calculate moments based on 5×31 data entries. For every scenario tree generated, hourly values from every scenario in every month are pooled together and moments are calculated on these values. If we look at 20 scenarios per month with 72 consecutive hours, this gives a total of 20×3 data entries for each hour in each month. If the data entries are all zero, or too few of the entries are non-zero to calculate a meaningful moment, the moments are set to zero. If v is moment from 1 to 4, h is hour of the day from 1 to 24 and m is month of year, then $mom_{hist}^{v,h,m}$ is the historic moment v of hour h in month m. Similarly, $mom_{tree}^{u,v,h,m}$ is the moment v of hour h in month m for scenario tree u. Thus, the absolute deviation $\delta_{u,m}$ of scenario tree u in month m can be calculated as follows.

$$\delta_{u,m} = \sum_{v=1}^{4} \sum_{h=1}^{24} \left| \frac{mom_{hist}^{v,h,m} - mom_{tree}^{u,v,h,m}}{mom_{hist}^{v,h,m}} \right| \tag{E.1}$$

These calculations are done for both wind and solar, thus obtaining a $\delta_{u,m}$ for each. As we're considering absolute deviation, these values are added together in order to compare the statistical fit of each monthly part of every tree for the two stochastic parameters. Finally, the best match tree u^*, is constructed by taking parts from the best matching tree for every month and merging them together.

$$\delta_{u^*,m} = min\left\{\delta_{1,m}, \delta_{2,m}, ..., \delta_{U-1,m}, \delta_{U,m}\right\} \qquad m = 1, ..., 12 \tag{E.2}$$

$$u^* = \{u_1^* \cup u_2^* \cup, ..., \cup u_{11}^* \cup u_{12}^*\} \tag{E.3}$$

Appendix F

Calculations VSS and EVPBD

Table F.1: VSS and EVPBD for all combinations with instance 3 and 4 for the MISSMDP

Instance	**Tree**	***RP***	***EEV***	***FRP***	***VSS***	***EVPBD***
3	1	20,295,651	427,635,456	20,551,266	*407,339,805*	*255,615*
3	2	20,886,736	544,929,883	21,109,017	*524,043,147*	*222,281*
3	3	21,489,205	446,766,518	21,792,784	*425,277,313*	*303,579*
3	4	19,812,041	448,825,916	20,114,356	*429,013,876*	*302,315*
4	1	25,407,409	558,935,343	25,845,326	*533,527,934*	*437,917*
4	2	25,898,752	706,294,339	25,967,231	*680,395,587*	*68,480*
4	3	25,898,752	571,270,843	27,331,581	*545,372,091*	*1,432,830*
4	4	24,935,289	674,870,450	25,114,367	*649,935,162*	*179,079*

Appendix G

Results from Chapter 7.5.1

Table G.1: Testing the matheuristic of increasing tolerance gap from 0.7 % to 5% on instance 3. Table shows average computation time and objective value with 0.7% and 5% tolerance gap, and the relative change on 4 different scenario trees.

		Objective value		**Computation time [s]**		**Relative change**	
Inst	Tree	0.7%	5.0%	0.7%	5.0%	Obj	Time
3	1	20,295,650	20,295,650	53,220.40	71,773.60	0%	+34.9%
3	2	20,886,735	20,892,457	87,960.40	10,322.10	+0.002%	-88.3%
3	3	21,489,205	21,496,014	47,727.70	12,263.70	+0.03%	-74.3%
3	4	19,812,040	19,836,638	23,588.50	10,977.70	+0.1%	-53.5%
Avg.		20,620,908	20,630,190	53,124.25	26,334.28	+0.04%	-50.4%

Table G.2: Testing the matheuristic of increasing tolerance gap from 0.7 % to 5% on instance 4. Table shows average computation time and objective value with 0.7% and 5% tolerance gap, and the relative change on 4 different scenario trees.

		Objective value		**Computation time [s]**		**Relative change**	
Inst	Tree	0.7%	5.0%	0.7%	5.0%	Obj	Time
4	1	25,407,408	25,407,408	196,433.00	144,692.00	0%	-26.3%
4	2	25,898,751	25,905,460	77,438.00	31,600.10	+0.02%	-59.2%
4	3	25,898,751	26,816,229	70,419.80	24,497.90	+3.54%	-65.2%
4	4	24,935,288	24,935,288	23,163.90	25,260.50	0%	+9.05%
Avg.		25,535,050	25,766,096	91,863.68	56,512.63	+0.90%	-38.5%